



ผลของโพรไบโอติกแบคทีเรียกรดแลคติกในการป้องกันการเกิดภาวะพังผืดในตับ
ของหนูที่ถูกเหนี่ยวนำด้วยสารไธโออะเซทาไมด์

HEPATOPROTECTIVE EFFECT OF PROBIOTICS LACTIC ACID BACTERIA
ON THIOACETAMIDE-INDUCED LIVER FIBROSIS IN RATS

CHITTAPON JANTARARUSSAMEE

Graduate School Srinakharinwirot University

2019

ผลของไฟรบไอบิติกแบคทีเรียกรดแลกติกในการป้องกันการเกิดภาวะพังผืดในตับ
ของหนูที่ถูกรบกวนด้วยสารไฮโออะเซทาไมด์



ปริญญานิพนธ์นี้เป็นส่วนหนึ่งของการศึกษาตามหลักสูตร
ปรัชญาดุษฎีบัณฑิต สาขาวิชาชีวภาพการแพทย์
คณะแพทยศาสตร์ มหาวิทยาลัยศรีนครินทรวิโรฒ
ปีการศึกษา 2562
ลิขสิทธิ์ของมหาวิทยาลัยศรีนครินทรวิโรฒ

HEPATOPROTECTIVE EFFECT OF PROBIOTICS LACTIC ACID BACTERIA
ON THIOACETAMIDE-INDUCED LIVER FIBROSIS IN RATS



A Dissertation Submitted in partial Fulfillment of Requirements
for DOCTOR OF PHILOSOPHY (Biomedical Sciences)
Faculty of Medicine Srinakharinwirot University

2019

Copyright of Srinakharinwirot University

THE DISSERTATION TITLED
HEPATOPROTECTIVE EFFECT OF PROBIOTICS LACTIC ACID BACTERIA
ON THIOACETAMIDE-INDUCED LIVER FIBROSIS IN RATS

BY
CHITTAPON JANTARARUSSAMEE

HAS BEEN APPROVED BY THE GRADUATE SCHOOL IN PARTIAL FULFILLMENT OF
THE REQUIREMENTS FOR THE DOCTOR OF PHILOSOPHY IN BIOMEDICAL
SCIENCES
AT SRINAKHARINWIROT UNIVERSITY

..... Dean of Graduate School
(Assoc. Prof. Dr. Chatchai Ekpanyaskul, MD.)
.....

ORAL DEFENSE COMMITTEE

..... Major-advisor Chair
(Assoc. Prof. Dr. Wisuit Pradidarcheep)	(Assoc. Prof. Dr. Sirinush Sricharoenvej)
..... Co-advisor Committee
(Asst. Prof. Dr. Malai Taweechotipatr)	(Asst. Prof. Dr. Amporn Jariyapongskul)
..... Co-advisor	
(Assoc. Prof. Dr. Udomsri Showpittapornchai)	

Title	HEPATOPROTECTIVE EFFECT OF PROBIOTICS LACTIC ACID BACTERIA ON THIOACETAMIDE-INDUCED LIVER FIBROSIS IN RATS
Author	CHITTAPON JANTARARUSSAMEE
Degree	DOCTOR OF PHILOSOPHY
Academic Year	2019
Thesis Advisor	Associate Professor Dr. Wisuit Pradidarcheep

Hepatic fibrosis is a reversible wound-healing response characterized by the accumulation of extracellular matrix. Probiotics have been used for the treatment of various disorders. The aim of the present study was to investigate the hepatoprotective effects of probiotics lactic acid bacteria (mixture of *Lactobacillus paracasei*, *Lactobacillus casei*, and *Weissella confusa*) on thioacetamide (TAA) -induced liver fibrotic rats. Thirty-five male Wistar rats were randomly divided into five groups: (A) Control group, (B) TAA group, (C) TAA+probiotics group, (D) TAA+silymarin group, and (E) Probiotic group. Group (A) were received standard diet. Group (B, C, and D) were induced by intraperitoneal injection of TAA (200 mg/kg BW) 3 times per week for consecutive 8 weeks. Group (D) received TAA plus 100 mg/kg BW of Silymarin 2 times per week. In probiotic group (C and E), the number of mixture of the viable microbial cells at 10^9 CFU/ml/day was administered orally daily. After sacrifice, liver tissues were collected and processed for histomorphology, lipid peroxidation, and Western blot analysis. Serum was obtained from blood for measurement of liver enzymes. It was found that the TAA group showed hepatic injury marked by increase in serum enzyme levels, area of inflammation, and expression of TNF- α , TGF- β 1, and α -SMA proteins. The collagen fibers were substantially accumulated in the hepatic lobules. Moreover, TAA+probiotics group and TAA+silymarin group significantly reduced the serum enzyme levels, area of inflammation, and accumulation of collagen. The liver damage was found to be lesser in the probiotic-treated group. Probiotics may be effective hepatoprotective agents and should be considered useful for the prevention of hepatic disorders.

Keyword : liver fibrosis, lactic acid bacteria, probiotics, thioacetamide

ACKNOWLEDGEMENTS

I would like to express profound gratitude and deep appreciation to my major advisor, Associate Professor Dr. Wisuit Pradidarcheep for invaluable support, encouragement, inspiration, enthusiasm, supervision and useful suggestions throughout this work. His continuous guidance enabled me to complete my work successfully. I am also thankful to Assistant Professor Dr. Malai Taweechoitipatr and Associate Professor Dr. Udomsri Showpittapornchai my co-advisor for their kindness, encouragement, immense knowledge, and support. I would like to thank the grants from Faculty of Medicine and The Graduate School, Srinakharinwirot University for financial support throughout my study. Moreover, I would like to thank Department of Anatomy and Microbiology, Faculty of Medicine, Srinakharinwirot University for providing me all instruments and facilities on my research. I also would like to thank everyone in Biomedical Sciences Program, Srinakharinwirot University for kindly assistance and giving me warm and friendly working environment. I am also indebted to all the animals that were sacrificed in this study. My special thanks must certainly go to Miss Siripa Rodniem, Miss Vilailak Ti Yao, Miss Vichununt Kerdput, Mr. Nattpawit Kaewnoonual, Mr. Thana Chaeyklinthes and everyone in Department of Anatomy, Faculty of Medicine, Srinakharinwirot University for their friendship and support academically.

Most especially to my family, I would like to thank my dad and mom who always believe in me, for their love, patience and support throughout my life. Thank you also to my brother who helps me in every issue whenever I needed it. I love you all and thank you very much.

CHITTAPON JANTARARUSSAMEE

TABLE OF CONTENTS

	Page
ABSTRACT	D
ACKNOWLEDGEMENTS.....	E
TABLE OF CONTENTS.....	F
LIST OF TABLES.....	L
LIST OF FIGURES	M
CHAPTER 1 INTRODUCTION	1
Hypothesis	5
CHAPTER 2 REVIEW OF THE LITERATURE.....	7
1. Definition of probiotics	7
2. Properties of probiotic strains.....	9
3. Mechanisms of action of probiotics.....	10
3.1 Enhancement of the epithelial barrier: maintain barrier function.....	11
3.2 Increased adhesion to intestinal mucosa	11
3.3 Colonization resistance: competitive exclusion of pathogenic microorganisms	12
3.4 Production of antimicrobial substances.....	12
3.5 Immune modulation.....	13
4. Probiotics in liver diseases	14
5. The liver.....	16
5.1 The human liver	16
5.2 Rat liver.....	16

5.2.1 Surfaces anatomy of the rat liver	17
5.2.2 The rat liver lobes.....	19
5.3 Histology of the Liver.....	20
5.3.1 Hepatic functional unites	20
5.3.2 Liver cell types	24
5.3.3 Sinusoids.....	27
5.3.4 Space of Disse.....	28
5.4 Liver function	29
5.4.1 Digestion	29
5.4.2 Metabolism.....	30
5.4.3 Protein synthesis.....	30
5.4.4 Detoxification.....	31
5.4.5 Immunity.....	31
6. Liver fibrosis.....	32
6.1 Pathophysiology of hepatic fibrosis	33
6.2 Hepatic stellate cells (HSCs) activation.....	34
6.2.1 Initiation	34
6.2.2 Perpetuation	34
6.2.2.1 Proliferation	35
6.2.2.2 Fibrogenesis	35
6.2.2.3 Chemotaxis	35
6.2.2.4 Matrix degradation.....	35
6.2.2.5 Retinoid loss	35

6.3 Liver specific enzymes in liver fibrosis	36
6.4 Patterns of liver fibrosis progression.....	37
6.4.1 Portal and periportal fibrosis.....	37
6.4.2 Pericellular fibrosis	37
6.4.3 Pericentral fibrosis	37
6.4.4 Bridging fibrosis.....	38
6.4.5 Cirrhosis	38
6.5 Assessment of liver fibrosis.....	38
6.5.1 Sirius red staining	39
6.5.2 The Ishak system	40
6.6 Liver regeneration in liver fibrosis	41
7. Thioacetamide (TAA)	41
7.1 Chemical structure	41
7.2 Bioactivation of TAA	42
7.3 Experimental hepatotoxicity of TAA	43
7.4 Histopathological caused by TAA.....	44
8. Silymarin	45
8.1 Chemistry of Silymarin.....	45
8.2 Mechanisms of action	46
8.3 Antifibrotic effects.....	47
CHAPTER 3 MATERIALS AND METHODS	48
1. Chemicals and antibodies	48
1.1 Chemicals.....	48

1.2 Antibodies.....	48
1.3 PrimePCR SYBR® Green gene assay and Primer sequences.....	49
2. Probiotic strains.....	50
3. Experimental animals.....	51
4. Preparation of probiotic constituents.....	52
5. Experimental designs	52
6. Methods	54
6.1 Gross examination of the liver.....	54
6.2 Liver enzyme markers	54
6.3 Histopathological studies from paraffin sections.....	54
6.3.1 Tissue preparation	54
6.3.2 Histopathological analysis	54
6.3.3 Immunohistochemical staining	55
6.4 Western blot analysis	56
6.5 MDA assay	57
6.6 Real-time quantitative PCR	57
6.6.1 RNA extraction	58
6.6.2 RNA qualification	58
6.6.3 Reverse transcription	58
6.6.4 Real time quantitative PCR	59
7. Statistical analysis.....	59
CHAPTER 4 RESULTS.....	60
1. Effects of probiotics on general properties	60

1.1 Body weights of the rats.....	60
1.2 The liver weight relative to body weight.....	60
2. Effects of probiotics on liver enzymes.....	62
2.1 Aspartate aminotransferase (AST).....	62
2.2 Alanine aminotransferase (ALT).....	63
2.3 Alkaline phosphatase (ALP).....	64
3. Effects of probiotics on gross and histomorphological changes in liver.....	66
3.1 External morphology of the rat livers.....	66
3.2 Histopathological changes.....	71
4. Effects of probiotics on collagen deposition in liver tissues.....	78
5. Effects of probiotics on lipid peroxidation in liver tissues.....	85
6. Effects of probiotics on the expression of TNF- α , TGF- β 1, and α -SMA proteins in liver tissues.....	86
Immunohistochemistry.....	86
6.1 Distribution of the TNF- α immunoreactivity.....	86
6.2 Distribution of the TGF- β 1 immunoreactivity.....	91
6.3 Distribution of the α -SMA immunoreactivity.....	95
Western blot analysis.....	99
7. Effects of probiotics on the mRNA expression of <i>Tnf</i> , <i>Tgfb1</i> , and <i>Acta2</i> genes in liver tissues.....	103
<i>Tnf</i> mRNA.....	104
<i>Tgfb1</i> mRNA.....	105
<i>Acta2</i> mRNA.....	106

CHAPTER 5 DISCUSSION 107

CHAPTER 6 CONCLUSION 113

REFERENCES..... 114

VITA 130



LIST OF TABLES

	Page
Table 1 Microorganisms considered as probiotics	8
Table 2 Criteria of ideal probiotic strains	9
Table 3 Ishak staging scale	40
Table 4 Assay details of all studied genes for real-time PCR.....	49
Table 5 List of primer sequences used for RT-PCR	50
Table 6 General characteristics of probiotic strains	51
Table 7 Comparison of the liver weight to body weight ratio	61
Table 8 Comparison of the liver enzyme makers.....	65
Table 9 Comparison of the index of liver damage and percentage of leukocyte infiltration.....	72
Table 10 The percentage of positive staining intensity quantified for the TNF- α , TGF- β 1, and α -SMA expressions in the liver tissue sections of all animal groups.....	86
Table 11 Comparison of the relative quantitative analysis of TNF- α , TGF- β 1, and α -SMA expression (% of control) in liver tissues	99
Table 12 The real-time PCR analysis of the <i>Tnf</i> , <i>Tgfb1</i> , and <i>Acta2</i> mRNA expression levels in liver tissues of all five animal groups	103

LIST OF FIGURES

	Page
Figure 1 Conceptual framework.....	6
Figure 2 Light micrograph of Gram-stained <i>Lactobacillus</i>	8
Figure 3 Major mechanisms of action of probiotics.....	10
Figure 4 Diagram illustrates the mechanisms involved in liver diseases and probiotic influences on them.....	15
Figure 5 Gross anatomy of the human liver.....	17
Figure 6 Gross anatomy of the rat liver.....	18
Figure 7 Ventral and dorsal surface of the rat liver showing lobes.....	20
Figure 8 Hepatic functional units-hepatic lobule, portal lobule and hepatic acinus.....	21
Figure 9 Diagram showing hepatic lobule.....	22
Figure 10 Diagram showing portal lobule.....	23
Figure 11 Diagram showing the hepatic acinus.....	24
Figure 12 Hepatocyte and its intracellular organelles.....	25
Figure 13 Cross-section of liver showing sinusoidal endothelial cells, hepatic stellate cell, and Kupffer cell.....	26
Figure 14 Illustration of hepatic sinusoids.....	28
Figure 15 The relationship between hepatocytes.....	29
Figure 16 Stage of liver damage.....	32
Figure 17 Normal liver to liver fibrosis.....	34
Figure 18 Activation of hepatic stellate cells (HSCs).....	36
Figure 19 The molecular formula of the dye Sirius red illustrating sulfonic groups.....	39

Figure 20 The structural formula of Thioacetamide (TAA)	42
Figure 21 The kinetics of a two-step bioactivation of TAA.....	43
Figure 22 Milk thistle.....	45
Figure 23 The structures of flavonolignan isomers of silymarin.....	46
Figure 24 Diagram illustrating the experimental groups.....	53
Figure 25 Graph illustrating the mean rat body weight of the five experimental groups from week 0 to week 8	61
Figure 26 Diagram showing the serum levels of aspartate aminotransferase (AST) in the five animal groups	62
Figure 27 Diagram showing the serum levels of alanine aminotransferase (ALT) in the five animal groups	63
Figure 28 Diagram showing the serum levels of alkaline phosphatase (ALP) in the five animal groups	64
Figure 29 Photomicrographs showing gross morphology of the liver (diaphragmatic surface) with magnifications of the liver surface.....	67
Figure 30 Photomicrographs showing gross morphology of the liver (visceral surface) with magnifications of the liver surface.....	68
Figure 31 Photomicrographs showing gross morphology of the liver (visceral surface) with magnifications of the liver surface.....	69
Figure 32 Photomicrographs showing gross morphology of the liver (viseral surface) with magnifications of the liver surface.....	70
Figure 33 Light micrographs of the liver sections stained with H&E	73
Figure 34 Light micrographs at higher magnification of the liver sections stained with H&E	75
Figure 35 Light micrographs at higher magnification of the liver sections stained with H&E in TAA group.....	77

Figure 36 Box plots of Ishak score according to liver fibrosis stage	79
Figure 37 Photomicrograph of the liver sections stained with Sirius red	80
Figure 38 Photomicrograph with higher magnification of the liver sections stained by with Sirius red	82
Figure 39 Quantitative analysis of comparison of the percentage of fibrotic collagen areas in the Sirius-red stained liver section of all animal different groups.....	84
Figure 40 Levels of serum malondialdehyde (MDA) (nmol/ul) in all animal groups.....	85
Figure 41 Photomicrographs showing immunoreactivity of TNF- α in rat liver sections of all animal groups.....	88
Figure 42 Photomicrographs at higher magnification showing immunoreactivity of TNF- α in rat liver sections of all animal groups	89
Figure 43 Quantitative analysis of TNF- α expression was shown as a percentage of positive staining intensity.....	90
Figure 44 Photomicrographs showing immunoreactivity of TGF- β 1 in rat liver sections of all animal groups.....	92
Figure 45 Photomicrographs at higher magnification showing immunoreactivity of TGF- β 1 in rat liver sections of all animal groups.....	93
Figure 46 Quantitative analysis of TGF- β 1 expression was shown as a percentage of positive staining intensity.....	94
Figure 47 Photomicrographs at higher magnification showing immunoreactivity of α -SMA in rat liver sections of all animal groups	96
Figure 48 Photomicrographs at higher magnification showing immunoreactivity of α -SMA in rat liver sections of all animal groups	97

Figure 49 Quantitative analysis of α -SMA expression was shown as a percentage of positive staining intensity.....	98
Figure 50 Hepatic TNF- α protein content was measured by Western blot analysis.....	100
Figure 51 Hepatic TGF- β 1 protein content was measured by Western blot analysis.....	101
Figure 52 Hepatic α -SMA protein content was measured by Western blot analysis.....	102
Figure 53 Quantitative real-time PCR analysis of the <i>Tnf</i> mRNA expression level in liver tissues.....	104
Figure 54 Quantitative real-time PCR analysis of the <i>Tgfb1</i> mRNA expression level in liver tissues.....	105
Figure 55 Quantitative real-time PCR analysis of the <i>Acta2</i> mRNA expression level in liver tissues.....	106
Figure 56 Schema showing of probiotic lactic acid bacteria protecting against liver fibrosis.....	111
Figure 57 Schematic depicting the gut-liver axis following the liver fibrosis induced by thioacetamide (TAA)	112

CHAPTER 1

INTRODUCTION

Liver fibrosis is a reversible wound-healing response to either acute or chronic cellular injury that reflects a balance between liver repair and scar formation. If the insult is acute or self-limited, these changes are transient, and liver architecture is restored to its normal composition. However, if the injury is prolonged, chronic inflammation and accumulation of ECM remain, leading to a progressive substitution of hepatic parenchyma by scar tissue.⁽¹⁾ This process results in cirrhosis, the end consequence of progressive fibrosis, which can have a poor outcome and high mortality. Liver cirrhosis is a significant cause of global health burden, with more than one million deaths in 2010.⁽²⁾ and have been projected to increase to make it the 12th cause of death in 2020.⁽³⁾ The most common causes of hepatic fibrosis globally are hepatitis B virus (HBV), hepatitis C virus (HCV), and alcohol. Other causes include immune-mediated liver injury, cholestatic diseases, hepatotoxic drugs, genetic abnormalities, and nonalcoholic steatohepatitis. Hepatic fibrosis and cirrhosis are defined by morphology and the pattern and extent of the morphologic changes depending on the cause and stage of fibrosis.^(1, 4)

Hepatic stellate cells (HSCs) are the major fibrogenic cells and their activation is the dominant event in hepatic fibrogenesis. Activation of HSCs refers to the conversion of quiescent, vitamin A-storing cells into proliferative, fibrogenic, and contractile myofibroblasts which are the main source of production of extracellular matrix such as synthesizing and secreting large amounts of fibril-forming collagens, particularly collagen type I and III.⁽⁵⁾ The activation of HSCs is a complex but tightly programmed response to liver injury. The earliest changes in HSCs reflect paracrine stimulation by all neighboring cells, including Kupffer cells (KCs), hepatocytes, and leukocytes, while autocrine cytokines (including transforming growth factor β (TGF- β) and connective tissue growth factor (CTGF)) play vital roles in regulating and

maintaining their activation. Moreover, damaged hepatocytes release cytokines (TGF- β , tumor necrosis factor α (TNF- α), epidermal growth factor (EGF) and insulin-like growth factor (IGF)) responsible for the activation of KCs and the recruitment of activated T-cells. Activated KCs, T-cells and damaged hepatocytes also release the proinflammatory cytokines (TNF- α , interferon γ (INF- γ), IL-6), free radicals, and growth factors (platelet-derived growth factor (PDGF), CTGF) which further promote HSCs activation and proliferation.^(1, 6, 7) Furthermore, it has known that TGF- β 1, a cytokine, plays an important role in pathogenesis of fibrosis. TGF- β 1 stimulates HSCs activation. The activated HSCs are characterized by loss of lipid and vitamin A storage but highly expression of alpha-smooth muscle actin (α -SMA). These cells also produce excessive amounts of collagen, glycoproteins and ECM.⁽⁸⁾ Malondialdehyde (MDA) is one of the final products of polyunsaturated fatty acids peroxidation in the cells. An increase in free radicals causes overproduction of MDA. MDA level is commonly known as a marker of oxidative stress, leading to KCs activation.⁽⁹⁾

Toxins and drugs are among the basic etiopathogenetic agents of liver diseases. The most common toxic substance used to mediate liver fibrosis in experimental animals is thioacetamide (TAA).⁽¹⁰⁻¹³⁾ TAA is a hepatotoxin frequently used for experimental purposes to induce hepatic inflammation and fibrogenesis.⁽¹⁴⁾ TAA triggers hepatic fibrosis through an increase of severe oxidative stress followed by an activation of HSCs.^(12, 15)

According to the Food and Agriculture Organization (FAO) of the United Nations and the World Health Organization (WHO), probiotics are live microorganisms that confer a health benefit to the host when administered in adequate amounts.⁽¹⁶⁾ Commonly used bacterial probiotics include *Lactobacillus* species, *Bifidobacterium* species, *Streptococcus* species, *Escherichia coli*, *Lactococcus lactis* and some *Enterococcus* species.^(17, 18) *Lactobacillus*, a major part of the lactic acid bacteria (LAB) is a genus of gram-positive facultative anaerobic, rod-shaped, non-sporulating, non-motile, and non-catalase producing bacteria. The general mechanisms underlying the health promotion of probiotics include enhancement of the epithelial barrier, increased

adhesion to intestinal mucosa, inhibition of pathogen adhesion, competitive exclusion of pathogenic microorganisms, production of anti-microorganism substances and modulation of the immune system.⁽¹⁹⁾

Interestingly, probiotics are proven to have the beneficial effects such as control of the flora bacteria quantity, decreases in compounds derived from bacteria, and lowers proinflammatory production such as TNF- α , IL-6, and IFN- γ via down-regulation of the nuclear factor kappa B (NF- κ B) in the liver diseases.⁽²⁰⁾ In an experimental rat model of liver fibrosis, *Saccharomyces cerevisiae* can suppress hepatic inflammation, steatosis, and necrosis.⁽²¹⁾ Moreover, the probiotics (*L. acidophilus* and *S. cerevisiae*) combined with selenium can protect the liver fibrosis by suppressing hepatic inflammation, attenuating hepatic oxidative stress, and inducing apoptosis of hepatic stellate cells.⁽²²⁾ Antioxidants alone or in combination with *L. johnsonii* La1 can be useful in preventing bacterial translocation in cirrhosis.⁽²³⁾ A combination of three types of live probiotic bacteria, *L. acidophilus*, *L. plantarum*, and *S. thermophilus* are protect the liver by reducing liver enzymes and level of morphological changes and necrosis.⁽²⁴⁾

Furthermore, Ladda B and her coworkers isolated probiotic strains which were screened for immune modulating effects on TNF- α production from Thai healthy infant feces in THP-1 human monocytic cell lines. They found that the Isolates *L. paracasei* MSMC 39-1, *L. casei* MSMC 39-3, and *W. confusa* MSMC 57-1, showed the strongest inhibitory effect on TNF- α production.⁽²⁵⁾ It is, therefore, probable that probiotics (*L. paracasei*, *L. casei*, and *W. confusa*) may be the useful hepatoprotective agents and should be used for prevention and treatment of hepatic disorders.

This study aims to determine whether probiotics lactic acid bacteria (*L. paracasei*, *L. casei*, and *W. confusa*) can prevent TAA-induced liver fibrosis in the rats. Six main investigations are as following.

1. Gross structure of the liver

To investigate the changes of external morphology of the liver.

2. Liver enzymes

To investigate liver functions by measuring the levels of liver enzymes including alanine aminotransferase (ALT), alkaline phosphatase (ALP), and aspartate aminotransferase (AST)

3. Histomorphology of the liver

To investigate the general histomorphological changes in liver tissue by hematoxylin and eosin staining.

To investigate the distribution of collagen fibers in the liver by sirius red staining.

4. Lipid peroxidation

To examine the changes of lipid peroxidation by measuring malondialdehyde (MDA) level by thiobarbituric acid (TBA) method.

5. Protein markers

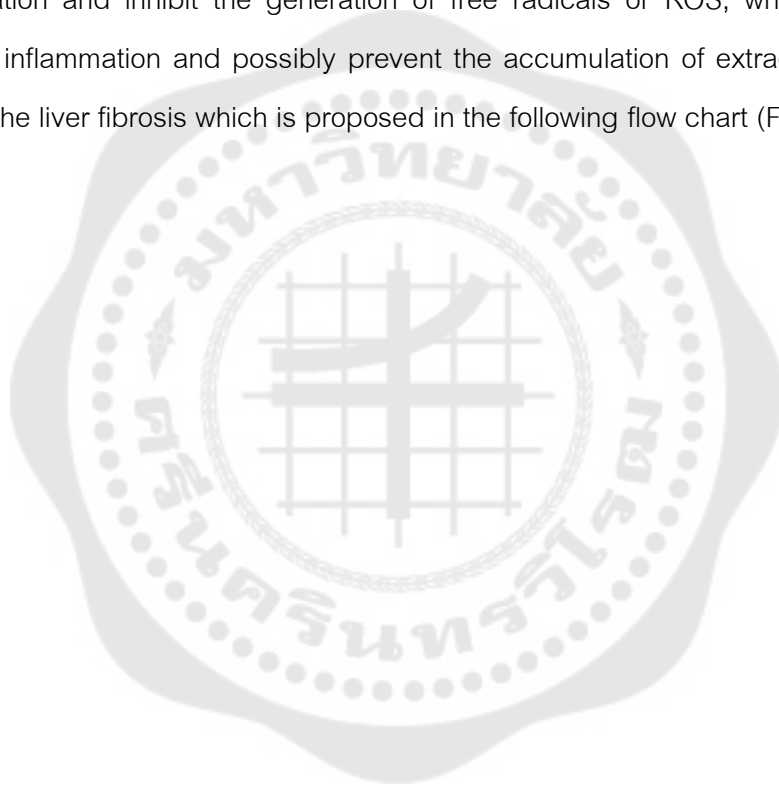
To investigate the changes and expression of transforming growth factor-beta 1 (TGF- β 1), alpha-smooth muscle actin (α -SMA), and tumor necrosis factor alpha (TNF- α) by immunohistochemical technique and Western blot analysis.

6. Gene expression

To investigate the expression of transforming growth factor-beta 1 (TGF- β 1), alpha-smooth muscle actin (α -SMA), and tumor necrosis factor alpha (TNF- α) by real-time PCR.

Hypothesis

Thioacetamide could induce liver fibrosis in rats by stimulation of an increase oxidative stress or reactive oxygen species (ROS) and lipid peroxidation detected by overproduction of MDA. The damaged hepatocytes release inflammatory cytokines TNF- α and TGF- β 1 which activates HSCs to express more proteins markers including of α -SMA. Then, the liver contains an excessive accumulation of extracellular matrix proteins. It might be that probiotics (*L. paracasei*, *L. casei*, and *W. confusa*) suppress inflammation and inhibit the generation of free radicals or ROS, which in turn could alleviate inflammation and possibly prevent the accumulation of extracellular matrix, or scar on the liver fibrosis which is proposed in the following flow chart (Figure 1):



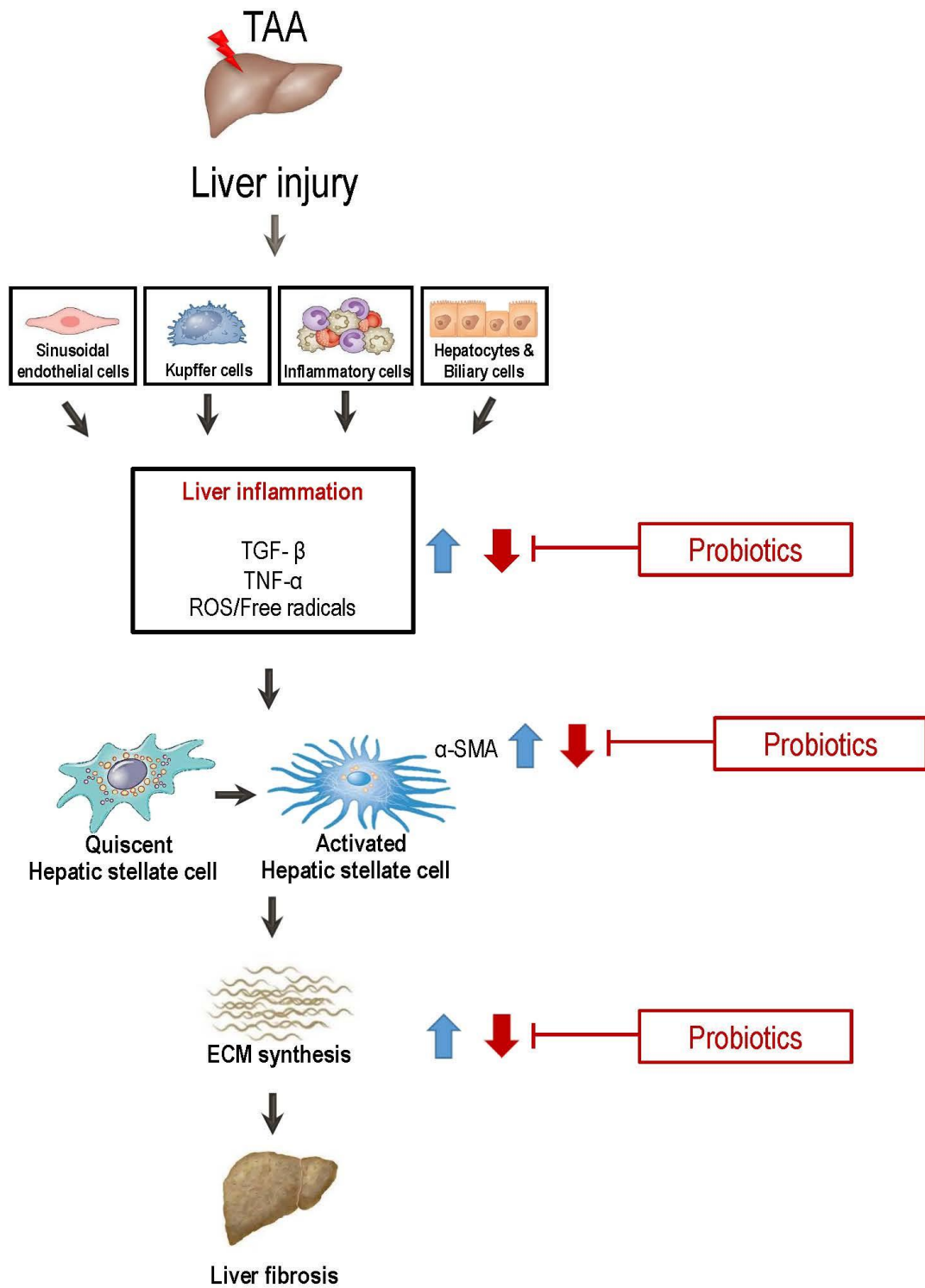


Figure 1 Conceptual framework

CHAPTER 2

REVIEW OF THE LITERATURE

1. Definition of probiotics

The term “probiotics” is derived from the Greek word which means “for life”.⁽²⁶⁾ This word was first used to describe substances which is produced by one microorganism that stimulate the growth another microorganism. The first definition of probiotics given by Fuller is “a live microbial feed supplement which beneficially affects the host animal by improving its intestinal microbial balance”.⁽²⁷⁾ According to Salminen, a probiotic is “a live microbial culture or cultured dairy product which beneficially influences the health and nutrition of the host”.⁽²⁸⁾ Schaafsma also defined “oral probiotics as living microorganisms which upon ingestion in certain numbers, exert health effects beyond inherent basic nutrition”.⁽²⁸⁾ Similarly the Food and Agriculture Organization (FAO) and World Health Organization (WHO) in 2002 defined probiotics as “live microorganisms which, when administered in adequate amount, confer a health benefit on the host”.⁽¹⁶⁾

Commonly used bacterial probiotics include *Lactobacillus* species (Figure 2), *Bifidobacterium* species, *Streptococcus* species, *Escherichia coli*, *Lactococcus lactis* and some *Enterococcus* species. Currently, the only probiotic yeast used is the nonpathogenic *Saccharomyces boulardii* (Table 1).^(17, 18)

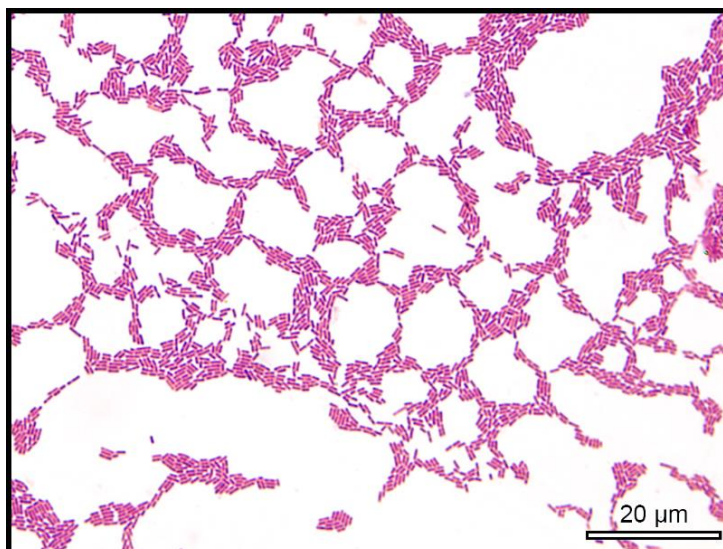


Figure 2 Light micrograph of Gram-stained *Lactobacillus*

Table 1 Microorganisms considered as probiotics

<i>Lactobacillus</i> species	<i>Bifidobacterium</i> species	Others
<i>L. acidophilus</i>	<i>B. bifidum</i>	<i>Bacillus cereus</i>
<i>L. casei</i>	<i>B. longum</i>	<i>Escherichia coli</i> Nissle
<i>L. paracasei</i>	<i>B. breve</i>	<i>Saccharomyces cerevisiae</i>
<i>L. reuteri</i>	<i>B. infantis</i>	<i>Enterococcus faecalis</i>
<i>L. rhamnosus</i>	<i>B. lactis</i>	<i>Streptococcus thermophilus</i>
<i>L. bulgaricus</i>	<i>B. adolescentis</i>	<i>Streptococcus salivarius</i>
<i>L. plantarum</i>	<i>B. animalis</i>	<i>Enterococcus durans</i>
<i>L. johnsonii</i>		
<i>L. lactis</i>		
<i>L. brevis</i>		
<i>L. fermentum</i>		
<i>L. helveticus</i>		
<i>L. kefirgranum</i>		
<i>L. kefiri</i>		

Table 1 Microorganisms considered as probiotics (Continued)

<i>Lactobacillus species</i>	<i>Bifidobacterium species</i>	<i>Others</i>
<i>L. delbrueckii</i>		
<i>L. crispatus</i>		
<i>L. amylovorus</i>		
<i>L. salivarius</i>		

2. Properties of probiotic strains

Selection of potential probiotics is most important are summarized in Table 2.⁽²⁹⁻

³¹⁾ The most suitable strains probiotic should be from human origin. This is because some health-promoting benefits may be species specific. Also, microorganisms may perform optimally in the species from which they were isolated.⁽³²⁾ The microorganisms used in probiotics preparation should be generally recognized as safe (GRAS) status. They could tolerate to gastric acidity and bile salt condition, able to produce the antimicrobial substance, and modulate immune response.⁽³⁰⁾ The probiotic microorganisms should be technologically suitable for incorporation into the food industry and commercial products.⁽³³⁾

Table 2 Criteria of ideal probiotic strains

Desirable Characteristics of an Ideal Probiotic Microorganism
Human origin
Generally recognized as safe (GRAS) status
Resistance to gastric acidity and bile salt
Adherence to gut epithelium
Production of antimicrobial substances
Ability to colonize the gastrointestinal tract
Ability to modulate immunity
Amenable to large scale fermentation and commercial production

3. Mechanisms of action of probiotics

Major mechanisms of probiotics action include enhances intestinal epithelial barrier function, promote mucus secretion, increased adhesion to the intestinal mucosa, and concomitant inhibition of pathogen adhesion, competitive exclusion of pathogenic microorganisms, inhibit the growth of pathogenic bacteria via production of anti-microbial substances, and modulation of the immune system. In the modulation of the immune system, probiotic bacteria interact with dendritic cells (DCs) which signal to trigger a variety of effector cell types, including T helper 1 (Th_1), Th_2 , and Th_{17} as well as regulatory T cells and B cells depending on the local cytokine/chemokine microenvironment (Figure 3).⁽¹⁹⁾ The followings are the major mechanisms of action of probiotics on the host.^(19, 34, 35)

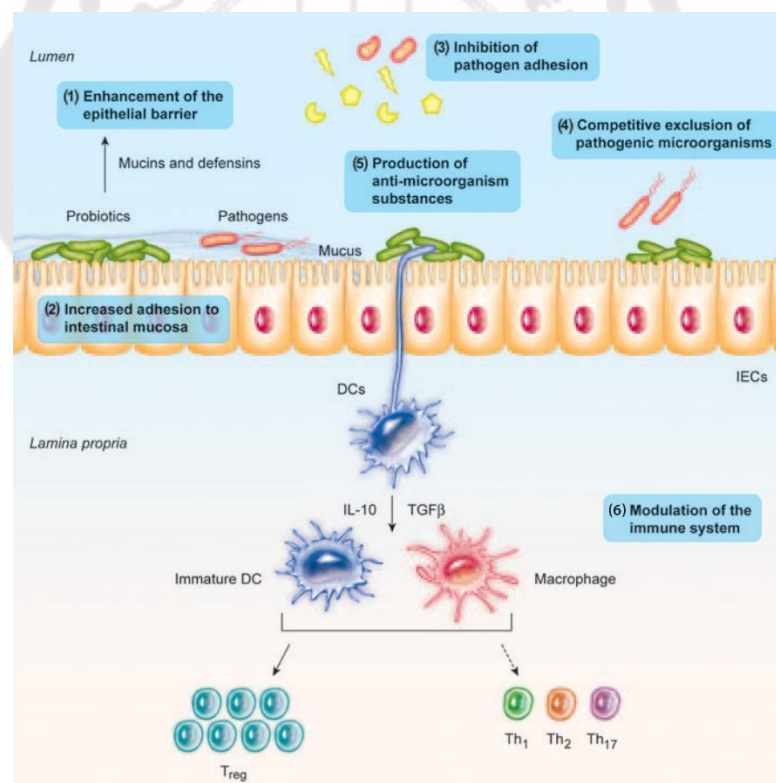


Figure 3 Major mechanisms of action of probiotics

IECs, intestinal epithelial cells; DCs, dendritic cells

Source: Bermudez-Brito M. (2012). Probiotic mechanisms of action.

3.1 Enhancement of the epithelial barrier: maintain barrier function

The intestinal barrier is a major defense mechanism used to maintain epithelial integrity and to protect the organism from the environment. Defenses of the intestinal barrier consist of the mucous layer, antimicrobial peptides, secretory IgA and the epithelial junction adhesion complex. When dysfunction of the barrier occurs, pathogenic bacteria can pass from mucosal to submucosal layer, which induce inflammatory responses.⁽³⁶⁾

Several studies have claimed that enhancing the expression of genes involved in tight junction signaling is a possible mechanism to reinforce intestinal barrier integrity.⁽³⁷⁾ In 2012, Hummel and coworkers found that lactobacilli can modulate the regulation of several genes encoding adherence junction proteins, such as E-cadherin and β -catenin, in T84 cell barrier model. Moreover, incubation of intestinal cells with lactobacilli differentially influences the phosphorylation of adherence junction proteins and the abundance of protein kinase isoforms, such as PKC, thereby positively modulating epithelial barrier function.⁽³⁸⁾ In 1999, Mack DR and coworkers investigated the *L. plantarum* (strain 2 9 9 v), have the capacity to enhance the production and secretion of mucins (MUC2 and MUC3) from human intestinal (HT2) epithelial cells. Probiotics, may promote mucus secretion as mechanism to maintain epithelial barrier integrity which resists to injurious agents, including enteric pathogens, by reducing breaks in the mucosal barrier.⁽³⁹⁾

3.2 Increased adhesion to intestinal mucosa

Adhesion of probiotics to intestinal mucosa is an important for colonization or immunomodulation and interaction between probiotic strains and the host.⁽⁴⁰⁾ Lactic acid bacteria (LABs) display various surface determinants that are involved in their interaction with intestinal epithelial cells (IECs) and mucus. IECs secrete mucin, which is a complex glycoprotein mixture that is the principal component of mucus, thereby preventing the adhesion of pathogenic bacteria.⁽⁴¹⁾ This specific interaction has indicated a possible association between the surface proteins of probiotic bacteria and the competitive exclusion of pathogens from the mucus. As mentioned above, several *Lactobacillus* proteins have been shown to promote attachment between mucus and

bacteria surface adhesins.⁽⁴²⁾ From clinical research, VSL#3 probiotic formula and/or its secreted components can augment the protective mucus layer *in vivo* and *in vitro*. VSL#3 probiotic increases the synthesis of cell surface mucins and to modulate mucin gene expression in a manner dependent on the adhesion of bacterial cells to the intestinal epithelium.⁽⁴³⁾

3.3 Colonization resistance: competitive exclusion of pathogenic microorganisms

Probiotic bacteria compete with invading pathogens for binding sites to epithelial cells and the overlying mucus layer in a strain-specific manner. Probiotics interact with epithelial lining cells of GI tract to prevent the binding and downstream effects of enteric pathogens. For example, the surface layer proteins purified from *L. helveticus* R0052 inhibits enterohemorrhagic *Escherichia coli* O157:H7 adherence and able to bind nonspecifically to host cell surfaces, including the apical microvillus membrane of epithelial cells.⁽⁴⁴⁾ In 2008, Wu and coworkers showed that *S. boulardii* secretes a heat-labile factor which in turn decreases bacterial *Citrobacter rodentium* adherence *in vivo*.⁽⁴⁵⁾

3.4 Production of antimicrobial substances

Probiotics can either induce host cells to produce peptides or directly release peptides to prevent pathogen invasion. Probiotics have been shown to suppress pathogen growth through the release of a variety of antimicrobial factors like defensins, bacteriocins, hydrogen peroxide, nitric oxide, and short chain fatty acids (SCFA), such as lactic and acetic acids, which reduce the pH of the GI lumen.⁽⁴⁶⁾ SCFA can disrupt the outer membranes of gram-negative pathogens causing inhibition of pathogen growth.⁽⁴⁷⁾ Defensins (hBD protein) and cathelicidins are the antimicrobial peptides expressed constitutively by the intestinal epithelial cells and display antimicrobial activity against a wide variety of bacteria, fungi and some viruses.⁽⁴⁸⁾ Microcins (produced by gram negative bacteria), on the other hand, can target the inner membrane bind essential enzymes or interact with the inner membrane to form a bacterial killing structure.⁽⁴⁹⁾ Bacteriocins can either permeabilize the inner membrane of gram-negative bacteria, leading to disruption and formation of pores.⁽⁵⁰⁾ Bacteriocin production may

enable the establishment and increase the prevalence of producing strains as well as enable the direct inhibition of pathogen growth within the gastrointestinal tract. Recently, the ability to modulate the fatty acid composition of the liver and adipose tissue of the host upon oral administration of conjugated linoleic acid (CLA) producing *bifidobacteria* and *lactobacilli* has been demonstrated in a murine model.⁽⁵¹⁾

3.5 Immune modulation

Some probiotic strains have the ability to promote the differentiation of B lymphocytes into plasma cells and increase the production of secretory immunoglobulin A.⁽⁵²⁾ Some bacteria are able to interact with epithelial and dendritic cells (DCs) and with monocytes/macrophages and lymphocytes. The immune system can be divided into the innate and adaptive systems. The innate immune system responds to common structures called pathogen-associated molecular patterns (PAMPs) shared by the vast majority of pathogens. In contrast, the adaptive immune response depends on B and T lymphocytes, which are specific for particular antigens.⁽⁵³⁾ Probiotics can also prevent activation of the proinflammatory nuclear transcription factor, nuclear factor kappa B (NF- κ B).⁽⁵⁴⁾ In 2005, Di Giacinto and coworkers studied the effect of probiotics (VSL#3) on immunoregulatory response in mice model. It has shown that probiotics (VSL#3) reduces the severity of intestinal inflammation, which is associated with the presence of regulatory T cells expressing TGF- β .⁽⁵⁵⁾ In 2006, Tien and coworkers demonstrated that *L.casei* attenuates the pro-inflammatory signaling induced by *Shigella flexneri* after invasion of the epithelial lining. This is because *L. casei* down-regulates the transcription of a number of genes encoding pro-inflammatory effectors such as cytokines, chemokines, and adherence molecules. This results in an anti-inflammatory effect which is presumably mediated by the inhibition of the NF- κ B pathway, particularly through stabilization of I- κ B α .⁽⁵⁶⁾

4. Probiotics in liver diseases

The liver and the gastrointestinal tract are informally associated, and there is bidirectional communication between these organs through the bile, inflammatory mediators, hormones, and products of digestion and absorption.⁽⁵⁷⁾ Receiving approximately 70% of its blood supply from the portal vein which is the direct venous outflow of the intestine, the liver is continually exposed to gut-derived factors including bacteria and bacterial components. The liver contains a large number of resident immune cells including Kupffer cells, natural killer cells, lymphocytes, dendritic cells, and B cells. Together, these immune cell populations in conjunction with endothelial cells and HSCs organized response to these potentially highly inflammatory factors. However, when normal liver physiology is disrupted and inflammatory cells are activated, gut-derived factors likely exacerbate certain liver diseases leading to enhanced tissue damage and propagation of inflammation.^(58, 59)

The close interaction of the gastrointestinal tract and the liver and the fact that the nutrients absorbed by the gut first reach the liver have fostered use of the term gut-liver axis.⁽⁶⁰⁾ The mechanisms of gut-liver interaction in these diseases (Figure 4)⁽²⁰⁾ include alterations in composition of gut microbiota, small intestine bacterial overgrowth, increase in permeability of small bowel, and alterations in mucosal and systemic immunity. Relationship of gut flora with liver disease may be influenced by several other factors, such as diet, toxin exposure, environmental factors, and probably genetic predisposition of an individual.^(20, 61-63)

In the absence of probiotic, liver fibrotic/cirrhotic patients have increased number and an altered composition of bacteria in their gut lead to increased intestinal permeability and bacterial translocation (BT), caused in part by portal hypertension and vascular congestion.^(64, 65) In an experimental mouse model of liver fibrosis, expression of profibrogenic genes (including transforming growth factor- β , matrix metalloproteinase-2, procollagen α -1, and tissue inhibitor of metalloproteinase-1), serum levels of proinflammatory cytokines (TNF- α and IL-6) and bacterial translocation showed progressive increase with increasing fibrosis.⁽⁶⁶⁾

When induction of anaerobes and gram positive bacteria growth, limiting gram negative bacteria, and preventing pathogens adherents are other antitranslocation effects of the probiotics. Probiotics can lead to decreased endotoxins and other toxic compounds derived from bacteria such as ethanol, phenol, which cause injury to the liver. Decreased levels of these substances in the liver result in lowering of proinflammatory production such as TNF- α , IL-6, and IFN- γ via down-regulation of the NF- κ B.

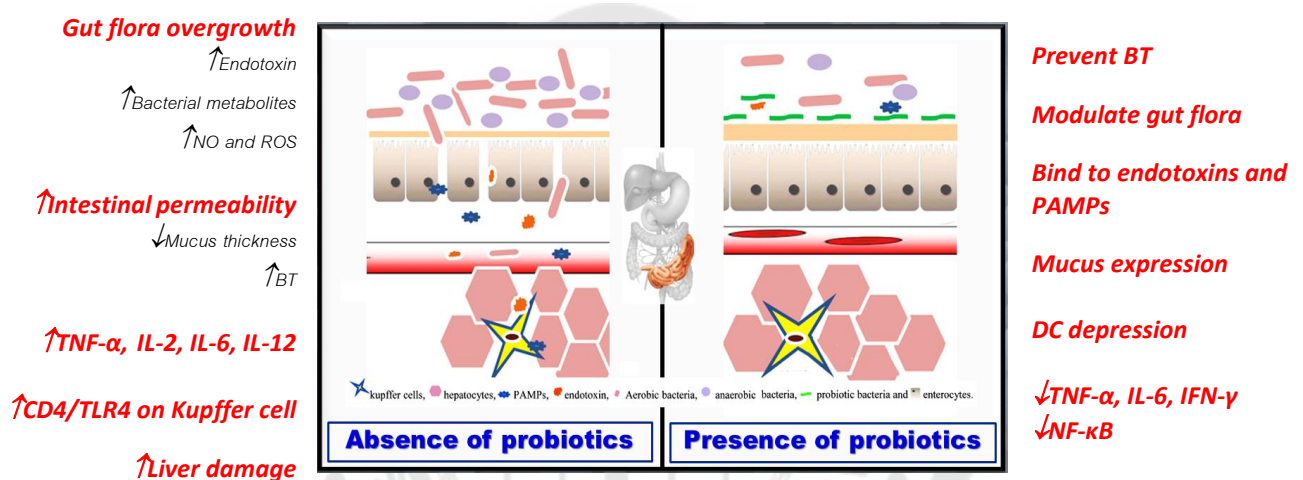


Figure 4 Diagram illustrates the mechanisms involved in liver diseases and probiotic influences on them

Source: Imani Fooladi AA. (2013). Probiotic as a novel treatment strategy against liver disease.

Thus, understanding the mechanisms both of control and of activation by gut-derived factors as well as the functionality of the gut barrier are critical to the development of new therapeutic modalities to treat or prevent acute and chronic liver diseases such as viral hepatitis, alcoholic liver disease, and/or liver cancer.

5. The liver

The liver is the largest mass of glandular tissue in the body and the largest internal organ, weighing about 1,500 g. in the adult. The liver is communication between the digestive system and the blood. The major blood supply from the hepatic portal vein (70-80%) and hepatic artery (20-30%), which carries the absorption of nutrients from the digestive system to the liver, which takes up and stores nutrients and vitamins. The liver is essential for protein, carbohydrate, and fat metabolisms. It also serves as an excretory organ for, cholesterol, bile pigments, various drugs and toxins while also performing important endocrine functions.^(67, 68)

5.1 The human liver

The liver is pyramidal or triangular-shaped organ and a reddish-brown (Figure 5) which lies in the right hypochondriac and epigastric region of the abdominal cavity. The most common of the liver's mass is established on the right side of the abdominal cavity. The anterosuperior surface (diaphragmatic surface) of the liver is smooth and dome shape, which is covered with visceral peritoneum, except the bare area of the liver, where it directly contacts with the diaphragm. The posteroinferior surface (visceral surface) of the liver is also covered with peritoneum, except at the gallbladder fossa and area of porta hepatis. The liver is very soft, reddish-brown tissues covered by Glisson's capsule. This capsule is covered and supported by the peritoneum of the abdomen, which protects and holds the liver within the abdominal cavity. The peritoneum attaches the liver at four areas as the left and right triangular ligaments, coronary ligament, and falciform ligament. The coronary ligament of the liver is located at the junction between of the falciform and triangular ligaments. It includes of two layers which are disconnected from each other by a space of bare area. The caudate lobe and quadrate lobe are subdivided from the right lobe of the liver.^(69, 70)

5.2 Rat liver

The rat is the most common used experimental model in scientific research because it is easy to handle and low-priced. The rat liver is multilobulated similar to other mammals. The approximately 5% of the total body weight represents the liver mass, weighing about 250 to 300 g, the liver mean weight is 13.6 g and transverse

measurement is about 7.5 to 8.0 cm. The superior to inferior diameter is about 3.8 to 4.2 cm (Figure 6).^(71, 72)

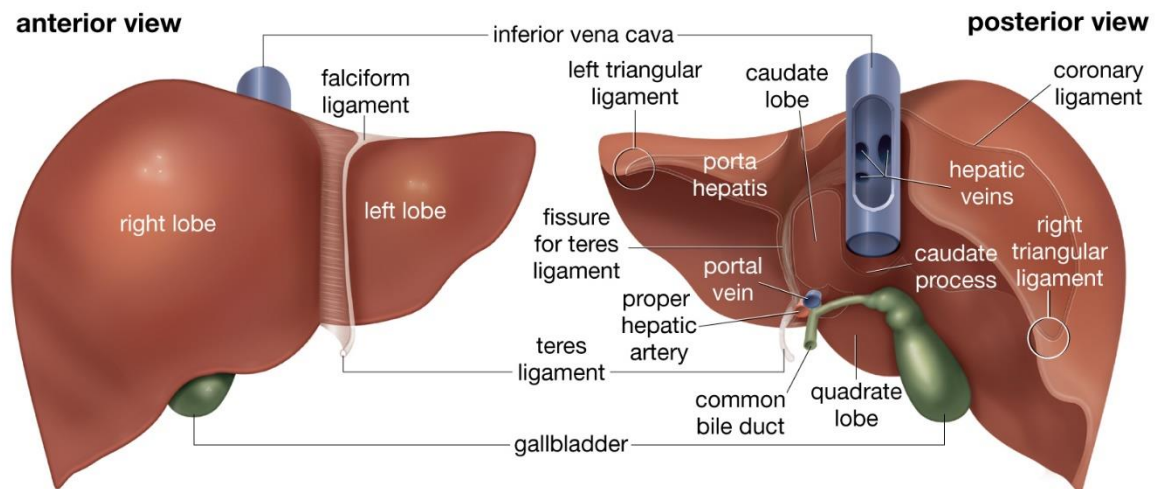


Figure 5 Gross anatomy of the human liver

Anterior view, the liver is divided the right lobe and left lobe by the falciform ligament. Posterior view of the right lobe is subdivided into caudate lobe and quadrate lobe.

Source: <https://www.britannica.com/science/human-digestive-system/Grossanatomy>

5.2.1 Surfaces anatomy of the rat liver

In the decubitus position, the rat liver has basically three surfaces: superior, inferior and posterior. The rat liver is lobated. The superior surface comprises a part of the left lateral and medial lobes, and as a whole, is convex, and fits under the vault of the diaphragm. It is completely covered by the peritoneum, except along the line of attachment of the falciform ligament. The falciform ligament divides the liver into two parts (left and right lobes). The difference from human livers is that the left and right sides of rat liver have approximately equal volume. The inferior surface is uneven, concave and is in relation to the stomach, duodenum. The inferior surface of the rat liver does not have the fossae H-shape fossae as in human. This surface is almost

completely invested by the peritoneum. The posterior surface is not covered by the peritoneum over some part of its extent and is directly contact with the diaphragm.^(72, 73)

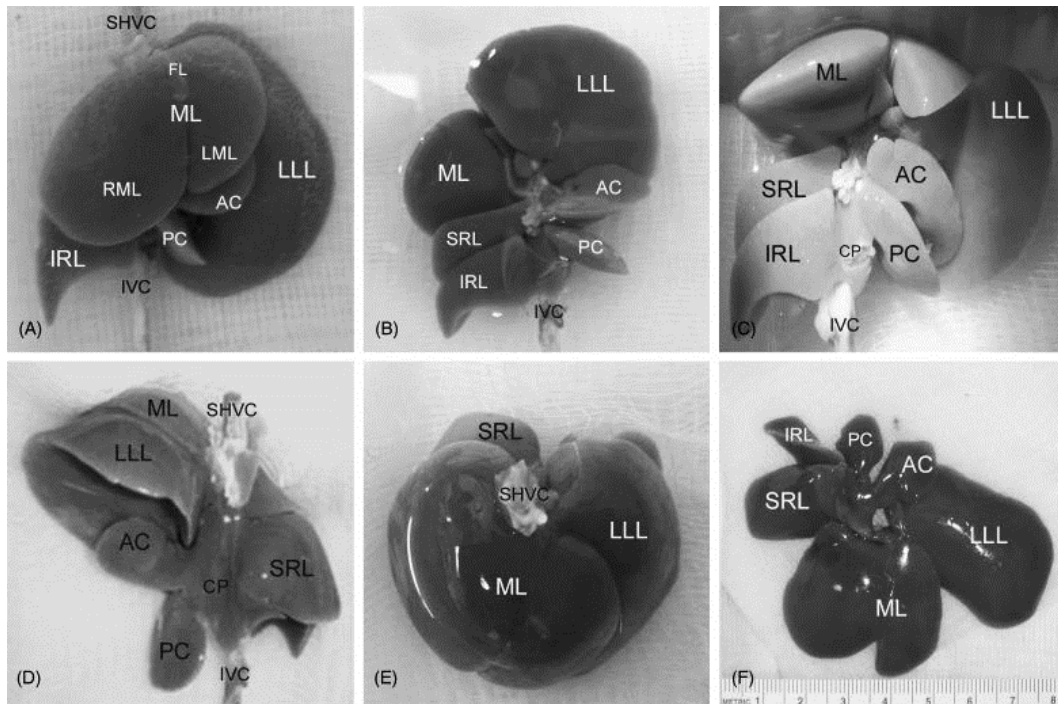


Figure 6 Gross anatomy of the rat liver

(A) Anterior view, (B) Inferior (visceral) view (C) Anterior after separating the lobes, (D) Posterior view, (E) Superior view with the lobes in normal position, (F) Superior view with lobes flattened and separated from each other. CP, Caudate process; AC, Anterior caudate lobe; PC, Posterior caudate lobe; SRL, Superior right lateral lobe; IRL, Inferior right lateral lobe; ML, Median lobe; RML, Right portion of the medial lobe; LML, left portion of the medial lobe; LLL, Left lateral lobe; MF, Median fissure; LF, Left fissure; RF, Right fissure; FL, Falciform ligament; PV, Portal vein and IVC, Inferior vena cava.⁽⁷²⁾

Source: Martins PN. (2007). Surgical anatomy of the liver, hepatic vasculature and bile ducts in the rat.

5.2.2 The rat liver lobes

The rat liver lobes like the human liver lobes, which are named after the portal branches that supply them. The portal system is the most constant anatomical reference (Figure 7).^(72, 74-76)

5.2.2.1 The median lobe is the largest, trapezoidal shape, and calculating for approximately 38% of the liver weight. It is fixed to the diaphragm and anterior abdominal wall by the falciform ligament. It is subdivided by a vertical fissure into a smaller left median lobe and a large right median lobe.

5.2.2.2 The left lateral lobe is flattened, rhomboid shape, and located in the left hypochondriac and epigastric regions over the anterior aspect of the stomach. It comprises about 30% of the liver weight. Its medial portion is covered by the left part of the median lobe. Its upper surface is slightly convex and is molded on the diaphragm.

5.2.2.3 The right lateral lobe is comprises about 22% of the liver weight. It located on the right of the vena cava and posteriorly in the right hypochondrium and is almost completely covered by the median lobe.

5.2.2.4 The caudate lobe is located behind the left lateral lobe and on the left of the vena porta and inferior cava vein. It consists 8–10% of the liver weight. The anterior part of the caudate lobe is located anterior to the esophagus and stomach and its pedicle lies superior, while the posterior is located behind these structures and its pedicle lies inferior. Both are covered by a very thin layer of peritoneum, the hepatogastric and hepatoduodenal ligaments.

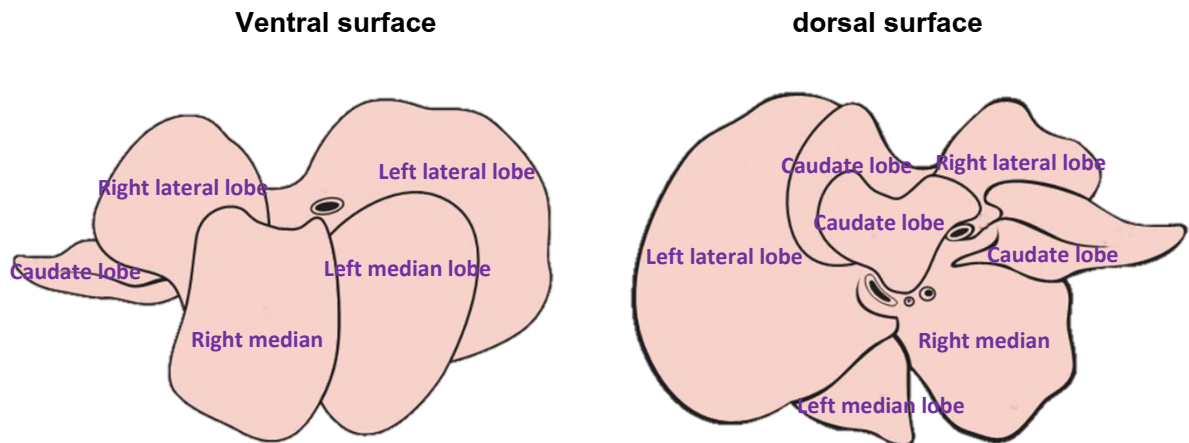


Figure 7 Ventral and dorsal surface of the rat liver showing lobes

5.3 Histology of the Liver

5.3.1 Hepatic functional unites

There are three ways to describe the structure of the liver in term of hepatic functional units: the hepatic lobule (classic lobule), the portal lobule, and the hepatic acinus (Figure 8).⁽⁷⁷⁾ The hepatic functional unites are based on the distribution of the branches of the portal vein and hepatic artery within the liver and the partway of the blood. The liver is a complex three-dimensional structure that consists of epithelial and mesenchymal elements arranged in repetitive microscopic units. Both structural and functional organization allows assessment of the most of liver diseases via a small representative biopsy specimens.^(68, 78, 79)

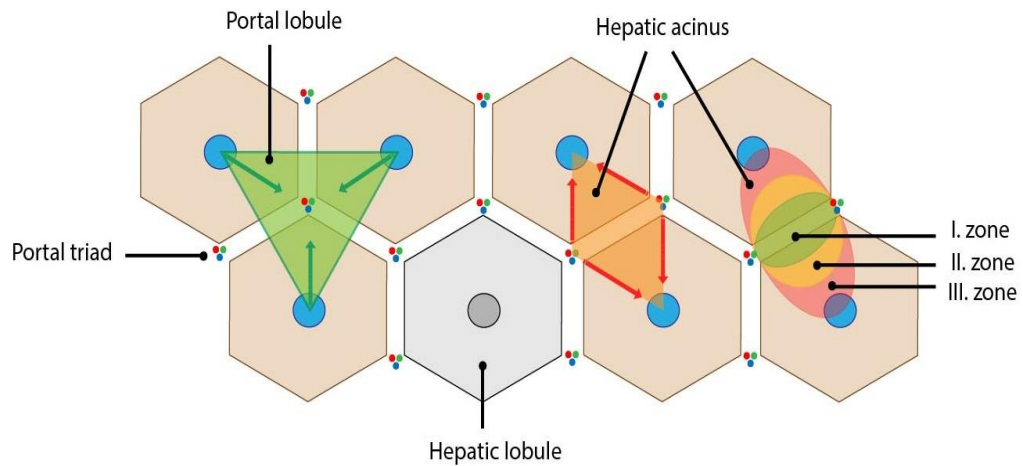
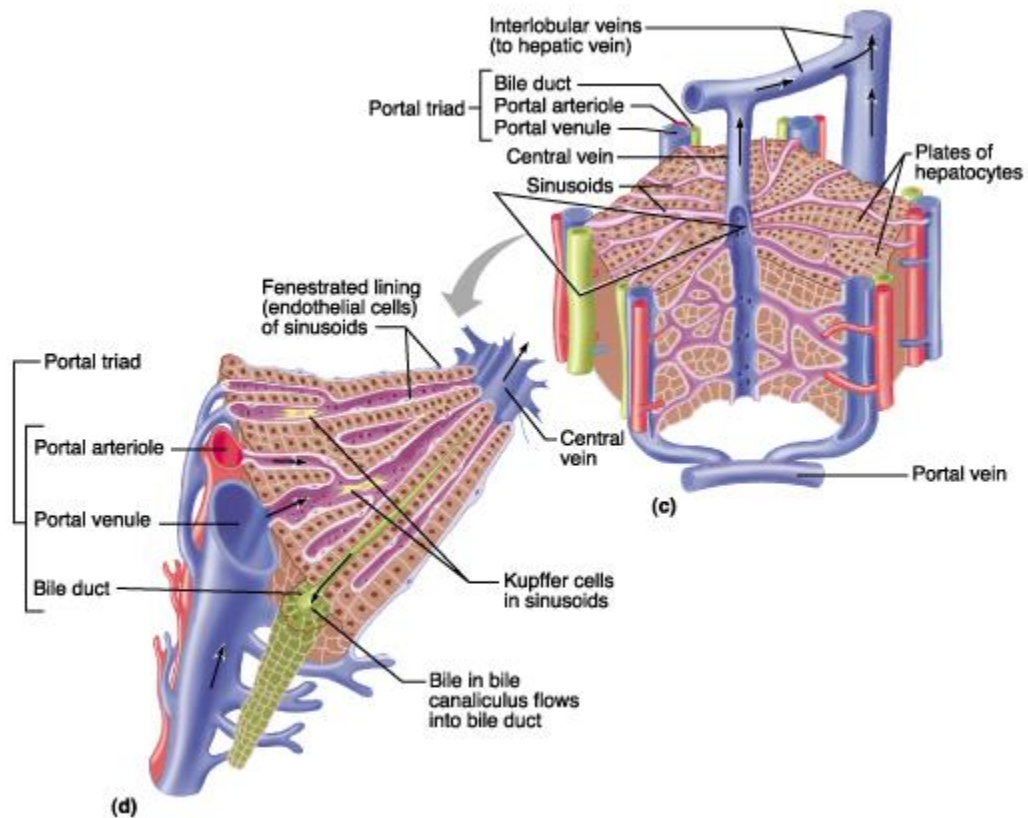


Figure 8 Hepatic functional units-hepatic lobule, portal lobule and hepatic acinus

Source:<http://fb.lt.cz/en/skripta/ix-travici-soustava/5-jatra-a-biotransformacexenobiotik/>

5.3.1.1 Hepatic lobule is a classical unit describing the organization of hepatic parenchyma. It is composed polygonal-shaped parenchyma and bordered by thin layer of collagenous connective tissue. A single vein marks the center of the lobule is the central vein that is a terminal hepatic venule and at the angles of hexagon are the portal triads, consisting of branches of hepatic artery, branches of hepatic portal vein, and bile ductule (Figure 9).⁽⁸⁰⁾ One hepatic lobule contains 3 to 6 portal triads. Pericentral hepatocytes, or hepatocytes enclosing the central veins the site that is contain drug metabolizing enzymes and is also found to be most susceptible to ischemic insults. Periportal hepatocytes, a group of hepatocytes surround the portal vein, are the first to receive blood, the last to undergo necrosis.^(77, 78)



Copyright © 2001 Benjamin Cummings, an imprint of Addison Wesley Longman, Inc.

Figure 9 Diagram showing hepatic lobule

Source: https://www.apsubiology.org/anatomy/2020/2020_Exam_Reviews/Exam_3/CH23_Liver_Anatomy.htm

5.3.1.2 The portal lobule emphasizes the exocrine function of the liver. Thus, triangular shape with a portal area at the center of portal lobule and the three of the central veins locate peripherally at each corner. It contains portions of three classic liver lobules that secrete the bile into one portal canal (Figure 10).⁽⁷⁷⁾ This lobule performs the portion of liver parenchyma that secrete and drain bile into the axial bile duct of portal triad.^(78, 79)

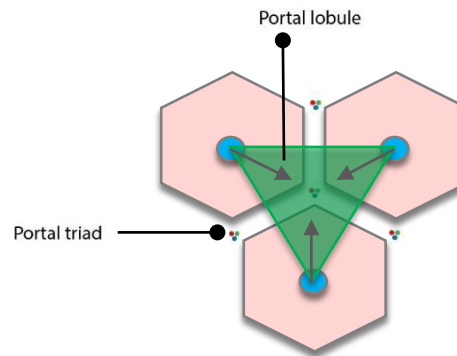


Figure 10 Diagram showing portal lobule

Source: <http://fbt.cz/wp-content/uploads/2013/12/jaterni-acinus-a-portalnilalucek-ENG-01.jpg>

5.3.1.3 Hepatic acinus is an irregular shaped, roughly ellipsoidal structure. The long axis is defined by connecting line between two adjacent central veins and the short axis of acinus is defined by the terminal branches of portal triads. It casually resembles two triangles attached together by their bases with central veins. The hepatic acinus is roughly divided into zones that correspond to distance from the arterial blood supply. It is divided into zone 1, 2, and 3, where in zone 1 (periphery of the classic lobules) locates the portal area and zone 3 (central part of the classic lobules) locates the hepatic venule (Figure 11).⁽⁸⁰⁾ Hepatic acinus is providing the best interaction between vascular perfusion, pathological processes, and metabolic activity in the liver. Because the low blood oxygen and low nutrient gradient from the portal tract flows through these zones to the venule. This classification is also important for explanation of histopathological conditions to selective destruction of hepatocytes.^(78, 79)

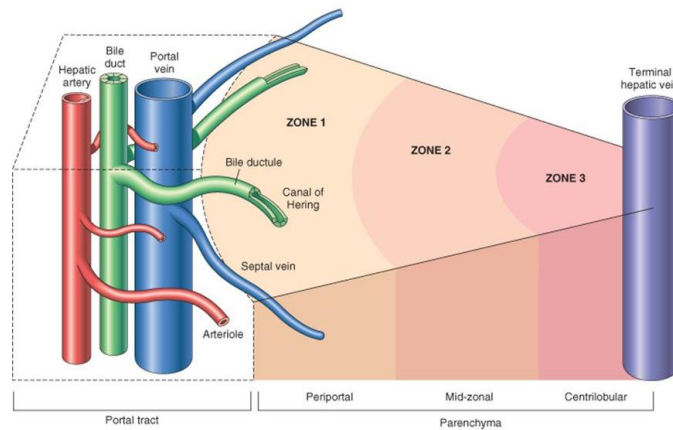


Figure 11 Diagram showing the hepatic acinus

Source: <http://people.upei.ca/eaburto/Liver1/Liver-L1-15.pdf>

5.3.2 Liver cell types

5.3.2.1 Hepatocytes (Liver cells) are epithelial cells that are normally arranged in cords separated by sinusoids. Sinusoidal surfaces of hepatocytes are separated from the sinusoidal vessel by the perisinusoidal space (space of Disse). They are covered by numerous of microvilli, which protrude into the perisinusoidal space to increase the surface area for absorption of substances and exchange from the portal blood. The sinusoidal surface of hepatocytes are the site where the material is transferred between the sinusoids and the hepatocytes. Canalicular surfaces of hepatocytes are across which bile drains from the hepatocytes into the canaliculi that attach to the neighboring hepatocyte with specialized junctions. The intercellular surfaces of hepatocytes are between adjacent hepatocytes that are not in contact with sinusoids or canaliculi. Hepatocytes are large polyhedral shape, 20-40 μm in diameter, and a concentric nucleus. The nucleus is oval or round in shape. Some nucleus are binucleated. Infrequently, nuclei are polyploid. The cytoplasm of the hepatocytes is typically acidophilic, with basophilic area. In addition, the hepatocytes are unusual in that they possess numerous smooth endoplasmic reticulum (SER) and rough endoplasmic reticulum (RER) in the same cells. The SER is associated with steroid metabolism and is also responsible for the processes of methylation, oxidation, and

conjugation required for detoxification of various substances before excretion from the body. The RER is associated with protein synthesis such as: albumin, prothrombin, fibrinogen, and globulin. The major processes in the SER is the conjugation of waterinsoluble toxic bilirubin to form a water-soluble nontoxic bilirubin glucuronide by glucuronyl-transferase. This conjugate is excreted by hepatocytes into the bile. Each liver cells has commonly 2,000 mitochondria. Golgi complexes are also abundant up to 50 per cell. The functions of this organelle include the lysosomal formation and the plasma proteins secretion, glycoproteins, and lipoproteins. Hepatocytes obtain lysosomes which are important in the turnover and degeneration of intracellular organelles. Peroxisomes are numerous which participle in a variety of metabolic reactions, including chemical detoxification and lipid metabolism. Glycogen and lipid droplet are found in varying amounts depend on the function of the cells. The hepatocyte is probably the most versatile cell in the body. It is a cell with both exocrine and endocrine functions. Exocrine secretion contains the production and release of bile. Endocrine secretion contains the production and release of several plasma proteins. (Figure 12).^(78, 79)

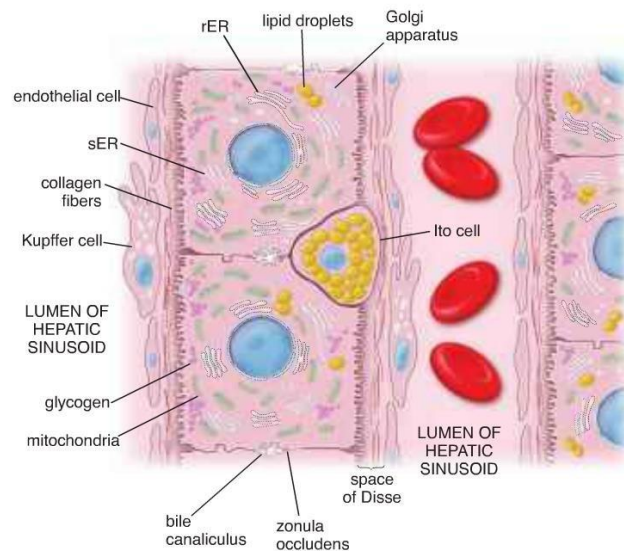


Figure 12 Hepatocyte and its intracellular organelles

Source: https://www.researchgate.net/figure/Cell-diagram-illustrates-a-one-cellthick-plate-of-hepatocytes-that-is-separated-from-the_fig8_270647723

5.3.2.2 Kupffer cells are the macrophage or monocyte derive from bone marrow or local proliferation. Kupffer cells are irregular shape, with cytoplasmic folds that promote their phagocytic function. Kupffer cells locate within the lumen of the hepatic sinusoids. The main of Kupffer cell function is the uptake, processing, and presentation of antigenic material. Kuffer cells are phagocytose the foreign material, cytokines production and defend the tumor cells which is similar to the macrophage function. The paracrine effects that they impact the function of hepatocytes, hepatic stellate cells, and sinusoidal endothelial cells. In the normal liver, they clear approximately 90% of bacteria transported by the sinusoidal blood. Kupffer cells proliferate markedly in acute viral hepatitis. Kupffer cells are closely involved in the liver's response to toxins, ischemia, infection resection, and other stresses. Kupffer cells play a substantial role in immunity and endotoxin-mediated. Kupffer cell activation as well as cytotoxic mechanisms induced by Kupffer cells appear to be major mechanisms in the pathogenesis of various liver diseases. Additionally to their endocytotic and phagocytotic properties, Kupffer cells are affected to exert paracrine effects on liver cells, sinusoidal endothelium, and HSCs by secreting cytokines and growth factors (Figure 13).⁽⁷⁹⁾

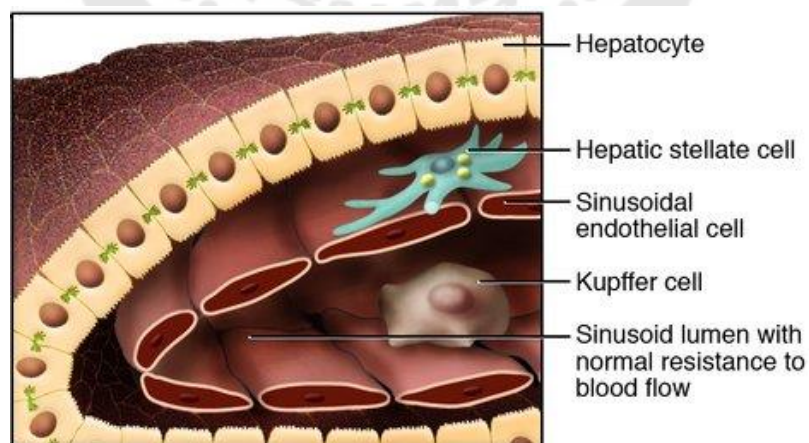


Figure 13 Cross-section of liver showing sinusoidal endothelial cells, hepatic stellate cell, and Kupffer cell

Source: Krishna M. (2013). Microscopic anatomy of the liver.

5.3.2.3 Sinusoidal endothelial cells are the fenestrated endothelium that is the endothelial cells consist of large holes that allow easy exchange between blood hepatocytes and blood through the perisinusoidal space. Endothelium contain numerous pinocytotic vesicle that actively transport substances between portal blood and hepatocytes (Figure 13).^(78, 79)

5.3.2.4 HSCs are called fat storing cells or Ito cells. It is the major cell type in the liver responsible for excess extracellular matrix synthesis during liver fibrosis. Normally, these cells store vitamin A, produce and secrete a hepatic growth factors and matrix components or collagen fibers and therefore act role in liver regeneration and fibrogenesis. Additionally, HSCs have an effect on growth and proliferation of hepatocytes and participate in the inflammatory and immune response in the liver. In every acute and chronic liver injury HSCs are activated. The phenotypical changes is the process of HSCs activation. The cell transforms from a resting, vitamin A storing HSCs, to activated HSC. It is characterize by proliferation, contractility, and fibrogenesis. HSCs increase in size and retinoid loss. Cytoskeletal markers of smooth muscle and fibroblasts are presented. The most strong activation and proliferation takes place in the severe liver injury (Figure 13).^(78, 81)

5.3.2.5 Pit cells are large granular lymphocytes (LGL) or liver-specific natural killer (NK) cells that are the primitive cellular immune host defense mechanism, active against virus-infected cells.⁽⁷⁹⁾

5.3.3 Sinusoids

Sinusoids are the spaces between the hepatic cell cords. They obtain blood and nutrient from the vessels in the portal areas to the central vein. They are irregular in shape and approximately 8-10 μm in diameter. The lining of the hepatic sinusoids consists of a discontinuous layer of fenestrated endothelial cells and also include Kupffer cells (Figure 14).^(6, 79)

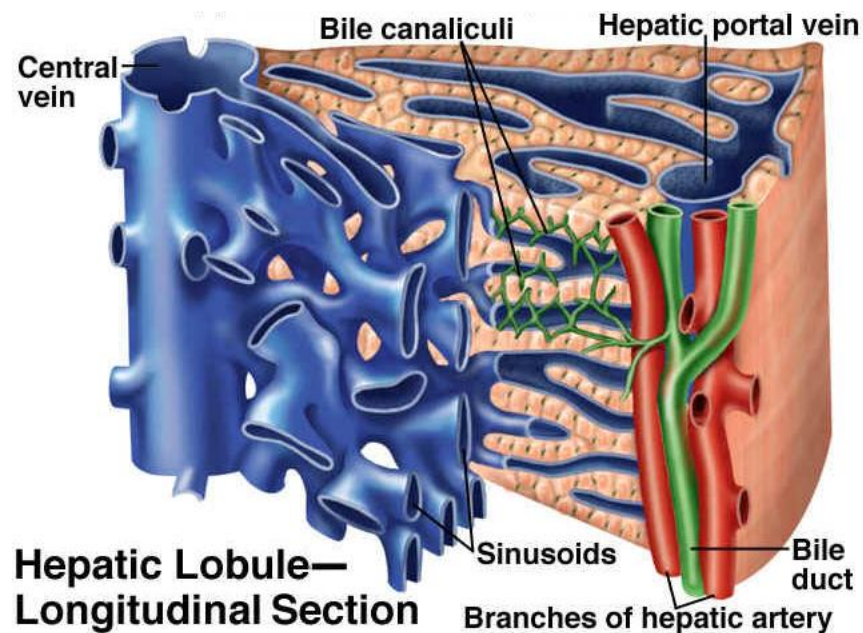


Figure 14 Illustration of hepatic sinusoids

Hepatic sinusoids pass between and through hepatic plates as they carry blood from the hepatic artery and portal vein to the central vein.

Source: Krishna M. (2013). Microscopic anatomy of the liver.

5.3.4 Space of Disse

Space of Disse or perisinusoidal space is located between hepatic cell cords and the hepatic endothelial cells (Figure 15). It contains microvilli of the hepatocytes, plasma, reticular fibers and HSCs. Blood plasma enters this space through openings between the endothelial cells that are too small for blood cells to pass. Blood-borne substances thus directly contact the microvilli of hepatocytes. These cells absorb oxygen and toxins from, nutrients, and release endocrine secretions into, these spaces. Its function is the exchange of material between the bloodstream and hepatocytes, which do not contact directly to the blood stream.^(78, 79)

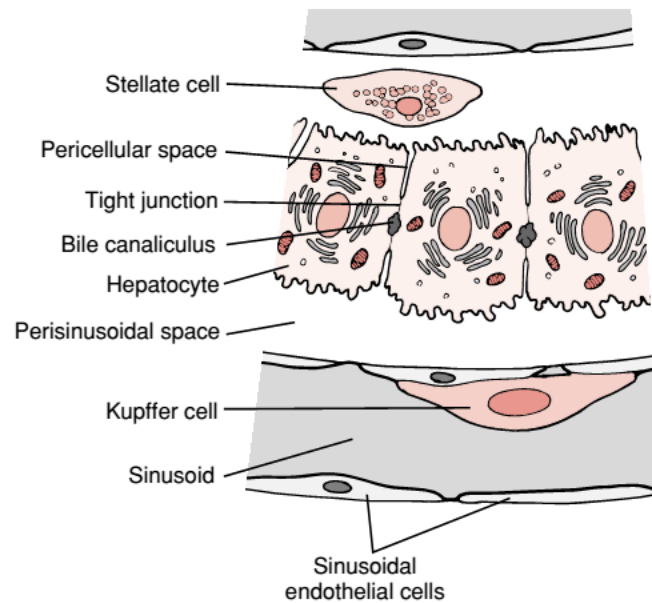


Figure 15 The relationship between hepatocytes

The perisinusoidal space and the sinusoid, the perisinusoidal space is the space between hepatocytes and sinusoids which is separated from the sinusoid by a layer of sinusoidal endothelium. Kupffer cells also line the hepatic sinusoids. A HSCs or Ito cells contains lipid droplets in the cytoplasm could be observed.

Source: Ross MH. (2003). Digestive system III : Liver, Gallbladder, and Pancreas. In Histology: A text and atlas p.628-55.

5.4 Liver function

The liver is responsible for numerous critical functions in the body. It plays a role in sugar and fat metabolism, digestion, and the body's immune defense. About 90% of the body's nutrients pass through the liver from the intestines. The liver convert food into energy, stores nutrients, and produces blood proteins. The liver also acts as a filter to remove harmful substances from the blood. In the developing fetus, blood cells are produced in the liver.^(82, 83)

5.4.1 Digestion

The liver acts an important role in the processing of food and digestion by producing bile, a greenish-yellow fluid digest fats. Bile is delivered to the small

intestine through the bile duct. By-products from the breakdown of drugs and toxic substances processed by the liver are carried in the bile and excreted from the body. A person with a damaged liver may experience impaired bile production and flow. The body may not be able to properly absorb nutrients. Liver cells has functions convert heme into bilirubin. When the liver is damaged, bilirubin may build up in the blood, causing jaundice.⁽⁸³⁾ The nutrients transported in portal blood circulation include, monosaccharides, fatty acids, and amino acids. A small amount of long-chain fatty acids, bound to albumin, is transported by the portal blood the most is transported in intestinal lymph.⁽⁸²⁾

5.4.2 Metabolism

The liver is important in regulating the metabolism of lipids, carbohydrates, and proteins. It likewise keeps up the blood glucose concentration level by converting different substances. The liver carries out many metabolic functions, providing the body with the energy it needs. It regulates the production, storage and release of sugar, fats and cholesterol. When food is eaten, the liver converts glucose into glycogen which is stored for later use. When energy is needed, the liver convert glycogen back into glucose in a process called gluconeogenesis.⁽⁸³⁾ The liver regulates the storage of fats by converting amino acids from digested food into fatty acids when the body does not have enough sugar, the liver converts fatty acids into ketones, which can be used for fuel. The liver also controls the production, metabolism and excretion of cholesterol, which is an important component of cell membranes and hormones.⁽⁸²⁾

5.4.3 Protein synthesis

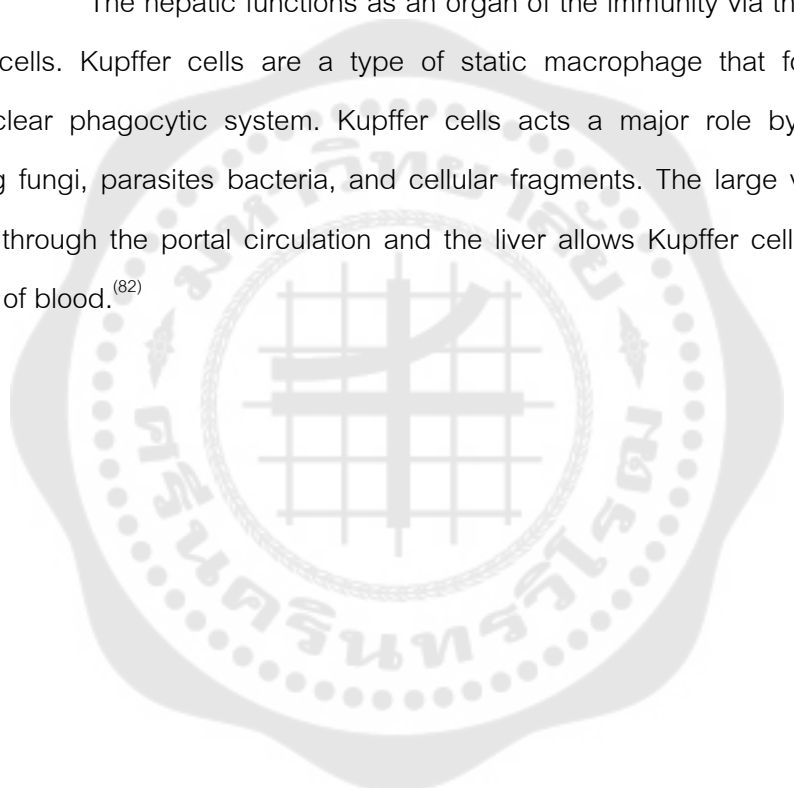
The liver synthesizes many important proteins consisting enzymes, clotting factors, hormones, and immune factors. Liver enzymes including aminotransferases or transaminases separate amino acids from digested food. When liver cells are damaged, these enzymes can leak out and build up to high levels in the blood. Several of the proteins synthesized by the liver are needed for proper blood functioning. These include various binding proteins and albumin. Other proteins synthesized by the liver include gamma-glutamyl transferase (GGT) and alkaline phosphatase (ALP).^(82, 83)

5.4.4 Detoxification

The liver plays an important role in substances detoxification these are harmful to the body such as alcohol, drugs, solvents, pesticides and heavy metals. Toxins are delivered to the liver by the portal vein. When the liver is damaged it may not be able to break down and excrete drugs efficiently, which could potentially lead to seriously high blood levels and severe side effects.⁽⁸³⁾

5.4.5 Immunity

The hepatic functions as an organ of the immunity via the function of the Kupffer cells. Kupffer cells are a type of static macrophage that form part of the mononuclear phagocytic system. Kupffer cells act a major role by capturing and engulfing fungi, parasites bacteria, and cellular fragments. The large volume of blood passing through the portal circulation and the liver allows Kupffer cells to clean large volumes of blood.⁽⁸²⁾



6. Liver fibrosis

Liver fibrosis/Hepatic fibrosis is a scarring response to liver damage, that progressive accumulation of extracellular matrix (ECM) in the liver proteins including three large families of proteins glycoproteins, collagens, and proteoglycans. Collagen occurs in most types of chronic liver diseases. Advanced liver fibrosis results in cirrhosis, liver failure, portal hypertension, and often requires liver transplantation. Cirrhosis is the end-stage of liver fibrosis which is characterized by bridging fibrosis, nodule formation, and altered liver function.⁽⁸⁴⁾

Fibrosis is caused by chronic inflammation arising from viral hepatitis, alcohol, drugs, and metabolic or autoimmune diseases. Progressive fibrosis distorts liver vasculature, architecture, and alters its normal function.^(1, 5)

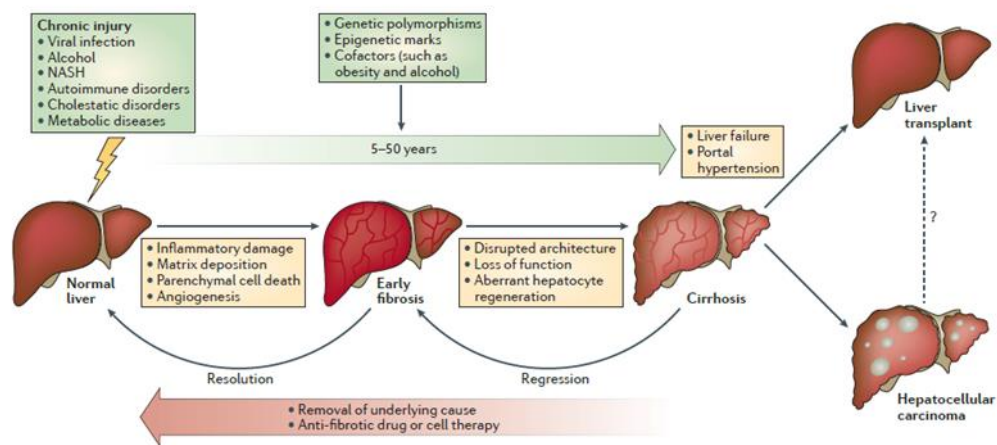


Figure 16 Stage of liver damage

Advanced hepatic fibrosis results in hepatic failure, portal hypertension and cirrhosis. The main causes of hepatic fibrosis are viral infection (hepatitis C and hepatitis B virus), drug or toxin (alcoholic liver disease), metabolic disease (non-alcoholic fatty liver disease: NAFLD), genetic disease (Wilson disease), and autoimmune disease (autoimmune hepatitis). Cirrhosis is the end-stage of hepatic fibrosis which is described by nodule formation, bridging fibrosis, and altered hepatic function (Figure 16).^(1, 84, 85)

Source: Pellicoro A. (2014). Liver fibrosis and repair: immune regulation of wound healing in a solid organ.

6.1 Pathophysiology of hepatic fibrosis

In the acute phase of liver injury and as the hepatic fibrosis progress (Figure 17), the injured hepatocytes secrete reactive oxygen species (ROS) and release proinflammatory cytokines.⁽⁸⁶⁾ TNF- α is mainly made by macrophage, monocyte, HSCs, and KCs. It has proinflammatory activities and cytotoxic effects in these cells, contributing to hepatocyte apoptosis, immune cell activation and HSC activation.⁽⁸⁷⁾ Consequently, oxidative stress takes place and the hepatocytes components entice tissue reactions secreting cytokines or growth factors such as transforming growth factor-beta1 (TGF- β 1). Kupffer cell function acts a considerable role in the pathogenesis induced by hepatotoxic substances.⁽⁸⁸⁾ Kupffer cells are the macrophages locating in the hepatic sinusoids. The HSCs undergoes a complex activation or transformation process where the cell changes from a restful, vitamin A-storing cell to be an activated HSCs, myofibroblast-like cell. HSCs activation include morphological changes such as, a loss in vitamin A storage, the presentation of the cytoskeletal protein such as alpha-smooth muscle actin (α -SMA), and an enhance in the presentation of rough endoplasmic reticulum. Furthermore, the presence of active tissue inhibitors of metalloproteinases (TIMPs) secreted by myofibroblast-like cells. The TIMP family function as important inhibitors of the extracellular activity of metalloproteinases (MMPs) by stabilizing the proenzyme and most essentially by inhibition of the active species. TIMP-1 expression is strongly linked to HSCs activation. In the perisinusoidal space, the activated HSCs improve the collagen accumulation. The overproduction and accumulation of collagens such as type I and IV, procollagen III, and elastin occur early in hepatic injury, and metalloproteinases that are directed at the different types of collagen are activated to degrade the depositions and maintain stability of the matrix. TIMPs are also expressed to regulate the degradation mechanism.⁽⁸⁹⁻⁹¹⁾

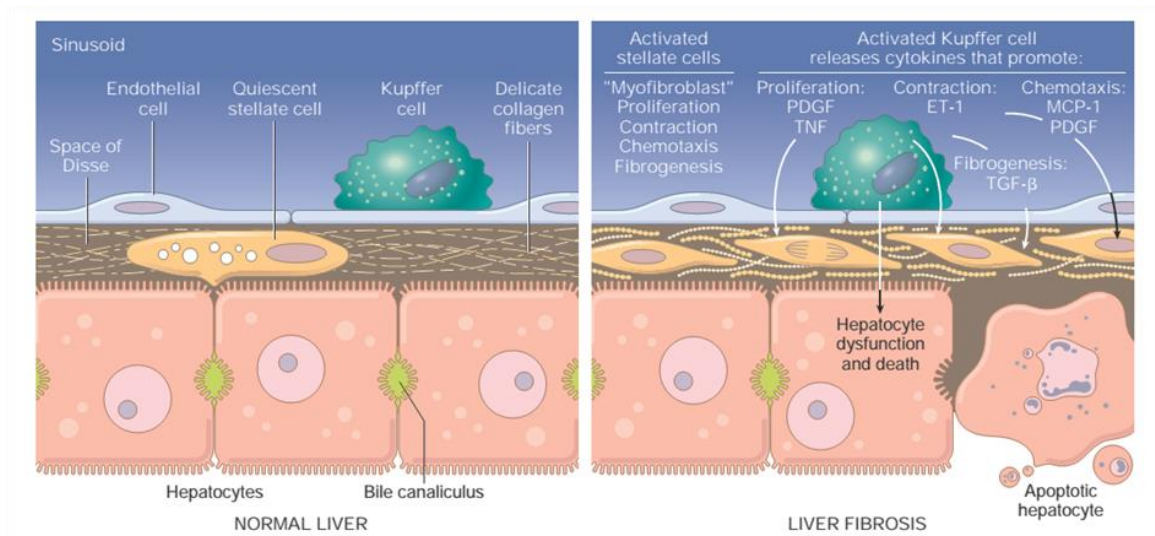


Figure 17 Normal liver to liver fibrosis

Source: Kumar V. (2007). Robbins Basic Pathology.

6.2 Hepatic stellate cells (HSCs) activation

6.2.1 Initiation

In liver injury, oxidative stress-mediated necrosis and $\text{TNF-}\alpha$ is another extremely pro-inflammatory cytokine. Effects of $\text{TNF-}\alpha$ are diverse, providing to hepatocyte apoptosis, immune cell activation and HSC activation. Moreover, liver injury is associated with infiltration of inflammatory cells and Kupffer cells to initiate local inflammation before the arrival of hepatic cells. In addition to oxidative stress, early injury of endothelium can stimulate HSCs activation. In injured liver are generating important mediators, including ($\text{TGF-}\beta 1$) and PDGF (Figure 18).^(92, 93)

6.2.2 Perpetuation

After initiation, activated HSCs undergo a series of phenotypic changes that collectively lead to the ECM accumulation. These include proliferation, contractility, fibrogenesis, matrix degradation, chemotaxis, loss of retinoid, and proinflammatory responses and cytokine release. The following sections detail the mechanisms underlying each of these events (Figure 18).^(92, 93)

6.2.2.1 Proliferation

An increase in the number of HSCs activation occurs after liver injury. PDGF act significant roles in the pathogenesis of hepatic fibrosis. PDGF promote, myofibroblast-liked cell proliferation, but also serves other functions including collagen stimulation and promotion of cell adhesion. PDGF is secreted by a variety of cell types in response to injury. Contractility by HSCs is a major determinant of early and late increases in portal resistance during hepatic fibrosis (Figure 18).^(92, 93)

6.2.2.2 Fibrogenesis

Fibrogenesis is the major component of the HSCs contribution to hepatic fibrosis. TGF- β 1 is a multifunctional growth factor, the most fibrogenic cytokine described for the HSCs and stimulates the ECM synthesis and accumulation. HSCs are a key source of TGF- β 1 but Kupffer cells, liver cells, and platelets can also secrete this cytokine (Figure 18).^(92, 93)

6.2.2.3 Chemotaxis

Activated HSCs are proliferate and migrate into regions of liver injury and promote leukocyte chemotaxis (Figure 18).^(92, 93)

6.2.2.4 Matrix degradation

Qualitative and quantitative changes in the activity of MMPs and their inhibitors play a key role in extracellular matrix remodeling in hepatic fibrogenesis (Figure 18).^(92, 93)

6.2.2.5 Retinoid loss

HSCs activation is attended by loss of perinuclear retinoid (vitamin A) droplets (Figure 18).^(92, 93)

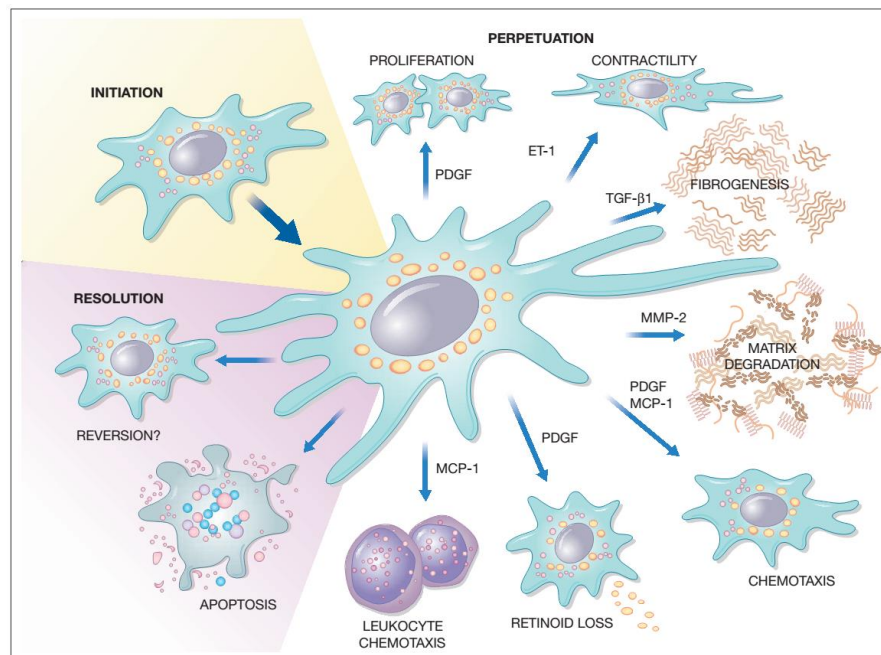


Figure 18 Activation of hepatic stellate cells (HSCs)

Source: Rockey DC. (2006). Hepatic fibrosis and cirrhosis.

6.3 Liver specific enzymes in liver fibrosis

The serum enzyme activities, which are located in hepatocytes, have been clinically used for the liver injury assessment. The liver enzymes may reflect the extent of hepatocellular necrosis is transaminases enzymes or cholestasis is alkaline phosphatase (ALP), gamma-glutamyltransferase (GGT). Aspartate aminotransferase (AST) and alanine aminotransferase (ALT) play a major role in amino acid metabolism by catalysing reversible transfer of the α -amino group.⁽⁹⁴⁾ ALT is essentially found in the liver cytosol, therefore is a more explicit marker of liver damage than AST. Because AST is found in the liver, skeletal muscles, heart, kidney, lungs, pancreas, and brain. Both ALT and AST are expressed in differing focuses in organs and physiologically quantifiable in the serum. While high activities of ALT are accessible in the periportal area of the liver, AST is found in high concentrations in various different organs. In general, serum transaminases activities are increased in the hepatic disorders. ALP is involved in the organic phosphate esters hydrolysis and though not exclusively showed

in the liver that used as a marker of cholestasis. GGT found in biliary epithelial cells and hepatocytes. GGT is responsible for the transfer of α , γ -glutamyl group between peptides or to an amino acid which is associated with microsomes or the cell membrane. In general, ALP and GGT may be useful for liver diseases follow-up associated with cholestasis. Liver function test is an ordinarily utilized clinical term but is regrettably a vague way of describing serologic tests used in the liver disease evaluation.^(7, 94, 95)

6.4 Patterns of liver fibrosis progression

The process of hepatic fibrosis can be partitioned into two main components. The first involves liver parenchyma. The second involves portal areas with inconstant extension into the adjacent periportal regions.⁽⁹⁶⁾

6.4.1 Portal and periportal fibrosis

In this pattern, collagen fibers accumulate within the portal areas, which consequently become darkly staining and expanded into the adjacent hepatic parenchyma. It may occur in any condition related with constant portal inflammation, including steatohepatitis, chronic hepatitis, biliary obstruction, inflammatory cholangiopathy, and various systemic diseases.⁽⁹⁶⁾

6.4.2 Pericellular fibrosis

This pattern is indicated by collagen fibers that stretch out along the hepatic sinusoid to surround single or small groups of liver cells. The most noticeable reason for pericellular fibrosis is steatohepatitis. At first emerging in the centrilobular region, the fibrosis is accompanied in active by liver cells swelling, inflammatory cells infiltration, and fatty change.⁽⁹⁶⁾

6.4.3 Pericentral fibrosis

The centrilobular fibrosis is mainly affected with collagen fiber deposition around the central vein. The degree of the deposition varies from minor vein wall thickening to marked scarring of the centrilobular region. When significant, perivenular fibrosis is generally characterized by pericellular fibrosis of differing degree.⁽⁹⁶⁾

6.4.4 Bridging fibrosis

In this pattern, bridging fibrosis alluded to as septal fibrosis, this example assigns the presence of collagen fibers septa that extend across lobules and interface portal areas and central vein in various arrangements. It represents an extension of periportal or pericentral fibrosis and as a marker of progressive disease, a significant marker of prognosis. Fibrosis septa demonstrate a shapes and sizes variety, ranging from slender, well-defined irregular collagenous bands that occasionally include whole lobules, portal-central, and central-central types.⁽⁹⁶⁾

6.4.5 Cirrhosis

Cirrhosis is resolved as a diffuse procedure described by annular fibrosis and a change of typical morphology into structurally abnormal nodules. Cirrhosis is related with extensive vascular changes. The portal-hepatic vascular shunts are developed. Regenerative nodules may form between the connective tissue fibrous septa. Several classifications of cirrhosis have been proposed dependent on morphology, pathogenesis or clinical features which depends on macroscopic appearance and dependent on the parenchymal nodules diameter. Cirrhosis has been divided into three categories consisting of micronodule cirrhosis, macronodule cirrhosis, and mixed cirrhosis.⁽⁹⁶⁾

6.5 Assessment of liver fibrosis

The significant parts of the histopathological appraisal of liver biopsies in the setting of biopsies in the setting of chronic liver disease is determination of the degree of hepatic fibrosis and architectural change. Liver biopsy is the standard tool for assessment of hepatic fibrosis. Nevertheless, liver biopsy has some drawbacks that must be recognized. Because liver biopsy includes just a minor piece of the entire organ, there is a risk that part might be insignificant for estimation of fibrosis in the whole liver due to heterogeneity in its distribution. The histopathological scoring systems increases reproducibility and several evaluation especially for liver fibrosis stage evaluation. Liver biopsy establishes and confirms the particular type of liver disease diagnosis. In addition, it is used to assess the severity of the disease including the grade and stage.⁽⁹⁶⁻⁹⁸⁾

6.5.1 Sirius red staining

The molecular formula of Sirius red is $C_{45}H_{26}N_{10}Na_6O_{21}S_6$ (Figure 19)⁽⁹⁹⁾. Sirius red is a powerfully acidic azo dye which contains six sulfonic group that had been used to stain collagen fiber in the tissue sections. It has four azo chromophoric groups and has therefore a high extinction coefficient that allows the detection of a small amounts of collagen fiber in tissue sections. Sirius red has affinity for most hepatic collagens, including fibril-forming types (types I and III). It has been shown that this dye binds to collagen through a strong connection of its acid sulfonic groups with the basic groups of collagen molecules. Sirius red staining is a commonly histological technique to visualize collagen in paraffin embedded tissue sections. Collagen appears red in light microscopy. The nuclei and cytoplasm appears yellow in color.⁽⁹⁷⁻⁹⁹⁾

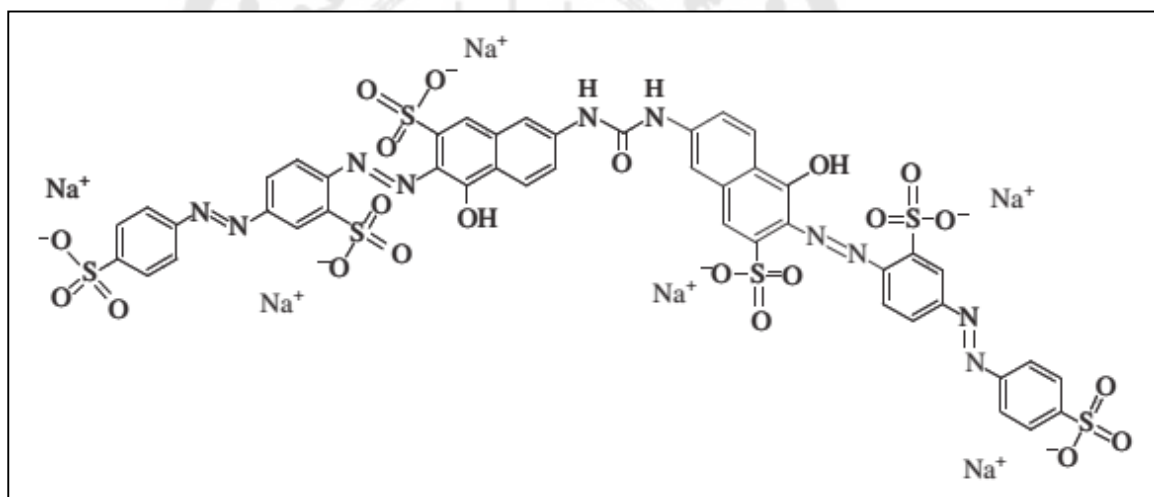


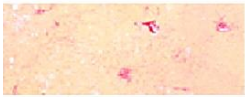
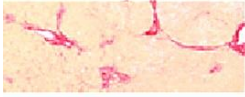
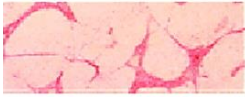
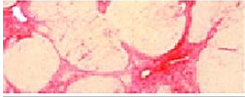
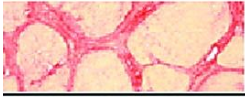
Figure 19 The molecular formula of the dye Sirius red illustrating sulfonic groups

Source: Weng CH. (2015). Effective decolorization of polyazo direct dye Sirius Red F3B using persulfate activated with Fe₀ aggregate. Separation and Purification Technology.

6.5.2 The Ishak system

Ishak score is the common widely approved scoring systems for assessment of hepatic fibrosis. The Ishak system evaluates fibrosis in seven categories, from normal liver to cirrhosis. All scoring systems basically use the same principles to record liver disease stage. The higher Ishak scores especially depend on architectural changes and degree of nodularity rather than amount of fibrous tissue. The Ishak system show that this variability is decreased if there are less classifications to choose from within each axis of assessment but this approach diminishes the distinct intensity of the more reduced scoring systems that have been projected (Table 3).⁽¹⁰⁰⁾

Table 3 Ishak staging scale

Appearance	Ishak stage: Categorical description	Ishak stage: Categorical assignment
	No fibrosis (normal)	0
	Fibrous expansion of some portal areas ± short fibrous septa	1
	Fibrous expansion of most portal areas ± short fibrous septa	2
	Fibrous expansion of most portal areas with occasional portal to portal (P-P) bridging	3
	Fibrous expansion of portal areas with marked bridging (portal to portal (P-P) as well as portal to central (P-C))	4
	Marked bridging (P-P and/or P-C), with occasional nodules (incomplete cirrhosis)	5
	Cirrhosis, probable or definite	6

Source: Standish RA. (2006). An appraisal of the histopathological assessment of liver fibrosis.

6.6 Liver regeneration in liver fibrosis

In adult liver has uncommon regenerative abilities. The healthy livers hide bipotent progenitors that can become either biliary cells or liver cells. Potential factors attracting reversibility probably include.^(101, 102)

1) A prolonged period of confirmed cirrhosis, which could indicate a longer period of collagen accumulation, rendering this collagen less sensitive to degradation by enzymes over time. Presently, support this possibility by animal studies.

2) Total content of collagen and other extracellular matrix molecules, which might lead to a large content of scar matrix that is physically unapproachable to degradative enzymes.

3) Reduction of enzymes expression that degrade matrix, or sustained increasing of proteins that inhibit the function of degradative enzymes, in particular elevated levels of TIMPs, which block matrix proteases and also prevent apoptosis of activated HSCs.

7. Thioacetamide (TAA)

Thioacetamide (TAA) is a thio-sulfur compound. It is formally used in leather processing, laboratories, paper industries, and textile. This white crystalline solid is dissolved in alcohol and water. TAA is one of the hepatotoxin, consumed to induce acute and chronic liver damage by means of its impacts on protein synthesis, RNA, DNA, and gamma-glutamyl transpeptidase activity.⁽¹⁰³⁾

7.1 Chemical structure

The chemical formula for TAA is C_2H_5NS . It is one of the common molecules containing a thiocarbonyl group and an amino group. Furthermore, TAA is a well-known source of hydrogen sulfide for inorganic analyses like the metal sulfides precipitation (Figure 20).^(104, 105)

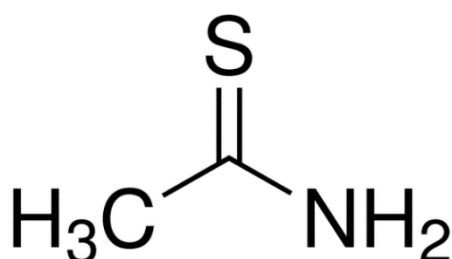


Figure 20 The structural formula of Thioacetamide (TAA)

Source: Axhausen J. (2013). The Protonation of Acetamide and Thioacetamide in Super-acidic Solutions: Crystal Structures of $[H_3CC(OH)NH_2]+AsF_6^-$ and $[H_3CC(SH)NH_2]+AsF_6^-$.

7.2 Bioactivation of TAA

TAA undergoes a two-step bioactivation to TAA-S-oxide (TASO) and afterward to TAA-S,S-dioxide (TASO₂) a reactive metabolite that is compromised by cellular enzymes including the cytochromes P450 (CYP) system. CYP is a heme containing enzyme that catalyzes the oxidation of a wide category of exogenous and endogenous compounds such as drugs, carcinogens and other xenobiotic chemicals. TAA requires metabolic activation to elicit its toxicity.⁽¹⁰⁶⁾ So, TAA is generally thought to be bioactivated by CYP systems interceded by microsomal CYP2E1. CYP450 system is thought to be responsible for metabolized of TAA in rat liver. Enzymes of CYP450 are display in the liver microsomes, a reactive intermediate with toxic nature and owing to oxidation process it induces oxidative stress in the hepatocytes that finally leads to centrilobular necrosis and liver injury. TASO is explainable for the nucleoli enlargement, increase intracellular concentration of Ca²⁺ and nuclear volume, change in cell permeability, and inhibit mitochondrial activity. TAASO₂ reacts with proteins via altering lysine side chains and response to release nitric oxide synthase (iNOS), leading to centrilobular necrosis. Previous studies demonstrated that TAA bioactivation is commonly mediated by hepatic CYP2E1. TAA and its initial metabolite TASO elicit a category of hepatotoxic responses in rodents relying upon the duration and dose of administration. TAA is an incredible inhibitor of the oxidation of TASO to its reactive

TASO₂ metabolite TASO, which can conceivably exist in two tautomeric forms. Then reacts with proteins by adjusting lysine side chains. This reasonable leads to cytotoxicity and impairment of function (Figure 21).^(15, 103)

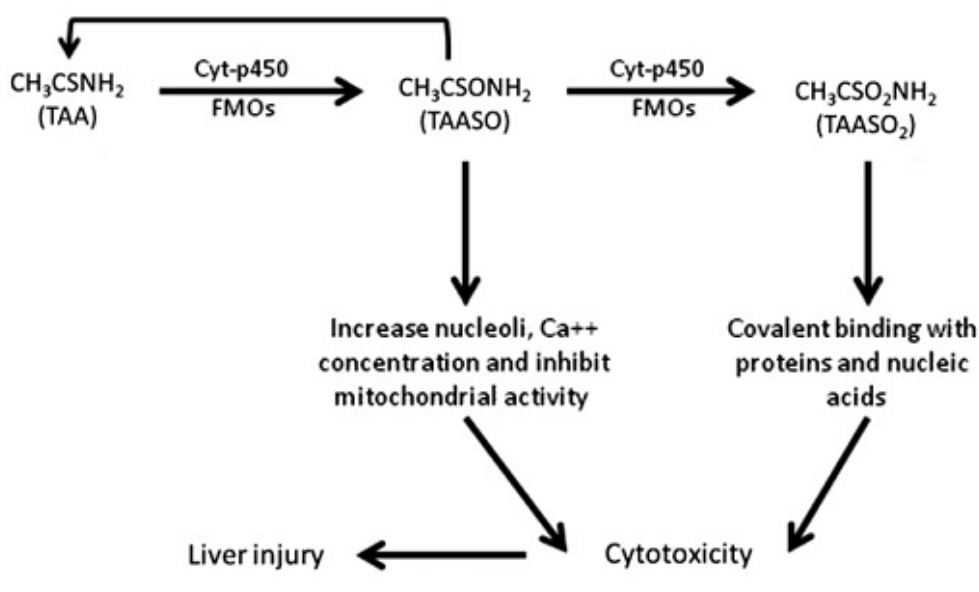


Figure 21 The kinetics of a two-step bioactivation of TAA

Source: Akhtar T. (2013). An overview of thioacetamide-induced hepatotoxicity.

7.3 Experimental hepatotoxicity of TAA

The experimental hepatotoxicity of TAA in animal modal was first investigated in 1948. Metabolite of TAA leads to the progression of reactive metabolites that are represented by radicals got from TASO and by reactive oxygen species (ROS) produced. Administration of TAA to animal models resulted in cell death by formation of apoptosis and necrosis. ROS production resulting from TAA administration was followed by lipid peroxidation.⁽¹⁴⁾ The metabolism of TAA and TASO in vivo induces the formation of acetamide derivatives on protein lysine side chains. In isolated hepatocytes, metabolism of TASO leads to extensive modification of both the amine groups of phosphatidylethanolamine lipids and protein lysine side chains. More recently, the in vivo utilization of TAA in rodents as a model hepatotoxin created profoundly particular

liver harm including hepatic necrosis or apoptosis, hepatic fibrosis, and cirrhosis.^(10, 13, 14)

TAA has been used extensively in the development of appropriate animal models of acute and chronic liver injury. Prolonged this compound directs to macro hepatic nodules, hepatocyte adenomas, cholangiomas, and hepatocarcinomas, histopathologically similar to that caused due to viral hepatitis infection.

7.4 Histopathological caused by TAA

The liver tissue sections of Wistar rats received chronic TAA treatment showed hepatotoxicity typified by vascular fibrosis, giant hepatocytes, degenerated hepaticlobular architecture, low degree cirrhosis, high level of necrotic cells infiltration, increased sinusoidal kupffer cells density, and mild level of hemorrhage. Inflammation is a feature and usually prominent characteristic of liver toxicity. Kupffer cells go through hyperplasia and hypertrophy and are loaded with pigment consequently of phagocytosis of hepatocellular debris. A mixture of inflammatory cells is usually infiltrated by portal tracts, causing periportal hepatocytes apoptosis. In the normal types of hepatic damage with TAA, irritation comprises of macrophages, lymphocytes, intermittent plasma cells and uncommon eosinophils or neutrophils and is restricted to portal tracts. Hepatic morphology is usually well preserved but apoptosis of hepatocyte all through the lobule may happen in all types of liver damage. Necrosis is also an extremely feature in liver chronic inflammation. As a result of accumulation of water, fat, and proteins, swelling occurs. Chronic hepatic injury is common always accompanied by prominent of sinusoidal stellate cells activation and portal tract fibroblasts or myofibroblast liked cells, giving increase to fibrosis. Most generally fibrosis is sinusoidal and perivenular, isolating parenchymal cells; incidentally, periportal fibrosis may prevail. In prolonged chronic inflammation, constant loss of hepatocytes and fibrosis brought about cirrhosis. Originally delicate fibrous septa develop and expand from central toportal regions. Fibrous tissue having wider bands merged hepatic parenchyma. Moreover, the liver is modified into a micronodular and macronodular pattern.^(10, 13)

8. Silymarin

Silymarin is a compound of flavonolignans from medicinal plant *Silybum marianum*.⁽¹⁰⁷⁾ *Silybum marianum* is the scientific name for St. Mary's thistle or Milk thistle. It is a common found in winter cereal fields, roadsides and undisturbed areas in the Mediterranean basin and other European regions. The typical name "milk thistle" is obtained from the "milky white" veins on the leaves.^(107, 108) It is characterized by spiny branches, height of 3-10 feet, and a milky sap, with its oval leaves reaching up to 30 cm. The flowers are bright purple or pink and can measure up to 8 cm in diameter (Figure 22).⁽¹⁰⁸⁾ Silymarin is arguably the most commonly used medication for various liver diseases.⁽¹⁰⁹⁻¹¹⁴⁾

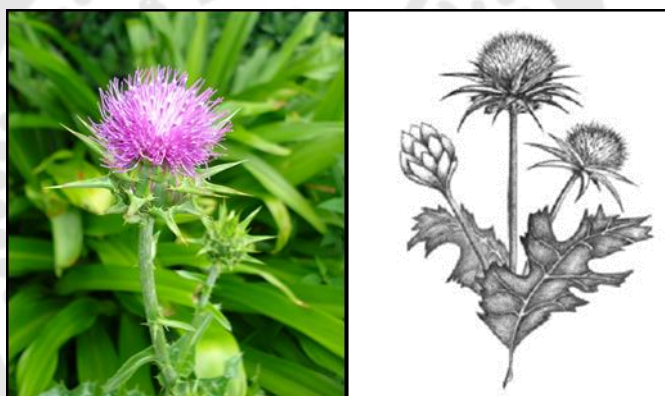


Figure 22 Milk thistle

Source: Abenavoli L. (2010). Milk thistle in liver diseases: past, present, future.

8.1 Chemistry of Silymarin

Silymarin is established in highest concentrations in the leaves and seeds but is also found in the fruit portion of the plant. It is a complex mixture of four flavonolignan isomers, isomers, namely silydianin silybin, isosilybin, and silychristin with an experimental formula $C_{25}H_{22}O_{10}$ (Figure 23).^(108, 115)

8.2 Mechanisms of action

Hepatoprotective effects of silymarin are performed by several mechanisms including restraint of lipid peroxidation, antioxidation, upgraded hepatic detoxification by inhibition of Phase I detoxification, and improved glucuronidation and protection of glutathione depletion. Previous studies show that silymarin presents several antiinflammatory effects, including inhibition of prostaglandin synthesis, Kupffer cell inhibition, mast cell stabilization, and restraint of neutrophil migration. Additionally, silymarin has been appeared to increment liver protein synthesis, thereby promoting liver tissue recovery. Animal studies have also exhibited silybin diminishes the change of HSCs into myofibroblasts, slowing or even reversing fibrosis. Clinical studies conducted in Hungary also shown silymarin to have immunomodulation on the liver diseases.⁽¹¹⁶⁾

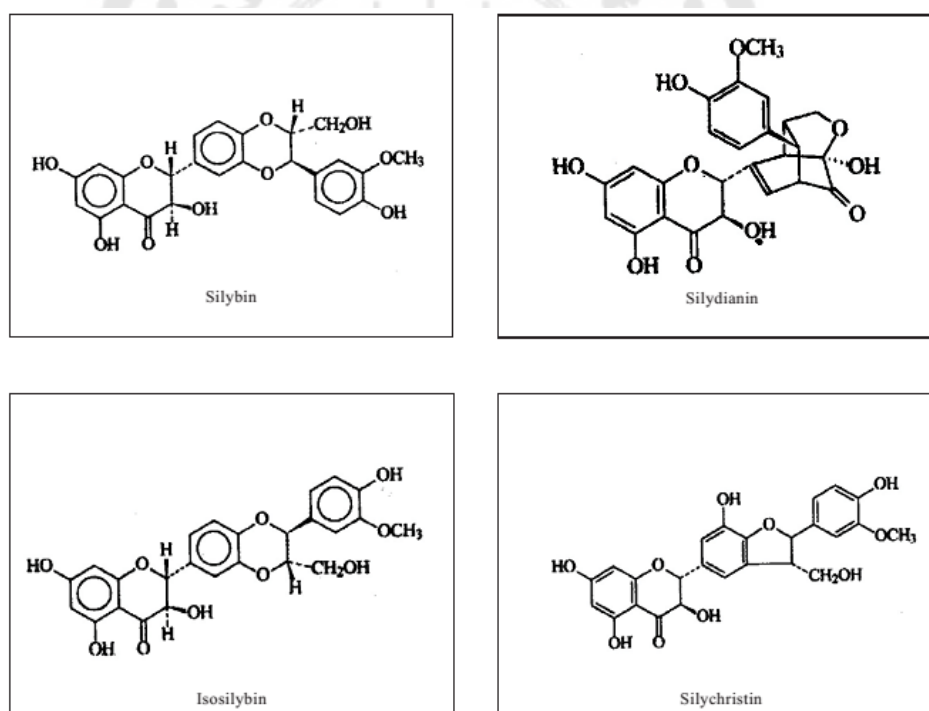


Figure 23 The structures of flavonolignan isomers of silymarin

Source: Féher J. (2012). Silymarin in the prevention and treatment of liver diseases and primary liver cancer.

8.3 Antifibrotic effects

Hepatic fibrosis can bring about renovating of hepatic histomorphology, leading to hepatic insufficiency, portal hypertension, and hepatic encephalopathy. These procedures concern a complex interaction of cell and mediators. In the underlying phase there will be proliferation of liver parenchymal cells. The conversion of HSCs into myofibroblast is determined as the central event in liver fibrogenesis. This decreases expression of the profibrogenic procollagen alpha I and the TIMP1, most likely by downregulation of profibrogenic cytokine, TGF- β 1. Past study show that silymarin have protective effects against CCl₄-induced hepatic fibrosis and ethanolinduced liver injury in rodents and silymarin act a protective role through their free redical scavenging properties.⁽¹¹⁷⁻¹¹⁹⁾



CHAPTER 3

MATERIALS AND METHODS

1. Chemicals and antibodies

1.1 Chemicals

Thioacetamide (TAA), silymarin, poly-L-lysine, direct red 80, NBT/BCIP stock solution, Fetal Bovine Serum, PermOUNT[®], and lipid peroxidation (MDA) assay kit were purchased from Sigma-Aldrich (St. Louis, MO). Hematoxylin and eosin were purchased from Bio-Optica (Milano, Italy). Man-Rogosa-Sharpe (MRS) agars was purchased from HiMedia (Mumbai, Maharashtra, India). Anaerobic GasPak and Anaerobic box were purchased from Mitsubishi (Tokyo, Japan). Radioimmunoprecipitation (RIPA) Lysis Buffer System and Polyvinylidene difluoride (PVDF) transfer membrane were purchased from Santa Cruz Biotech (Santa Cruz, CA, USA). Paraformaldehyde and paraffin were purchased from Electron Microscopy Science (Hatfield, PA, USA). High-Capacity cDNA reverse transcription kit and TRIzol reagent were acquired from Invitrogen (Carlsbad, CA, USA). SsoAdvanced SYBR[®] Green Supermix, PrimePCR SYBR[®] Green gene assay, the clarity[™] western chemiluminescence (ECL) blotting substrate, and Protein assay dry reagent concentrate were purchased from Bio-Rad (Hercules, CA, USA). Diethylpyrocarbonate (DEPC)-treated water was purchased from Applied Biosystems (Foster City, CA, USA). Non-fat milk powder was purchased from EMD Millipore Corporation (Billerica, MA, USA). All other chemicals used in this study were obtained from Ajax finechem and Sigma-Aldrich (St. Louis, MO).

1.2 Antibodies

Rabbit polyclonal antibody against TGF- β 1 (ab92486) and rabbit polyclonal antibody against TNF- α (ab6671) were ordered from Abcam (Cambridge, MA, USA). Mouse monoclonal antibody against α -SMA (A5228), anti-rabbit IgG, and anti-mouse IgG - conjugated with alkaline phosphatase (A3562) from Sigma-Aldrich (St. Louis, MO,

USA) were utilized. Anti-rabbit IgG; HRP-linked antibody, Anti-mouse IgG; HRP-linked antibody, and Biotinylated protein ladder detection pack were purchased from Cell Signaling Technology (Danvers, MA, USA). PageRuler prestained protein ladder were purchased from Pierce Biotechnology (Rockford, IL, USA). GAPDH Loading Control Monoclonal Antibody were purchased from Invitrogen (Carlsbad, California, USA).

1.3 PrimePCR SYBR® Green gene assay and Primer sequences

The specific primer and probe assays used to analyze the mRNA levels of five target genes; *Tgfb1* and *Tnf* in real-time PCR were selected from the PrimePCR SYBR® Green gene assay. The differences in sample RNA content were normalized by rat β -actin (*Actb*). The details of assays are shown on Table 4.

The primer sequences used for RT-PCR were designed to be specific for α -SMA Encyclon and Primer3 software. In RT-PCR study, β -actin was used to normalize the relative abundance of each band as endogenous control. The sequences of primers are shown on Table 5.

Table 4 Assay details of all studied genes for real-time PCR

Genes	Interrogated sequence		Amplicon Length (bp)
	Unique Assay ID	Ref. sequence	
<i>Tgfb1</i>	qRnoCID0009191	NM_021578	109
<i>Tnf</i>	qRnoCED0009117	NM_012675	112
<i>Actb</i>	qRnoCID0056984	NM_031144	74

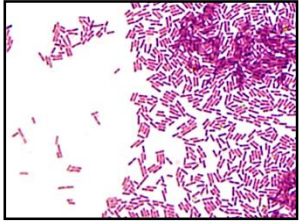
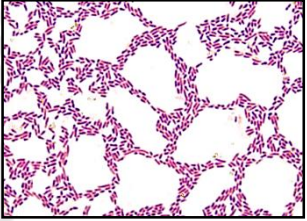
Table 5 List of primer sequences used for RT-PCR

Genes	Forward Primer (5'-3')	Reverse Primer (5'-3')	Size (bp)
<i>Acta2</i>	GAGCGTGGCTATTCCTTCGTG	CAGTGGCCATCTCATTTCAAAGT	106
<i>β-actin</i>	GTGGGGCGCCCCAGGCAC	CTCCTTAATGTCACGCAC	540

2. Probiotic strains

The probiotics were obtained from Asst. Prof. Malai Taweechotipatr, Department of Microbiology, Faculty of Medicine, Srinakharinwirot University. Three different probiotic lactic acid bacteria strains (*L. paracasei* MSMC 39-1, *L. casei* MSMC 39-3, and *W. confusa* MSMC 57-1) were kept frozen cultures in de Man-Rogosa-Sharpe (MRS) broth with 20% glycerol at -80 °C until experimental use.

Table 6 General characteristics of probiotic strains

Strain	Colony morphology	Gram reaction	Morphology
<i>Lactobacillus paracasei</i>	Large colonies white/creamy Circular	Gram positive long bacilli	
<i>Lactobacillus casei</i>	Large colonies white/creamy Circular	Gram positive Big long bacilli	
<i>Wasilla confusa</i>	Medium colonies White Circular	Gram positive short bacilli	

3. Experimental animals

Male Wistar rats, 5-8 weeks (200-250 g), were obtained from the National Laboratory Animal Center, Mahidol University, Salaya, Nakhonphathom, Thailand. The animals were housed in standard cages with free access to water and standard pellet diet in a temperature and humidity-controlled environment and maintained on a 12:12 hrs light-dark cycle at Medical Center Animal Care Laboratory, Srinakharinwirot University. All rats were acclimatized for 2 weeks before experimentation. All procedures involving animals were followed by the Animal Ethics Committee of the Faculty of Medicine, Srinakharinwirot University (License no. 11/2561).

4. Preparation of probiotic constituents

L. paracasei, *L. casei*, and *L. confusus* were spread onto de Man-Rogosa-Sharpe (MRS) agar plates which is selective for lactic acid bacteria. The plates were incubated at 37 °C for 24–48 hours under anaerobic conditions using an anaerobic GasPak in an anaerobic box. Single, pure colonies were isolated and sub-cultured anaerobically at 37 °C for 24-48 hours. Then, the bacterial cells were collected by centrifugation, washed twice in PBS, and adjusted to 10^9 CFU/ml as determined by spectrophotometer (OD_{600}). The bacterial cells were mixed at 1:1:1 ratio and suspended in sterile distilled water for experimental use.

5. Experimental designs

The rats were randomly divided into five groups of seven animals each (Figure 24). The groups were as follow: (A) Control group, (B) TAA group, (C) TAA+probiotics group, (D) TAA+silymarin group, and (E) Probiotics group.

Group (A) rats were received standard diet. Groups (B to D) rats were received intraperitoneal injection with TAA 200 mg/kg b.w. dissolved in sterile water 3 times per week for 8 weeks.⁽¹⁰⁾ Groups (C and E) rats were orally treated with probiotics daily by an intragastric stainless steel feeding tube. The number of viable microbial cells were used approximately 10^9 CFU/ml.^(120, 121) Group (D) rats were received silymarin 100 mg/kg b.w. 2 times per week (Silymarin is a well-known standard drug with hepatoprotective activity: positive control).^(122, 123) All groups were treated for 8 weeks.

At the end of treatment, the rats were sacrificed under anesthesia. Blood was collected by cardiac puncture for liver enzyme tests. Livers were collected for histopathological study and stored at -80°C for western blot analysis, lipid peroxidation (MDA) assay, and real-time PCR assay.

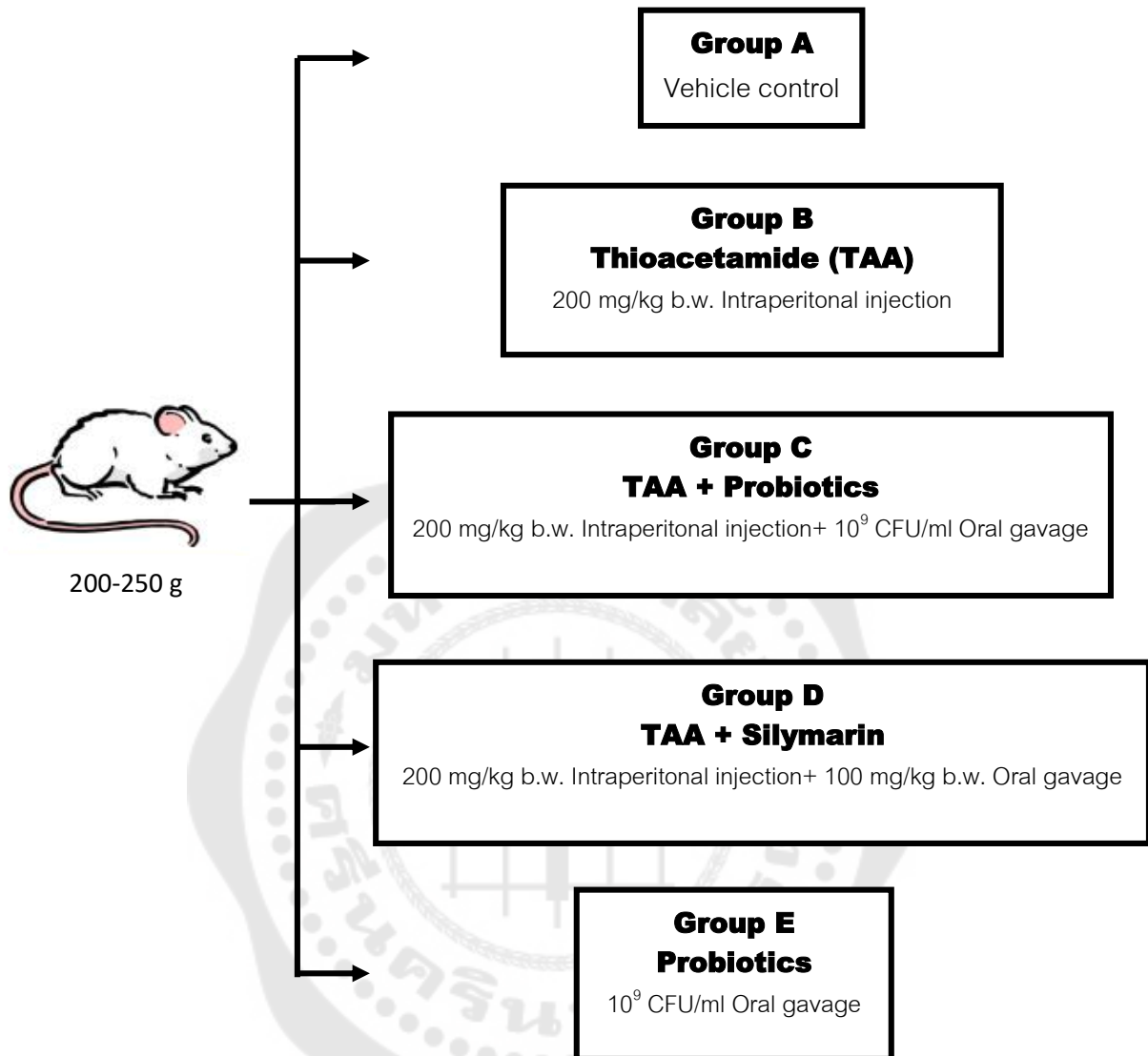


Figure 24 Diagram illustrating the experimental groups

6. Methods

6.1 Gross examination of the liver

The liver of the rats were isolated, dissected and then rinsed in phosphate buffer saline (PBS). Gross examination were checked for gross abnormalities of the organs and a photograph were taken. The body weight and relative liver weight were measured. The liver indices were calculated as the percentage of the body weight.

$$\text{The liver weight relative to body weight ratio (\%)} = \frac{\text{Liver weight (g)}}{\text{Body weight(g)}} \times 100$$

6.2 Liver enzyme markers

The blood samples were collected from the heart to analyze liver enzyme markers including serum aspartate aminotransferase (AST), alanine aminotransferase (ALT) and alkaline phosphatase (ALP). Serum AST, ALT, and ALP were measured in a standard clinical lab (Bangkok R.I.A. Laboratory, Bangkok, Thailand).

6.3 Histopathological studies from paraffin sections

6.3.1 Tissue preparation

The liver specimen were immediately removed and then rinsed in PBS. Then it were excised into five pieces and fixed in 4% paraformaldehyde at 4 °C and then dehydrated in a graded alcohol series. The specimens were embedded in paraffin blocks.

6.3.2 Histopathological analysis

The paraffin blocks were sectioned at 5-7 micron thick by microtome. Then the sections were deparaffinized and dehydrated in xylene and a graded alcohol series, respectively. The sections were stained with hematoxylin and eosin (H&E) for observing the histopathological features or with Sirius red for visualizing the collagen distribution. After rehydration quickly in a graded series of ethanol and clearing in xylene, the sections were covered with Permount[®] and observed under a light

microscope (Olympus, Tokyo, Japan). Histological evaluation were selected the section randomly at 40 sections per group (40x magnification). The degree of hepatocyte injury was determined by a point-counting method using an ordinal scale by pathologist as follows:⁽¹²⁴⁾

Grade 0	Minimal or no evidence of injury
Grade 1	Mild injury consisting of cytoplasmic vacuolation and focal nuclear pyknosis
Grade 2	Moderate to severe injury with extensive nuclear pyknosis, cytoplasmic hypereosinophilia, and loss of intercellular borders
Grade 3	Severe necrosis with the disintegration of hepatic cords, hemorrhage, and neutrophil infiltration

To describe leukocyte infiltration, a scale from one to four was used: grade 1, <10 leukocytes/field (focal infiltration); grade 2, 10–20 leukocytes/field (mild infiltration); grade 3, 21–50 leukocytes/field (moderate infiltration); and grade 4, >50 leukocytes/field (severe infiltration).^(124, 125) The degree of fibrosis was assessed by percent of fibrotic area measuring the threshold intensity in the Sirius-red stain sections (40 randomly selected sections per group at 10x magnification) using Cell Sense Dimensions software (Olympus Germany, Hamburg, Germany) and Ishak score from 0 to 6.⁽⁹⁶⁾

6.3.3 Immunohistochemical staining

Paraffin sections were mounted on poly-L-lysine coated glass slides. Specimens were deparaffinized and rehydrated in a graded series of ethanol. After washing, specimens were processed for antigen retrieval performed by boiling in sodium citrate buffer (pH 6.0) for 10 min at 120°C. After cooling down at room temperature and washing in PBS, the specimens were incubated in TENG-T (10mM Tris, 5mM EDTA, 150 mM NaCl, 0.25% gelatin, 0.05% Tween-20; pH 8.0) with 10% normal

goat serum for 30 min in humidity chamber. After that, the samples were incubated with rabbit anti-TGF- β 1 polyclonal clonal antibody, or mouse anti- α -SMA monoclonal, or rabbit anti-TNF- α polyclonal antibodies overnight at room temperature in humidity chamber. After washing with PBS, the sections were incubated in the alkaline phosphatase-conjugated goat anti-mouse IgG for 2 h at room temperature. Then, the samples were washed in PBS and incubated in substrate (NTM+NBT/BCIP) for 30 min to 2 h in order to visualize the immunopositive regions in the tissue. After stop reaction with double distilled water, the tissue sections were dehydrated quickly in an ascending graded series of ethanol, cleared in xylene and covered with Permount[®] before being examined and photographed under a light microscope (Olympus, Tokyo, Japan). For semiquantitation immunoreactivity were performed using Olympus cellSens Dimension software, Version 17.1 (Olympus). Five images per animal were analyzed to give a single value. The Mean intensity was quantified as $(255 - \text{Mean gray value})$ and OD as $\log(255 / (255 - \text{Mean intensity}))$. The immunoreactivity value were calculated as the percentage of positive staining intensity.

6.4 Western blot analysis

After sacrifice, the livers were immediately removed and stored at -80°C until use. Liver samples, about 50 mg were homogenized in RIPA (Radioimmunoprecipitation) Lysis Buffer containing 1X lysis buffer (pH 7.4 \pm 0.1), 200 mM PMSF in DMSO, protease inhibitor cocktail in DMSO, 100 mM sodium orthovanadate in water and then, centrifuged at 12,000 rpm for 15 minutes at 4°C . The supernatants were used for Western blot analysis. The concentration of protein were determined by the Bradford protein assay. Bovine serum albumin (BSA) were used as a protein standard. Protein extracts from liver tissue samples were denatured at 95°C for 5 min in sample buffer (62.5 mM Tris-HCl pH 6.8, 10% SDS, 10% glycerol, 2% mercaptoethanol and 0.01% bromophenol blue). After that, lysate proteins were separated by sodium dodecyl sulfate-polyacrylamide gel electrophoresis (SDS-PAGE) and transferred proteins onto a polyvinylidenedifluoride (PVDF) membrane. The PVDF membrane was stained with Ponceau Red solution to detect the transfer efficacy. The

membranes were washed with Tris-buffer saline that contained 0.1% Tween-20 (TBST), the membrane was incubated in blocking buffer (5% non-fat milk in TBST) for 1 hr at room temperature. TGF- β 1, α -SMA, and TNF- α were detected by using rabbit anti-TGF- β 1 polyclonal antibody (1:1000), mouse anti- α -SMA monoclonal antibody (1:1000), mouse anti-TNF- α monoclonal antibody (1:1000), respectively together with GAPDH Monoclonal Antibody (1:1000) as standard. All primary antibodies were diluted in 1% non-fat milk in TBST and incubated at 4 °C overnight. After washing with TBST (x3), the membranes were incubated with a 1:5000 anti-mouse IgG, HRP-linked antibody, or 1:5000 anti-rabbit IgG, HRP-linked antibody for 1 hr at room temperature. Then, the membrane was washed with TBST and immunoreactive proteins were detected with enhanced chemiluminescence (ECL). Protein bands were visualized and recorded using a UVITEC Chemiluminescence Documentation Systems (UVItec Limited, Cambridge, UK). The immunoblot bands were quantified by measuring the density of each band using densitometry with Scion image program (National Institutes of Health, Bethesda, MD). The optical density of the TNF- α , TGF- β 1, α -SMA, and GAPDH bands were normalized relative to the optical density of corresponding GAPDH.

6.5 MDA assay

After sacrifice, the livers were immediately removed and stored at -80°C until use. Liver samples, about 200 mg were homogenized and centrifuged at 3500 rpm for 10 minutes at 4°C. The supernatant were collected for estimation of lipid peroxidation product, MDA content, by using a commercially available kit. The absorbance of the supernatants were measured at 532 nm by using spectrophotometer

6.6 Real-time quantitative PCR

The Real-time PCR were performed in CFX96 Real-Time PCR Detection System (Bio-Rad, Hercules, CA, USA), using by PrimePCR SYBR® Green gene assay which is a primer set designed for the detection and quantitation of rat *Tnf*, *Tgfb1*, and *Acta2* genes in RNA samples converted to cDNA. Assay of rat β -actin (*Actb*) gene were performed as an endogenous control for relative quantification study.

6.6.1 RNA extraction

Total RNA were extracted from frozen rat liver using the TRIzol reagent (Invitrogen, Carlsbad, CA, USA). Briefly, 20 mg of the liver sample were homogenized with a sonicator (brand; 130 Watt, 20 kHz, Amp 35%) for 10 seconds in 1 ml of TRIzol reagent and then incubated at room temperature for 5 minutes before adding 0.2 ml of chloroform (CHCl_3), then were mixed vigorously by hand for 15 seconds, incubated at room temperature for 3 minutes, and centrifuged at 12,000 rcf for 15 minutes at 4 °C. After centrifugation, the RNA in the upper aqueous phase was transferred to a fresh tube and then precipitated with 0.5 ml of isopropanol, mixed gently by vortex, and incubated at room temperature for 10 minutes. The pellet of total RNA was collected by centrifugation at 12,000 rcf for 10 minutes. The supernatant was discarded. The RNA pellet were washed with 0.1 ml of cold 75% ethanol, and centrifuged at 7,500 rcf for 5 minutes. Finally, the RNA was dissolved in a small volume of DEPC-treated water (30-40 μl) and stored at -80 °C to be used later.

6.6.2 RNA qualification

The RNA concentrations were determined using a NanoDrop® spectrophotometer (Thermo Scientific, Waltham, MA, USA). RNA quality were assessed by the 260/280 nm absorbance ratio (~2.0) and gel electrophoresis.

6.6.3 Reverse transcription

Reverse transcription were performed using High Capacity cDNA Reverse Transcriptase Kit according to the manufacturer's instructions. First strand cDNA was synthesized with 2X RT master mix per 20 μl reaction (2 μl of 10X RT Buffer, 0.8 μl of 25X dNTP Mix (100 mM), 2 μl of 10X RT random primers, 1 μl of RNase inhibitor, 1 μl of Multiscribe™ reverse transcriptase, and 3.2 μl of DEPC-treated water). Then 10 μl of diluted RNA samples (2 ug of total RNA) were mixed with the 10 μl RT master mix and run on thermal cycler (Eppendorf Mastercycler® personal; Eppendorf AG, Hamburg, Germany) at 25°C for 10 minutes, 37°C for 120 minutes, 85°C for 5 minutes, and then were stored at -20°C until use.

6.6.4 Real time quantitative PCR

The real-time PCR reactions were set up using the SsoAdvanced SYBR® Green Supermix (Bio-Rad, California, USA) along with 1 µl of cDNA and the gene-specific primers (Bio-Rad, Hercules, CA, USA). The primer was used as follow; Rat *Tgfb1* (reference GenBank accession no. NM_021578) Unique Assay ID: qRnoCID0009191, Rat *Tnf* (reference GenBank accession no. NM_012675) Unique Assay ID: qRnoCED0009117. The differences in sample RNA content were normalized by rat *Actb* (reference GenBank accession no. NM_031144) Unique Assay ID: qRnoCID0056984. The real-time PCR reactions were carried out in CFX96 Real-Time PCR Detection System (Bio-Rad, Hercules, CA, USA). The thermal cycler protocol were consisted of 2 min activation at 95°C followed by 40 cycles of denaturation at 95°C for 5 sec, and then annealing/extension at 60°C for 30 sec. At the end of each run, a melting curve analysis were performed from 65-95 °C with a heating rate of 0.1°C per sec. Target genes and *Actb* reactions were performed in separate tubes and all samples were run in triplicate to ensure the accuracy of data. Analysis of the mRNA expression levels was performed by Bio-Rad CFX manager™ software version 1.3.1 (Hercules, CA) and quantification of relative mRNA expression was calculated using the comparative $\Delta\Delta C_t$ method of relative quantification. The change of target gene expression, relative to the mRNA amount of ΔC_t calibrator value was calculated using the equation $2^{-\Delta\Delta C_t}$ where $\Delta\Delta C_t = \Delta C_t (\text{calibrator}) - \Delta C_t (\text{target})$.

7. Statistical analysis

Statistical analysis was performed using GraphPad Prism 7 software (GraphPad Software Inc., San Diego, CA). All values were represented as mean \pm SEM. The data were analyzed using one-way analysis of variance (ANOVA) with Tukey's post hoc test to compare between each group. The significance levels will set at p -values less than 0.05.

CHAPTER 4

RESULTS

1. Effects of probiotics on general properties

1.1 Body weights of the rats

The average body weight of the control and the probiotics groups gradually increased in a parallel manner from week 0 to week 8. The body weights of the TAA+probiotics and TAA+silymarin groups also increased but was less than the first two groups mentioned earlier. Treatment with TAA caused, as expected, a significant decrease in body weight compared to the control group ($P<0.01$). The mean body weights of the five animal groups from week 0 to week 8 was depicted in Figure 25.

1.2 The liver weight relative to body weight

Although the liver weights of the TAA, TAA+probiotics, and TAA+silymarin groups, increased they were not of significance when compared with the control group. The liver weight of only the probiotics group significantly decreased when compared with the TAA group ($P<0.05$ and Table 7). Moreover, the liver-to-body weight ratio of the TAA group was significantly increased when compared with the control group ($P<0.01$). It was noteworthy that the ratios of liver-to-body weight were only insignificantly increased in the TAA+probiotics and TAA+silymarin groups, compared to the TAA group. Comparison of the liver- to-body weight ratio was shown in Table 7.

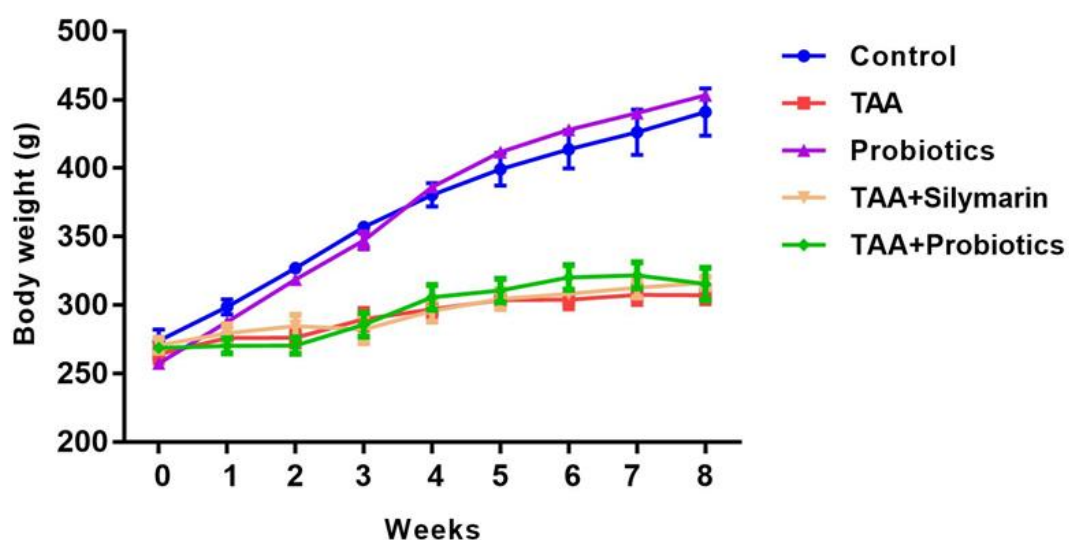


Figure 25 Graph illustrating the mean rat body weight of the five experimental groups from week 0 to week 8

Table 7 Comparison of the liver weight to body weight ratio

Parameters	Groups				
	Control	TAA	TAA+Probiotics	TAA+Silymarin	Probiotics
Liver weight (g)	11.93±0.9	12.98±0.2**	12.87±0.4**	12.83±0.2**	10.85±0.27 [#]
Body weight (g)	452±12.5	319.37±7.2**	319.61±14.0**	341.63±9.8**	453.05±1.6 ^{##}
Liver weight to body weight ratio (%)	2.7±0.3	4.07±0.1**	4.1±0.2**	4.1±0.1**	2.4±0.1 ^{##}

The data are presented as the mean ± S.E.M. (n = 7). ** $P < 0.01$ compared with the control group; [#] $P < 0.05$ and ^{##} $P < 0.01$ compared with the TAA-treated group.

2. Effects of probiotics on liver enzymes

2.1 Aspartate aminotransferase (AST)

Serum AST concentration in the TAA-treated group was significantly elevated when compared with the control group ($P < 0.01$). Its concentrations in the TAA+silymarin and probiotics groups, were significantly lower than those in the TAA group ($P < 0.05$ and $P < 0.01$, respectively). Surprisingly, serum levels of AST in the TAA+probiotics and the control groups were not significantly different (Figure 26). Comparison of the liver AST enzyme level was illustrated in Table 8.

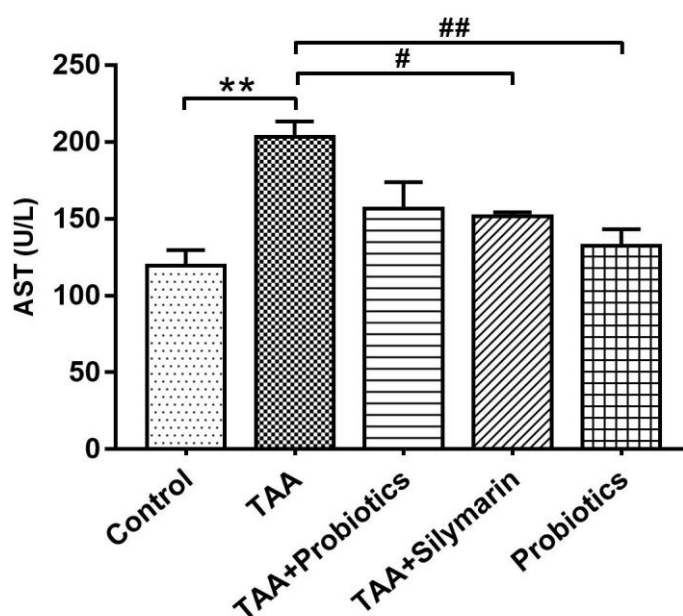


Figure 26 Diagram showing the serum levels of aspartate aminotransferase (AST) in the five animal groups

The data are presented as the mean \pm S.E.M. ($n = 7$). ** $P < 0.01$ compared with the control group; # $P < 0.05$ and ## $P < 0.01$ compared with the TAA-treated group.

2.2 Alanine aminotransferase (ALT)

Serum ALT level in the TAA group increased significantly when compared with the control group ($P < 0.01$). ALT concentrations in the TAA+probiotics, TAA+silymarin, and probiotics groups were significantly lower than those in the TAA group ($P < 0.01$ and Figure 27). Comparison of the liver ALT enzyme is demonstrated in Table 8.

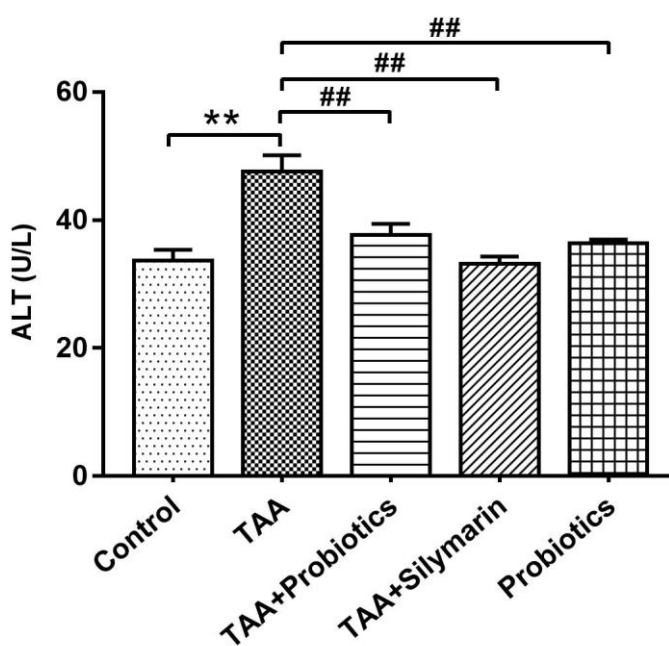


Figure 27 Diagram showing the serum levels of alanine aminotransferase (ALT) in the five animal groups

The data are presented as the mean \pm S.E.M. ($n = 7$). ** $P < 0.01$ compared with the control group; ## $P < 0.01$ compared with the TAA-treated group.

2.3 Alkaline phosphatase (ALP)

Serum ALP level in the TAA-treated group was significantly higher than those in the control group ($P < 0.01$). In rats treated with TAA+probitocs and TAA+silymarin, the levels of ALP were significantly lower than those treated with TAA only ($P < 0.05$ and Figure 28). Serum levels of ALP in the control and probiotics groups were almost identical. Comparison of the liver ALP enzyme was shown in Table 8.

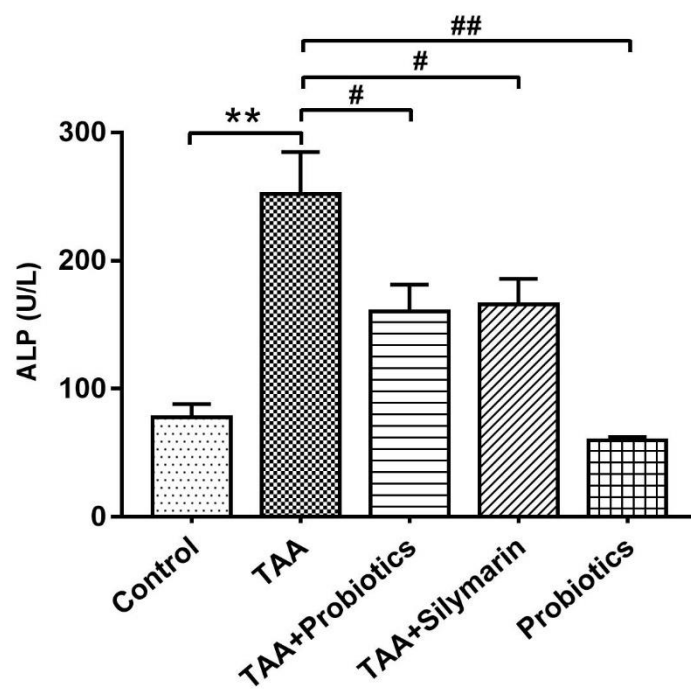


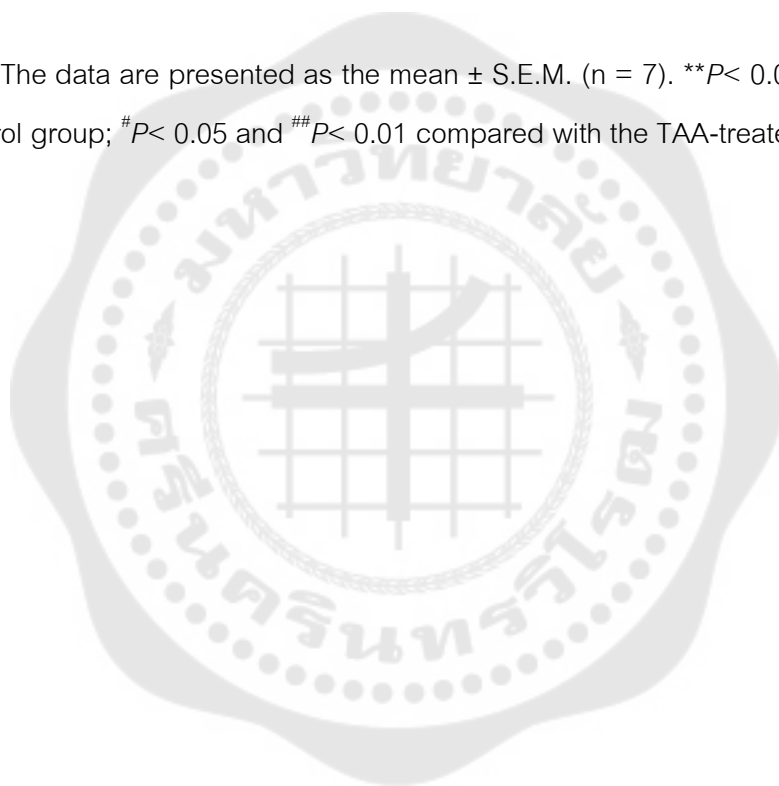
Figure 28 Diagram showing the serum levels of alkaline phosphatase (ALP) in the five animal groups

The data are presented as the mean \pm S.E.M. ($n = 7$). $**P < 0.01$ compared with the control group; $\#P < 0.05$ and $##P < 0.01$ compared with the TAA-treated group.

Table 8 Comparison of the liver enzyme makers

Parameters	Groups				
	Control	TAA	TAA+Probiotics	TAA+Silymarin	Probiotics
AST (U/L)	120±10	204±10**	157±17	152±2.8 [#]	132±11 ^{##}
ALT (U/L)	34±1.7	48±2.5**	38±1.8 ^{##}	33±1.1 ^{##}	36±0.56 ^{##}
ALP (U/L)	78±11	252±33**	160±21 [#]	166±20 [#]	60±2.6 ^{##}

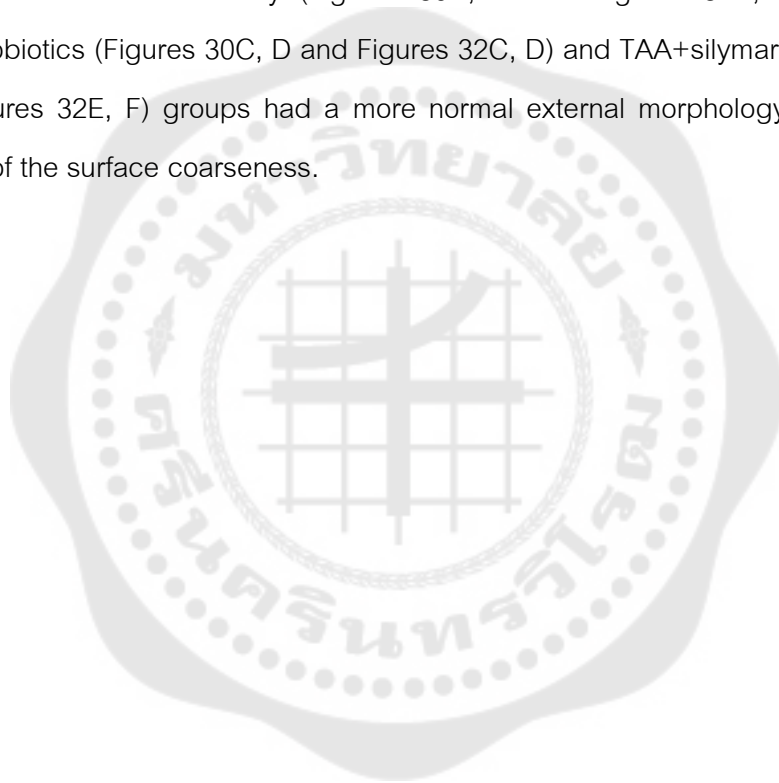
The data are presented as the mean ± S.E.M. (n = 7). ** $P < 0.01$ compared with the control group; [#] $P < 0.05$ and ^{##} $P < 0.01$ compared with the TAA-treated group.



3. Effects of probiotics on gross and histomorphological changes in liver

3.1 External morphology of the rat livers

The external morphology both in diaphragmatic and visceral surfaces of the rat livers in the control (Figures 29A, B and Figures 31A, B) and probiotics groups (Figures 29C, D and Figures 31C, D) had the normal brownish-red color and were glossy with sharp edges together with a smooth contour and soft consistency. In contrast, the liver surface of the TAA-treated group at 8 wk was slightly irregular and coarse with hard consistency (Figures 30A, B and Figures 32A, B). Livers in the TAA+probiotics (Figures 30C, D and Figures 32C, D) and TAA+silymarin (Figures 30E, F and Figures 32E, F) groups had a more normal external morphology due to a lesser degree of the surface coarseness.



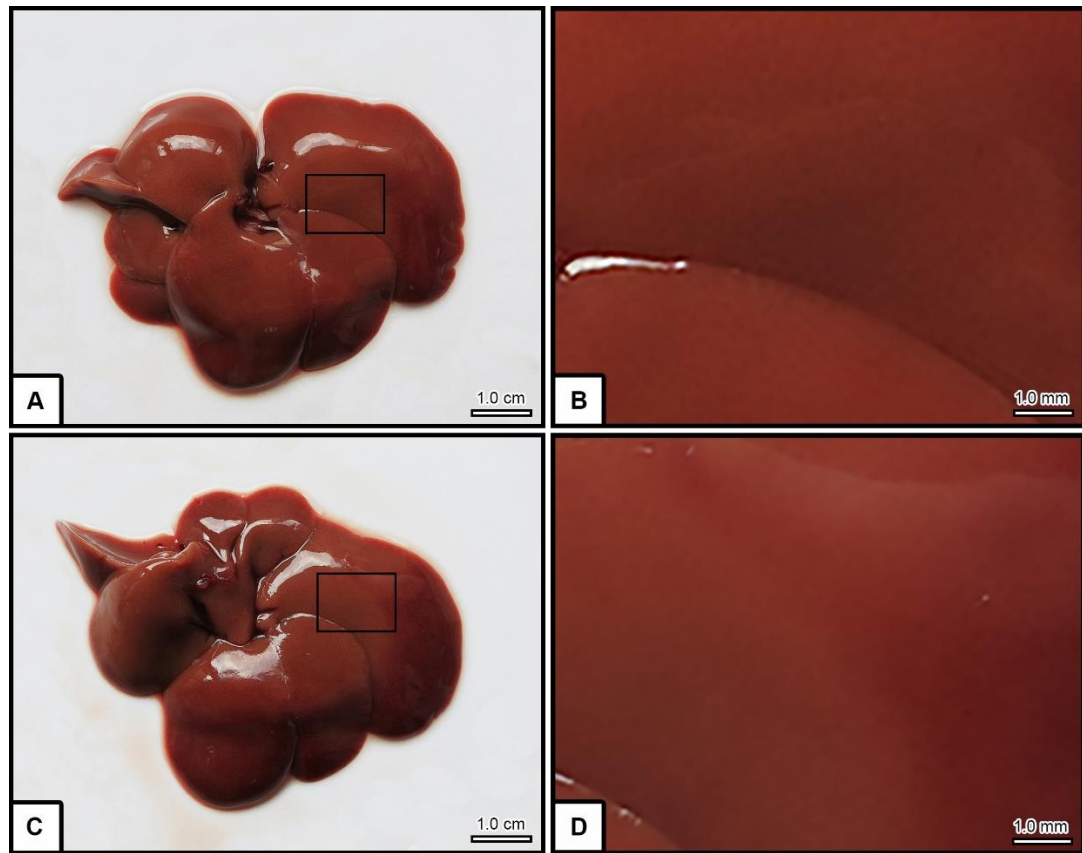


Figure 29 Photomicrographs showing gross morphology of the liver (diaphragmatic surface) with magnifications of the liver surface Control group (A,B) and Probiotics group (C,D).

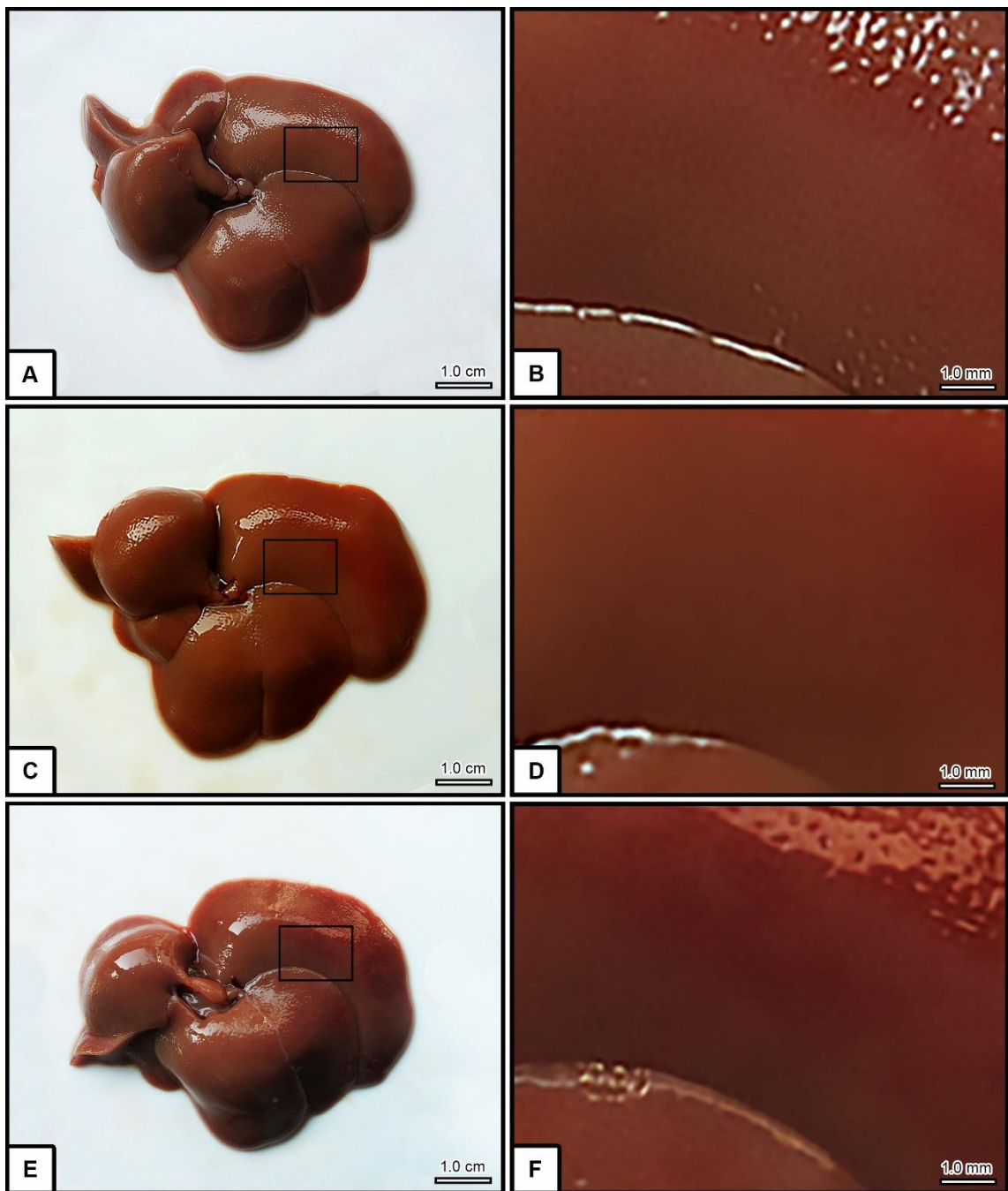


Figure 30 Photomicrographs showing gross morphology of the liver (visceral surface) with magnifications of the liver surface

TAA-treated group (A,B), TAA+Probiotics group (C,D), and TAA+Silymarin group (D,F)

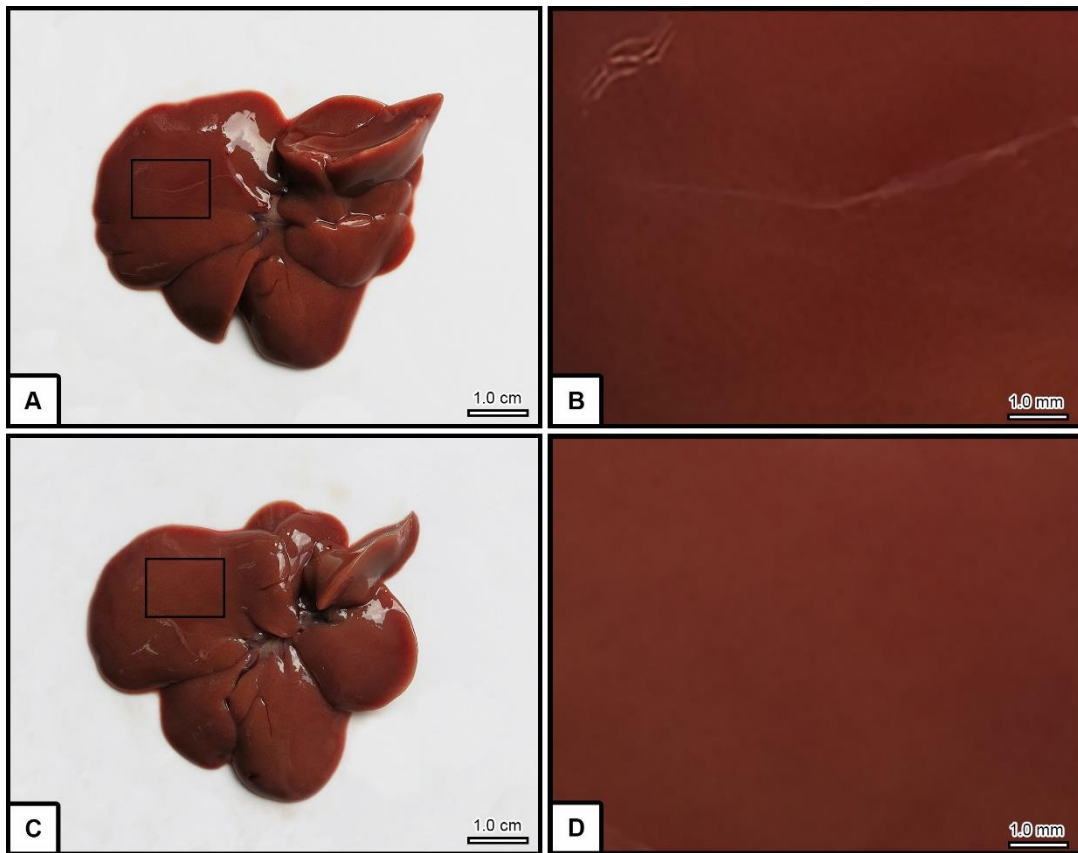


Figure 31 Photomicrographs showing gross morphology of the liver (visceral surface) with magnifications of the liver surface
Control group (A,B) and Probiotics group (C,D).

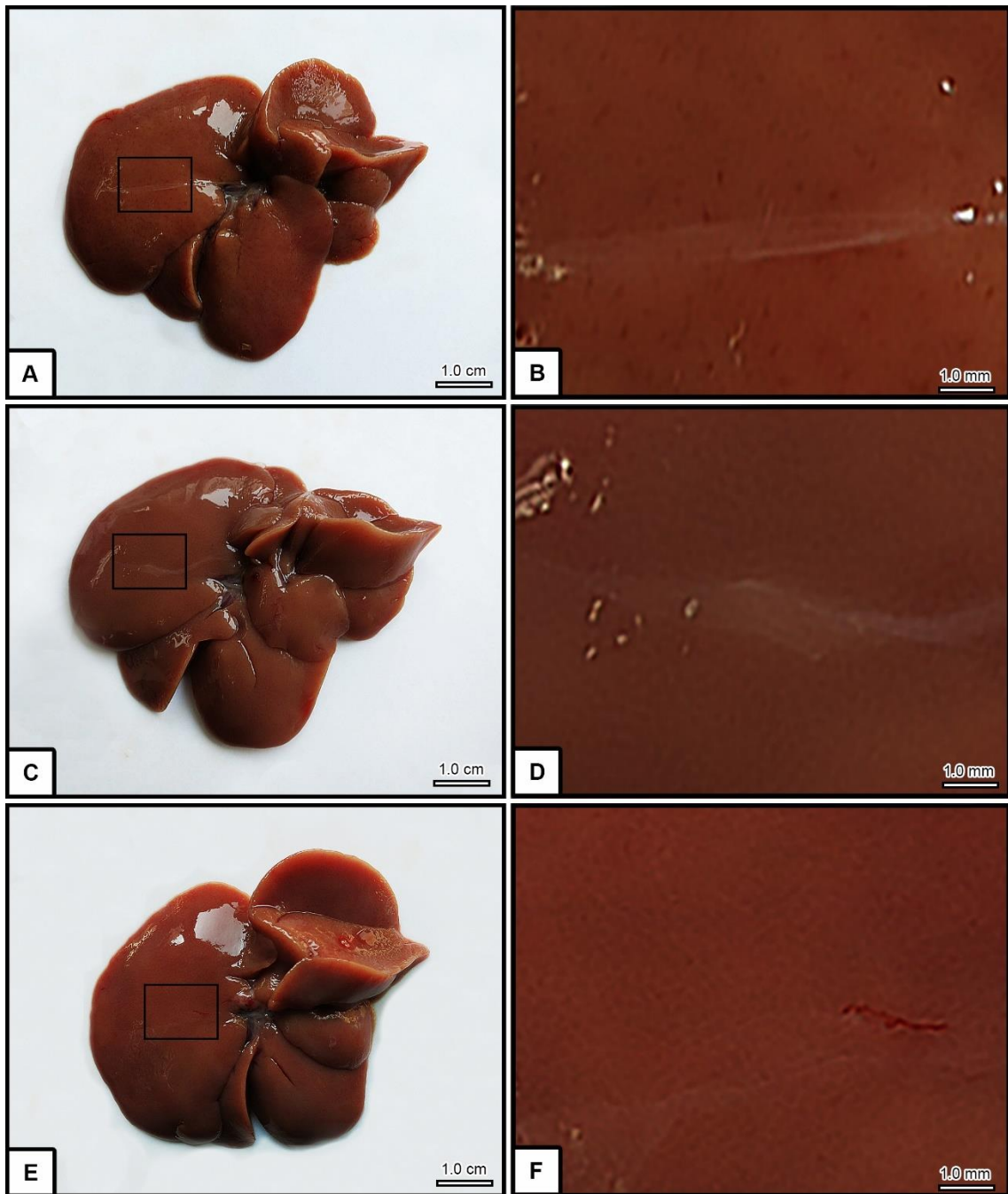


Figure 32 Photomicrographs showing gross morphology of the liver (viseral surface) with magnifications of the liver surface

TAA-treated group (A,B), TAA+Probiotics group (C,D), and TAA+Silymarin group (E,F)

3.2 Histopathological changes

As anticipated, the normal architecture of hepatic lobule with hepatic cell cords alternating with blood sinusoids radiating between a central vein to portal triads was observed in the livers of control and probiotics groups (Figures 33A and 33E). Hepatocytes in each hepatic lobule had polygonal shape with rounded vesicular nuclei and uniform staining of cytoplasm (Figures 34A and 34E).

In TAA-treated rat, the liver histology revealed a modified architecture with a grade 2 (moderate-to-severe) injury together with mild leukocyte infiltration ($P < 0.01$ and Table 9). These livers suffered from centrilobular necrosis and giant hepatocytes together with areas of inflammation (Figures 33B, 34B and 35). Two populations of hepatocytes in TAA-treated rats were observed as 1) dark eosinophilic-stained cells in the perivenular areas and 2) pale hydropic degenerated hepatocytes in the central area (Figure 32B and 35). Moreover, presence of the strands of myofibroblast-like cells in the connective tissue connecting between portal triads and central veins resembling hepatic nodule were clearly demonstrated (Figures 33B). In addition, cells with brownish cytoplasmic vacuoles were frequently observed in the portal areas (Figure 35).

The livers in the TAA+probiotics and TAA+silymarin groups show fewer areas of inflammation, accumulation of myofibroblast-like cells, pale hydropic degenerated cells and giant hepatocytes than the TAA groups. In agreement, the index of liver damage in the TAA+probiotics (Figures 33C and 34C) and TAA+silymarin groups (Figures 33D and 34D) was significantly decreased compared with the TAA group. This exhibited grade 1 mild injury and mild leukocyte infiltration ($P < 0.01$ and Table 9).

Table 9 Comparison of the index of liver damage and percentage of leukocyte infiltration

Parameters	Groups				
	Control	TAA	TAA+Probiotics	TAA+Silymarin	Probiotics
Index of liver damage	0.5±0.11	2.7±0.06**	1.3±0.06** ^{##}	1.6±0.09** ^{##}	0.55±0.11 ^{##}
Leukocyte infiltration (%)	3.2±0.61	19±1.20**	7.5±0.66** ^{##}	9.8±0.84** ^{##}	3.9±0.79 ^{##}

The data are presented as the mean ± S.E.M. ** $P < 0.01$ compared with the control group; ^{##} $P < 0.01$ compared with the TAA-treated group.

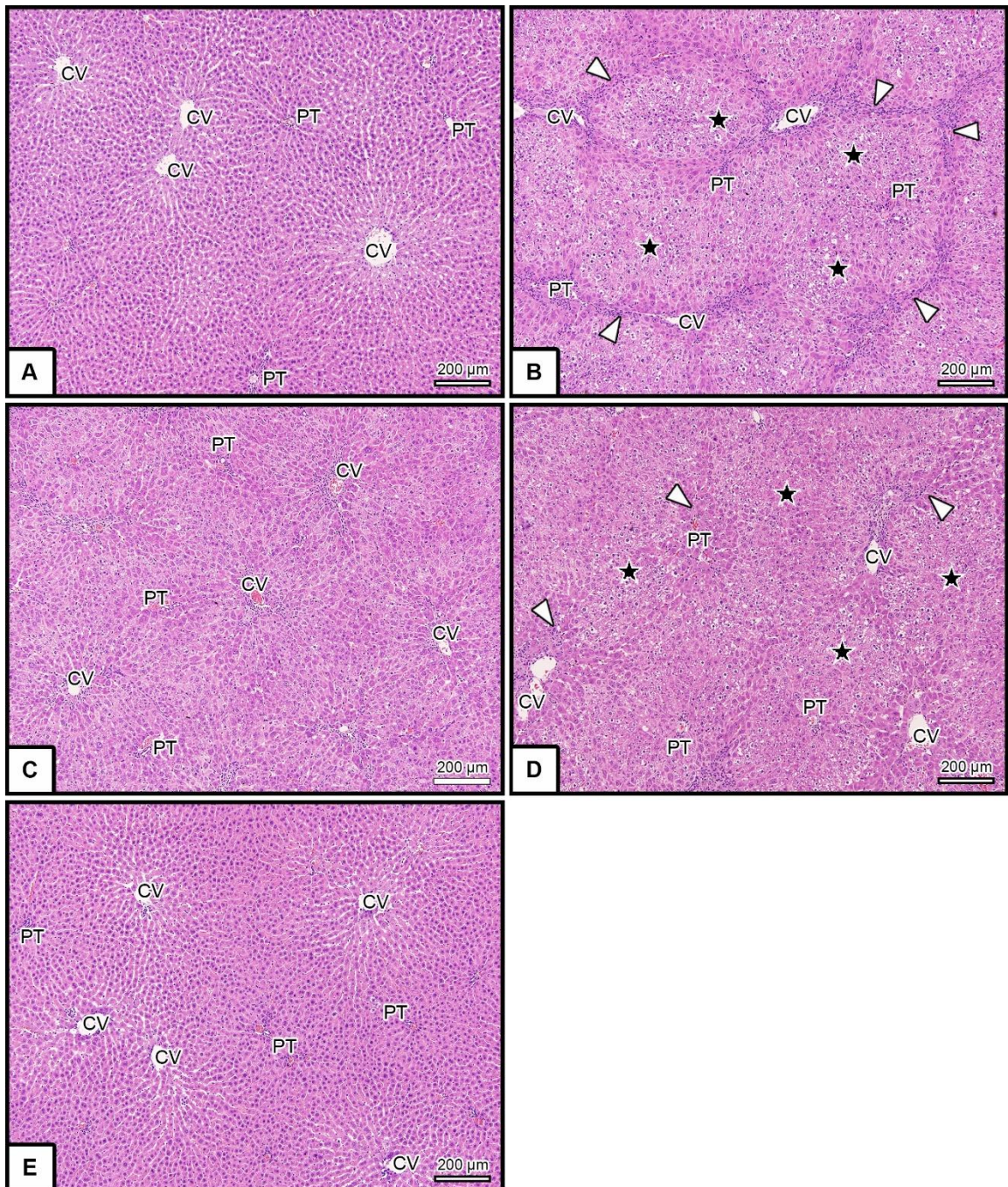


Figure 33 Light micrographs of the liver sections stained with H&E

From the control group (A), TAA group (B), TAA+Probiotics group (C), TAA+Silymarin group (D), and Probiotics only group (E). A and E showed normal histomorphology of liver whereas B showed the typical pattern of centrilobular necrosis (black stars) and accumulation of myofibroblast-like cells (white arrowheads) after TAA-

induced liver fibrosis for 8 weeks. The TAA group (B) showed more severe liver inflammation than the TAA+Probiotics group (C) or the TAA+Silymarin group (D).
CV=central vein, PT=portal triads.



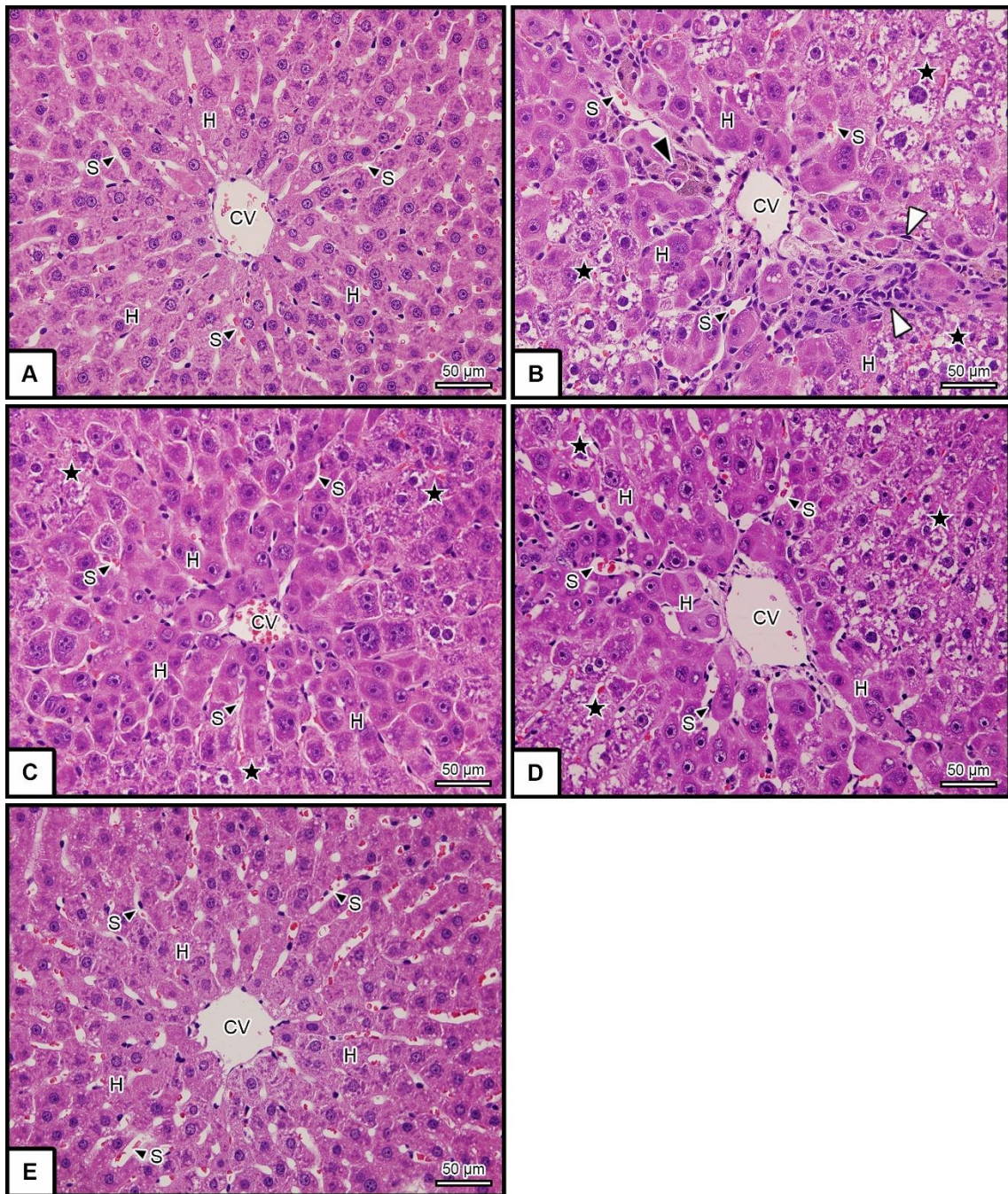


Figure 34 Light micrographs at higher magnification of the liver sections stained with H&E

From the control group (A), TAA group (B and F), TAA+Probiotics group (C), TAA+Silymarin group (D), and Probiotics only group (E). A and E showed normal histomorphology of liver whereas B showed the typical pattern of centrilobular necrosis

(black stars), accumulation of myofibroblast-like cells (white arrowheads), and brownish cytoplasmic vacuoles cells (black asterisks) after TAA-induced liver fibrosis for 8 weeks. The TAA group (B) showed more severe liver inflammation than the TAA+probiotics group (C) and or the TAA+silymarin group (D). CV= central vein, H=hepatocytes, PT=portal triads (PT), and S=sinusoid. S could be recognized in all figures (A to E).



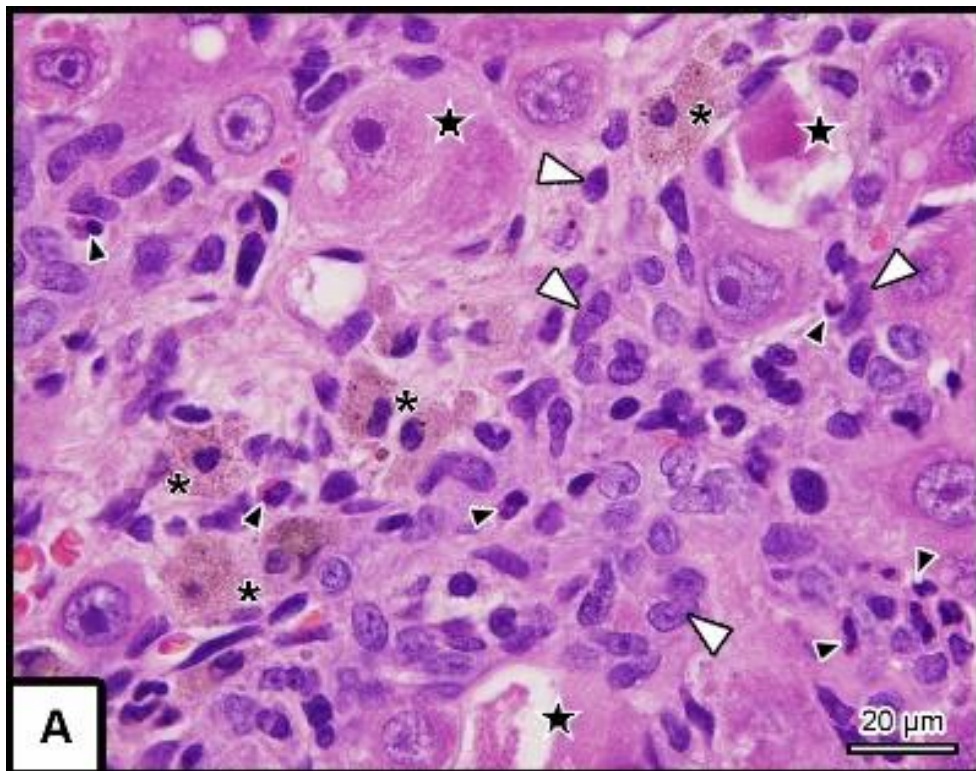


Figure 35 Light micrographs at higher magnification of the liver sections stained with H&E in TAA group

A showed the typical pattern of centrilobular necrosis (black stars), accumulation of myofibroblast-like cells (white arrowheads), leukocyte infiltration (dark arrowheads), and brownish cytoplasmic vacuoles cells (black asterisks) after TAA-induced liver fibrosis for 8 weeks.

4. Effects of probiotics on collagen deposition in liver tissues.

Sirius red staining in the liver sections of the control and the probiotics only groups revealed the presence of the collagen fibers only around the vessels and bile ducts (Figures 37A and 38A). The percentage of collagen area in the control and the probiotics only groups was 14 ± 0.72 and 16 ± 1.4 , respectively (Figure 39). This, however, was equivalent to fibrotic score 0 according to Ishak score (Figure 36). In contrast, the liver sections of TAA-treated rats revealed the presence of collagen fibers arranged into thick connective tissue septa which invaded the liver parenchyma, leading to the formation of many hepatocellular micronodules (Figures 37B and 38B). This was the typical feature of fibrotic liver with the Ishak score of 3 to 4 (Figure 36). The percentage of such collagen fibers in the TAA-treated group accounted for $28\pm 2.6\%$ which was significantly higher than the control group ($P<0.01$, Figure 39).

In the animals of TAA+probiotics (Figures 37C and 38C) and TAA+silymarin groups (Figures 37D and 38D). The collagen fibers formed as only a few tiny, short septa with some fibers distributed around blood vessels. The percentage of the total collagen contents in the TAA+probiotics ($19\pm 1.9\%$) and TAA+silymarin ($16\pm 0.42\%$) groups was significantly lower than those in the TAA-treated group ($P<0.01$, Figure 39). The fibrotic score of the TAA+probiotics group (1.6 ± 0.22) was a bit lower than that in the TAA+silymarin group (1.8 ± 0.2) (Figure 36).

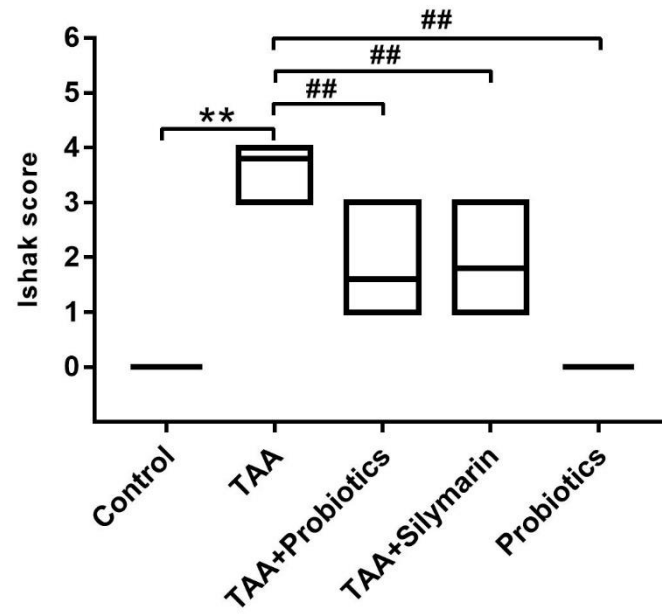


Figure 36 Box plots of Ishak score according to liver fibrosis stage

Ishak scores ranged from 0 to 6. The data are presented as the mean \pm S.E.M.

** $P < 0.01$ compared with the control group; ## $P < 0.01$ compared with the TAA-treated group.

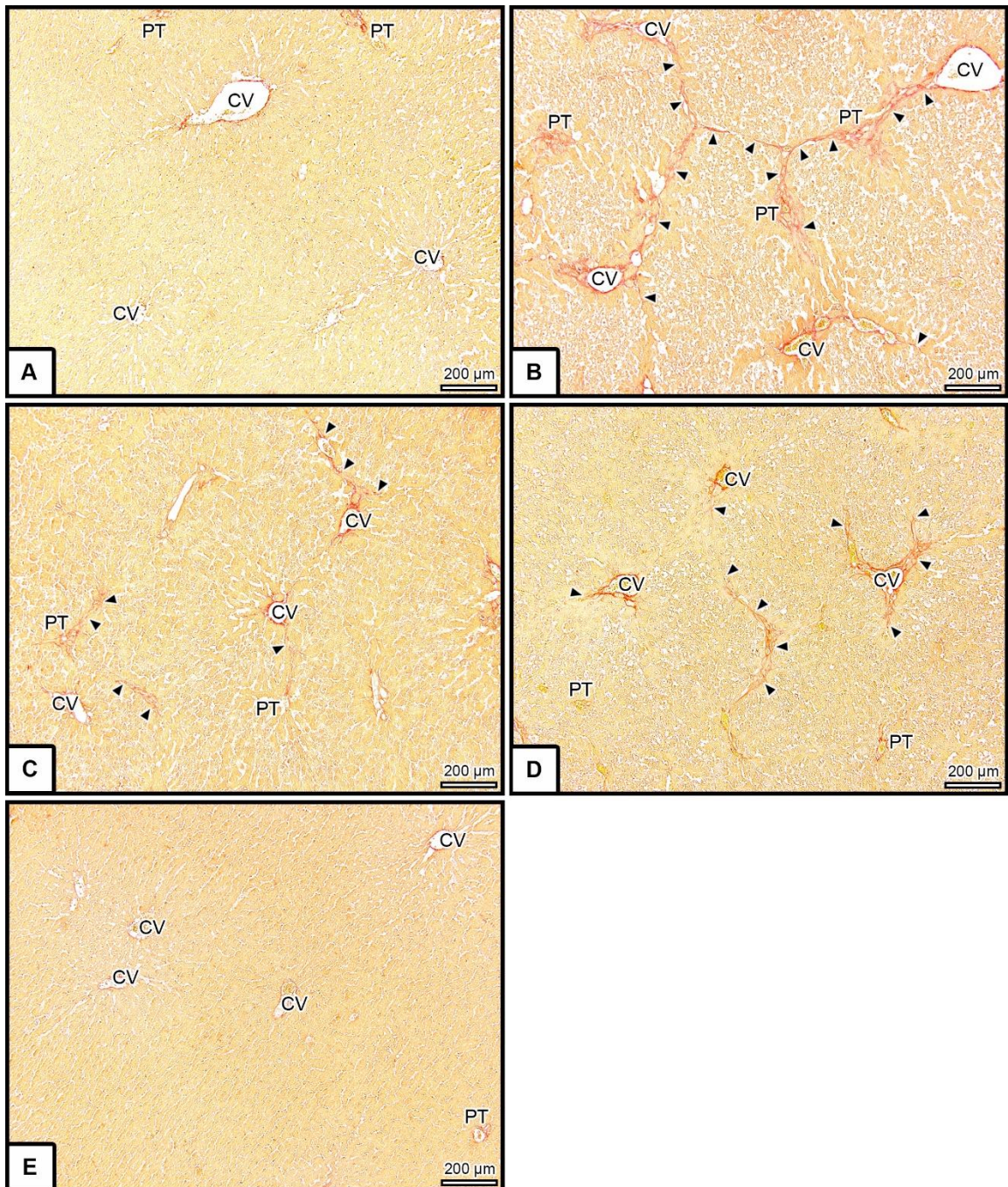


Figure 37 Photomicrograph of the liver sections stained with Sirius red

From the control group (A) and probiotics only group (E) showing the collagen fibers deposition around the central vein (CV) and portal triads (PT). Collagen fibers with bridging fibrosis (black arrowheads) were observed in TAA-treated group (B). Only short septa of the collagen fibers (black arrowheads) were illustrated in both the

TAA+probiotics (C) and TAA+silymarin (D) groups Note the red color staining in the collagen fibers.



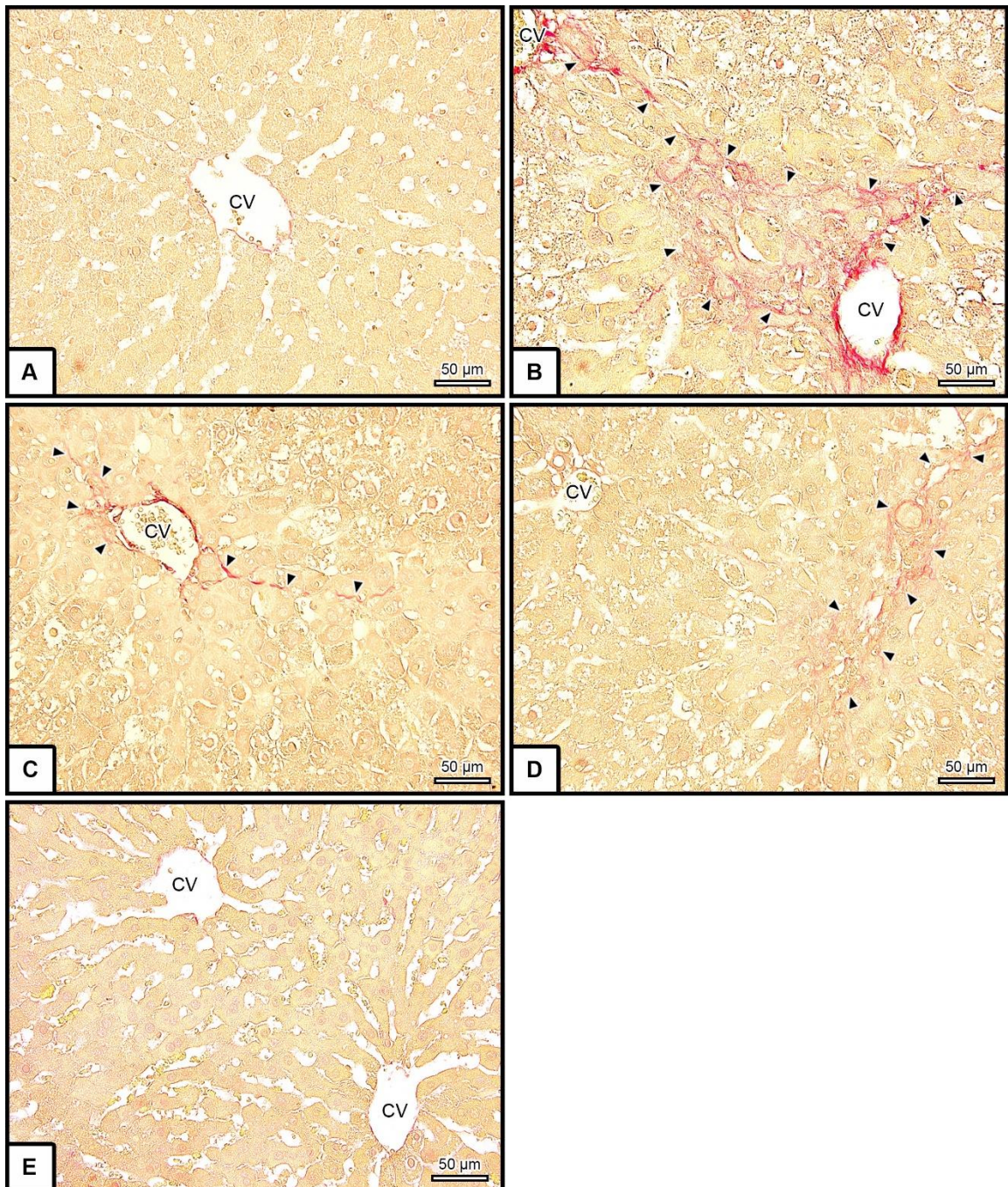


Figure 38 Photomicrograph with higher magnification of the liver sections stained by with Sirius red

From the control group (A) and probiotics only group (E) showing the collagen fibers deposited deposition around the central vein (CV) and portal triads (PT). TAA group (B) was accumulation of collagen fibers with bridging fibrosis (black arrowheads)

could be were observed in TAA-treated group (B). Only short septa of the collagen fibers (black arrowheads) were illustrated in both the TAA+probiotics group (C) and TAA+silymarin group (D) illustrating collagen fibers which appeared as short septa (black arrowhead). Note: The collagen fibers were stained in red color.



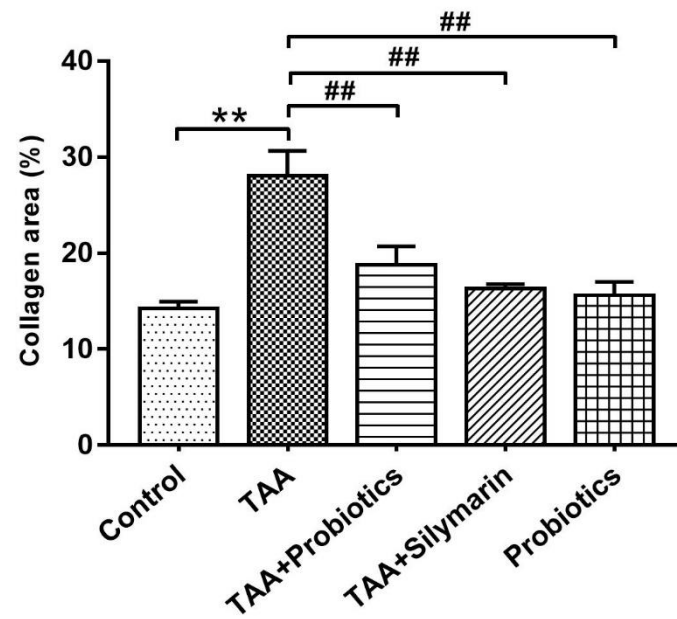


Figure 39 Quantitative analysis of comparison of the percentage of fibrotic collagen areas in the Sirius-red stained liver section of all animal different groups

The collagen areas were identified by color threshold in the Cell Sense Dimensions software and calculated as a percentage of the total collagen area. The data are presented as the mean \pm S.E.M. ** $P < 0.01$ compared with the control group; and ## $P < 0.01$ compared with the TAA-treated group.

5. Effects of probiotics on lipid peroxidation in liver tissues.

Malondialdehyde (MDA) is a product of lipid peroxidation following oxidative damage to cell structures that lead to cell death. After TAA administration, the hepatic concentration of MDA was significantly increased compared with the control group ($P < 0.05$, Figure 40). The MDA concentration in the TAA+probiotics group was significantly lower than that in the TAA group ($P < 0.05$, Figure 40). There was no difference in hepatic MDA concentration between the control and probiotics groups.

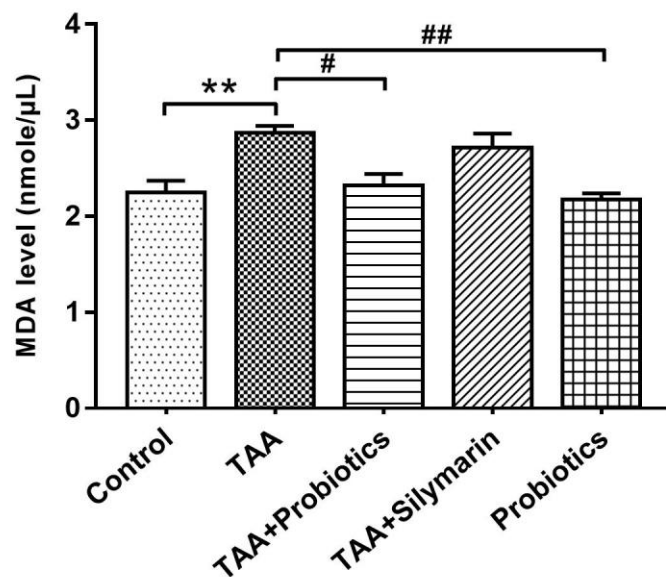


Figure 40 Levels of serum malondialdehyde (MDA) (nmol/ul) in all animal groups

The data are presented as the mean \pm S.E.M. $**P < 0.01$ compared with the control group; $^{\#}P < 0.05$ and $^{\#\#}P < 0.01$ compared with the TAA-treated group.

6. Effects of probiotics on the expression of TNF- α , TGF- β 1, and α -SMA proteins in liver tissues.

Immunohistochemistry

TNF- α , TGF- β 1, and α -SMA have been reported to be important for the development of hepatic fibrosis. Their expressions in rat liver tissue were determined by using immunohistochemical technique. The expression of each protein in term of the staining intensity was summarized in Table 10.

Table 10 The percentage of positive staining intensity quantified for the TNF- α , TGF- β 1, and α -SMA expressions in the liver tissue sections of all animal groups

Parameters	Groups				
	Control	TAA	TAA+Probiotics	TAA+Silymarin	Probiotics
TNF- α	19 \pm 0.35	21 \pm 0.40**	20 \pm 0.37 [#]	20 \pm 0.20	19 \pm 0.17 [#]
TGF- β 1	20 \pm 0.09	22 \pm 0.37**	21 \pm 0.25 [#]	21 \pm 0.37 [#]	20 \pm 0.28 ^{##}
α -SMA	18 \pm 0.26	25 \pm 0.37**	20 \pm 0.37 ^{##}	21 \pm 0.41 ^{##}	19 \pm 0.19 ^{##}

The data are presented as the mean \pm S.E.M. ** P < 0.01 compared with the control group; [#] P < 0.05 and ^{##} P < 0.01 compared with the TAA-treated group.

6.1 Distribution of the TNF- α immunoreactivity

TNF- α is a proinflammatory cytokine involved in fibrogenesis. In the control and the probiotics groups, very mild immunoreactivity for TNF- α was shown (Figures 41A, 41E). Positive areas of TNF- α were found in the cytoplasm of hepatocytes (Figure 42A, 42E). The positive staining intensity of TNF- α in the control and the probiotics groups was 19 \pm 0.35 and 19 \pm 0.17 %, respectively (Figure 43).

After TAA administration, the strong immunoreactivity of TNF- α was found in most areas of the liver sections of both parenchymal and non-parenchymal cells (Figures 41B, 42B). The percentage of positive staining intensity of TNF- α in the

TAA treated group was significantly higher than that in the control group ($P<0.01$, Table 10).

Similarly, the immunoreactivity of TNF- α in the TAA+probiotics and TAA+silymarin groups was also found in the cytoplasm of parenchymal and nonparenchymal cells. The immunopositive staining areas of TNF- α in those two groups were lesser than that of in the TAA-treated group (Figures 41C, 41D, 42C, 42D). However, of the two groups, only the TAA+probiotics group showed significantly lower than that in the TAA group ($P<0.05$) (Table 10).



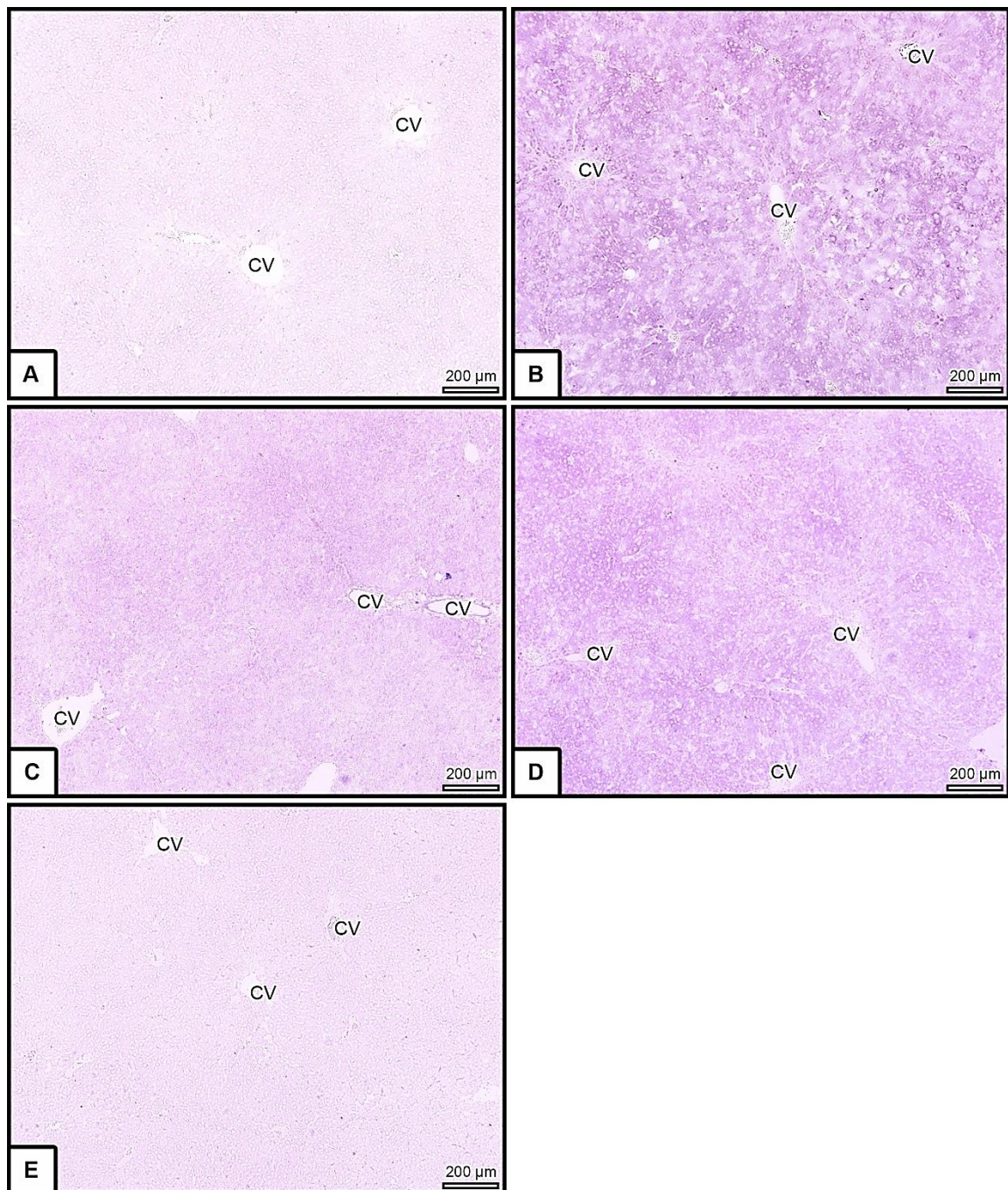


Figure 41 Photomicrographs showing immunoreactivity of TNF- α in rat liver sections of all animal groups

Positive immunostaining of TNF- α was strongest in the TAA-treated group (B), moderate in the TAA+Probiotics (C) and TAA+Silymarin (D) groups while very weak in the control (A) and probiotics only (E) groups. CV= central vein.

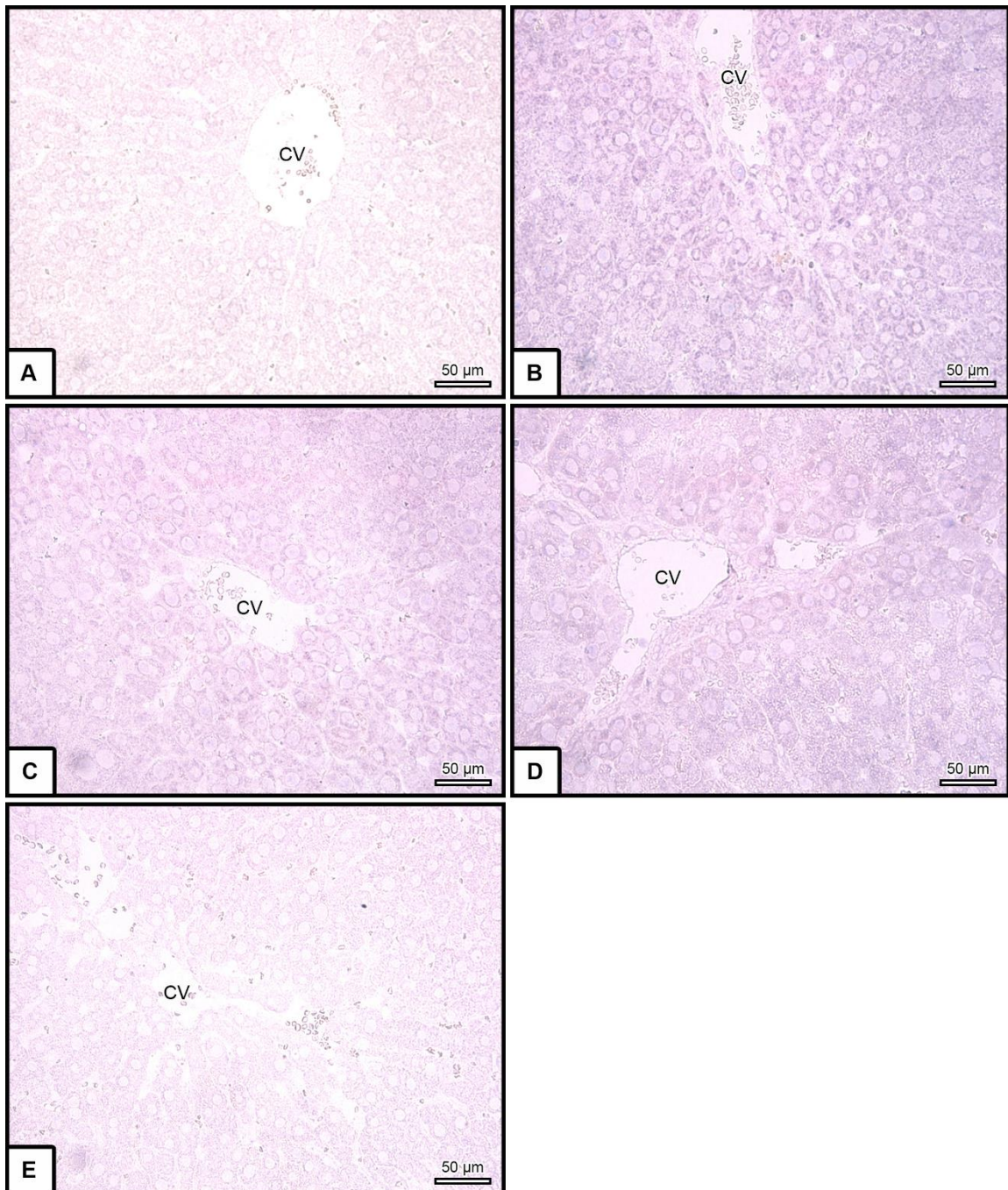


Figure 42 Photomicrographs at higher magnification showing immunoreactivity of TNF- α in rat liver sections of all animal groups

Positive immunostaining of TNF- α was strongest in the TAA-treated group (B), moderate in the TAA+Probiotics (C) and TAA+Silymarin (D) groups while very weak in the control (A) and probiotics only (E) groups. CV= central vein.

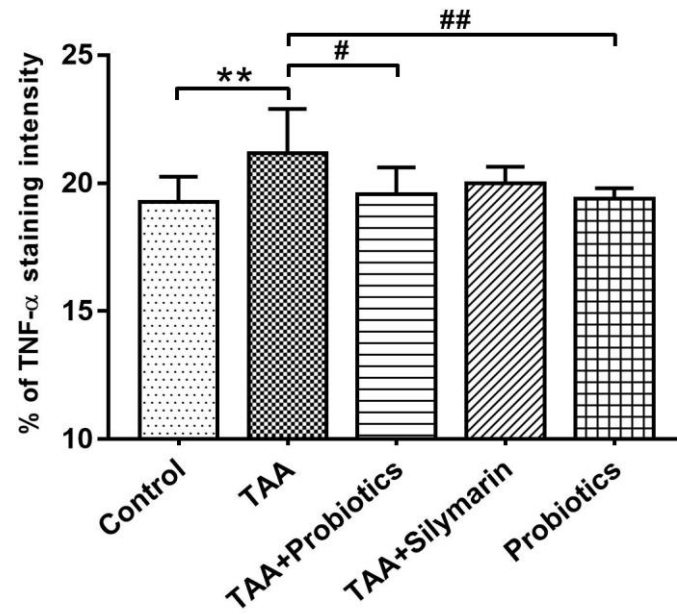


Figure 43 Quantitative analysis of TNF- α expression was shown as a percentage of positive staining intensity

The data are presented as the mean \pm S.E.M. $**P < 0.01$ compared with the control group; $\# P < 0.05$ and $##P < 0.01$ compared with the TAA-treated group.

6.2 Distribution of the TGF- β 1 immunoreactivity

TGF- β 1 is the major stimulus cytokine for HSCs to synthesize extracellular matrix in the fibrotic liver. The immunoexpression of TGF- β 1 was present in the cytoplasm of both parenchymal (hepatocyte) and non-parenchymal cells in all animal groups. However, its immunoreactivity intensity was varied among groups. Such intensity was strongest in the TAA-treated group ($22\pm 0.37\%$), being moderate in the TAA+probiotics ($21\pm 0.25\%$) and TAA+silymarin ($21\pm 0.37\%$) groups and was only mild in the control ($20\pm 0.09\%$) and probiotics ($20\pm 0.28\%$) groups (Figures 44-46, Table 10).



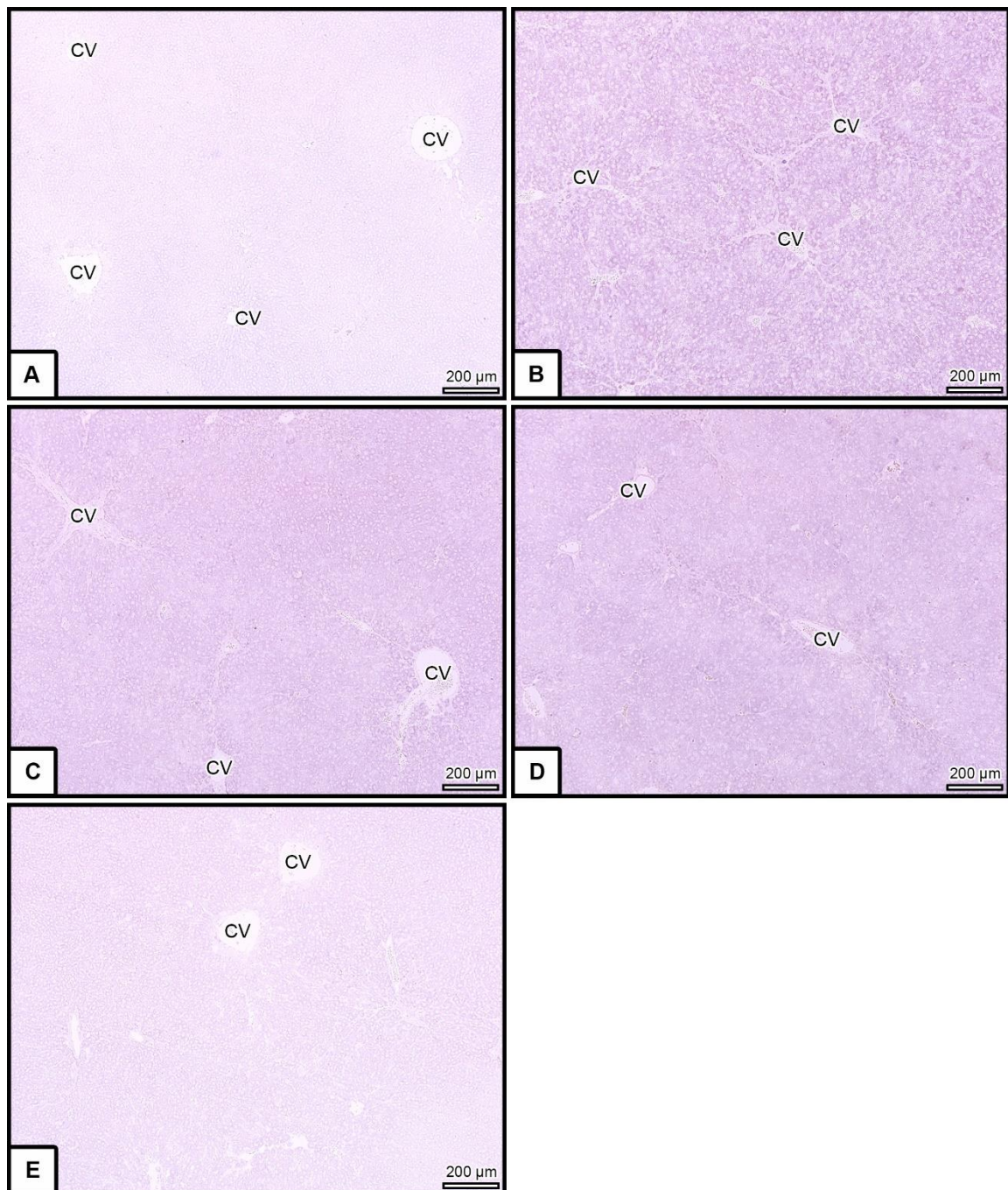


Figure 44 Photomicrographs showing immunoreactivity of TGF- β 1 in rat liver sections of all animal groups

Positive immunostaining of TGF- β 1 was strongest in the TAA-treated group (B), moderate in the TAA+Probiotics (C) and TAA+Silymarin (D) groups while very weak in the control (A) and probiotics only (E) groups. CV= central vein.

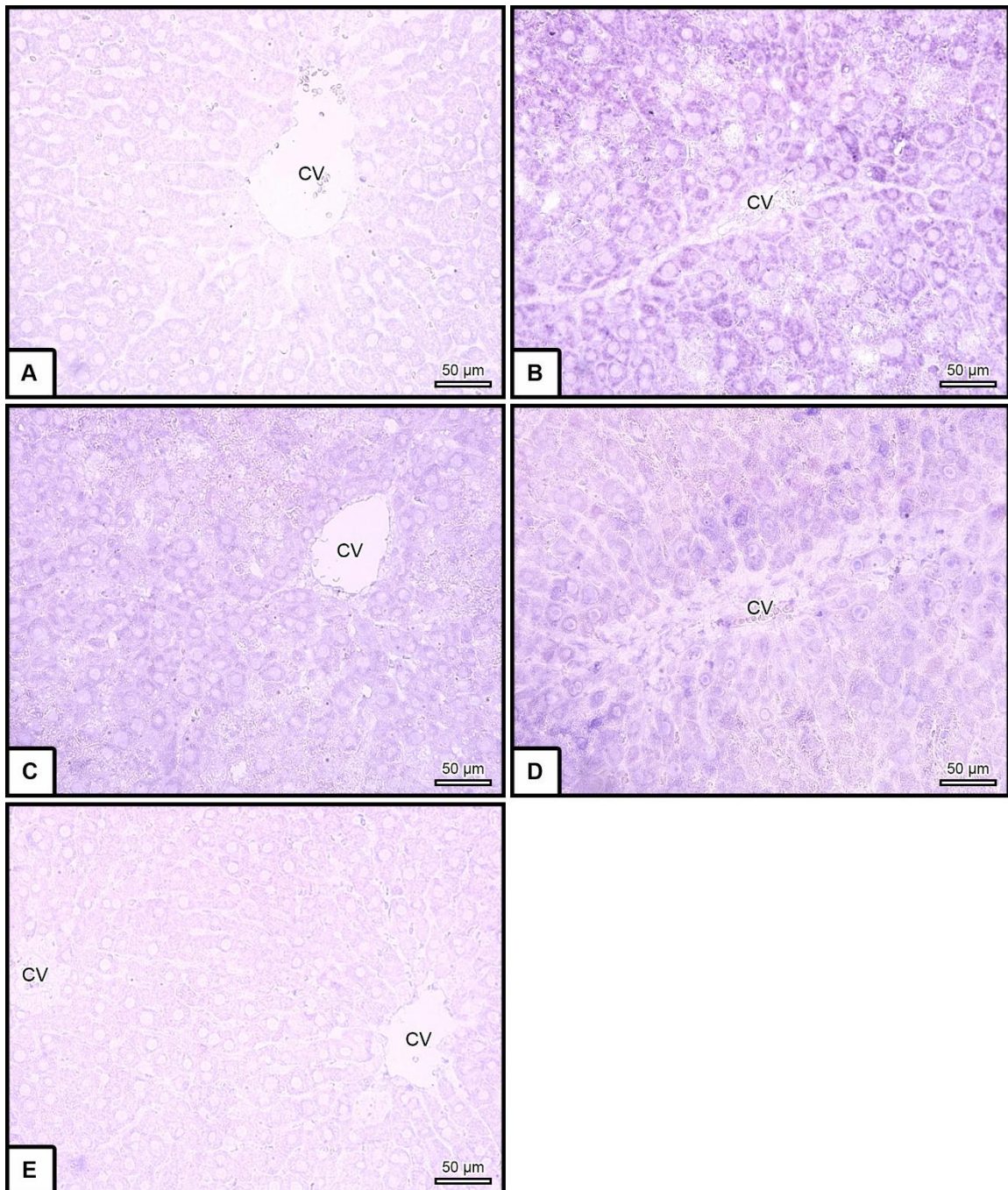


Figure 45 Photomicrographs at higher magnification showing immunoreactivity of TGF- β 1 in rat liver sections of all animal groups

Positive immunostaining of TGF- β 1 was strongest in the TAA-treated group (B), moderate in the TAA+Probiotics (C) and TAA+Silymarin (D) groups while very weak in the control (A) and probiotics only (E) groups. CV= central vein.

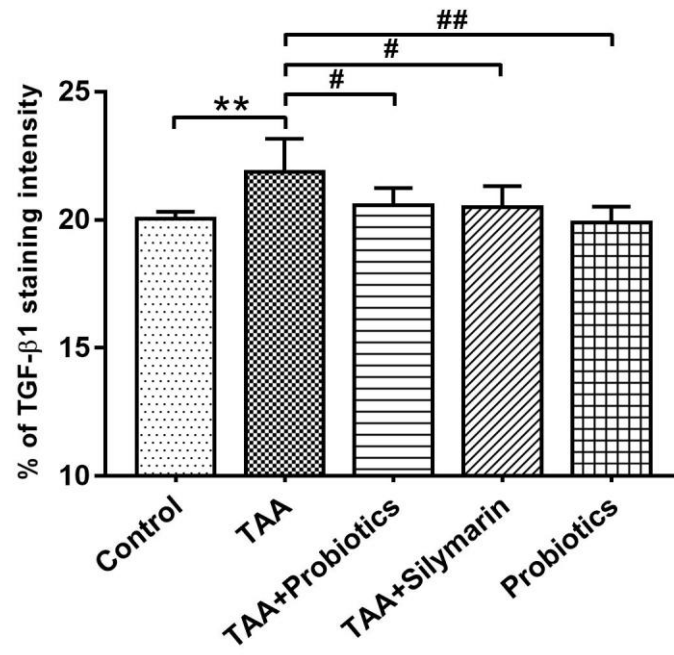


Figure 46 Quantitative analysis of TGF- β 1 expression was shown as a percentage of positive staining intensity

The data are presented as the mean \pm S.E.M. ** P < 0.01 compared with the control group; # P < 0.05 and ## P < 0.01 compared with the TAA-treated group.

6.3 Distribution of the α -SMA immunoreactivity

The α -SMA is a marker for HSCs activation. The higher percentage of its expression reflected the higher number of activated hepatic cells presented in the fibrotic area. The immunoreactivity of α -SMA was very mild in the control group (18 ± 0.26 %) and mild in the probiotics (19 ± 0.19 %) groups which was present mainly around blood vessels and bile ducts in portal triads area (Figures 47A, 47E, 48A, 48E) In contrast, the immunostaining of α -SMA in the TAA-treated group was observed in the fibrotic area and pericentral zone (Figures 47B, 48B) and its staining intensity (25 ± 0.37 %) was significantly increased when compared with the control group ($P < 0.01$ and Figure 49). Interestingly only moderate immunoreactivity of α -SMA was analyzed in the TAA+probiotics (20 ± 0.37 %) and TAA+silymarin (21 ± 0.41 %) groups and was presented in the cytoplasm of parenchymal and non-parenchymal cells particularly in the pericentral zones of the liver sections (Figures 47C, 47D, 48C, 48D). The percentage of positive staining intensity of α -SMA in both the TAA+probiotics and TAA+silymarin groups was significantly lower when compared with the TAA group ($P < 0.01$, Figure 49, Table 10).

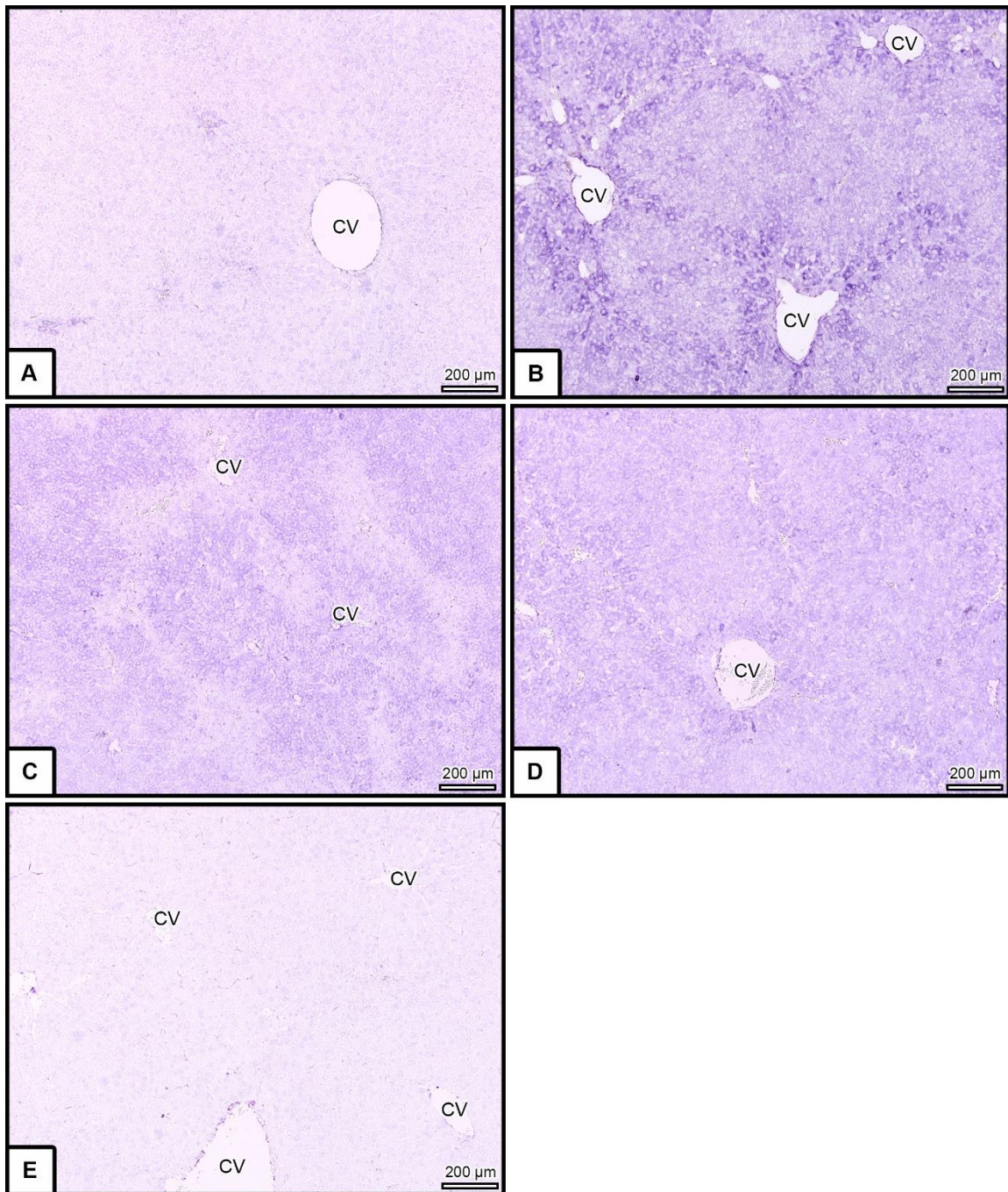


Figure 47 Photomicrographs at higher magnification showing immunoreactivity of α -SMA in rat liver sections of all animal groups

Positive immunostaining of α -SMA was strongest in the TAA-treated group (B), moderate in the TAA+Probiotics (C) and TAA+Silymarin (D) groups while very weak in the control (A) and probiotics only (E) groups. CV= central vein.

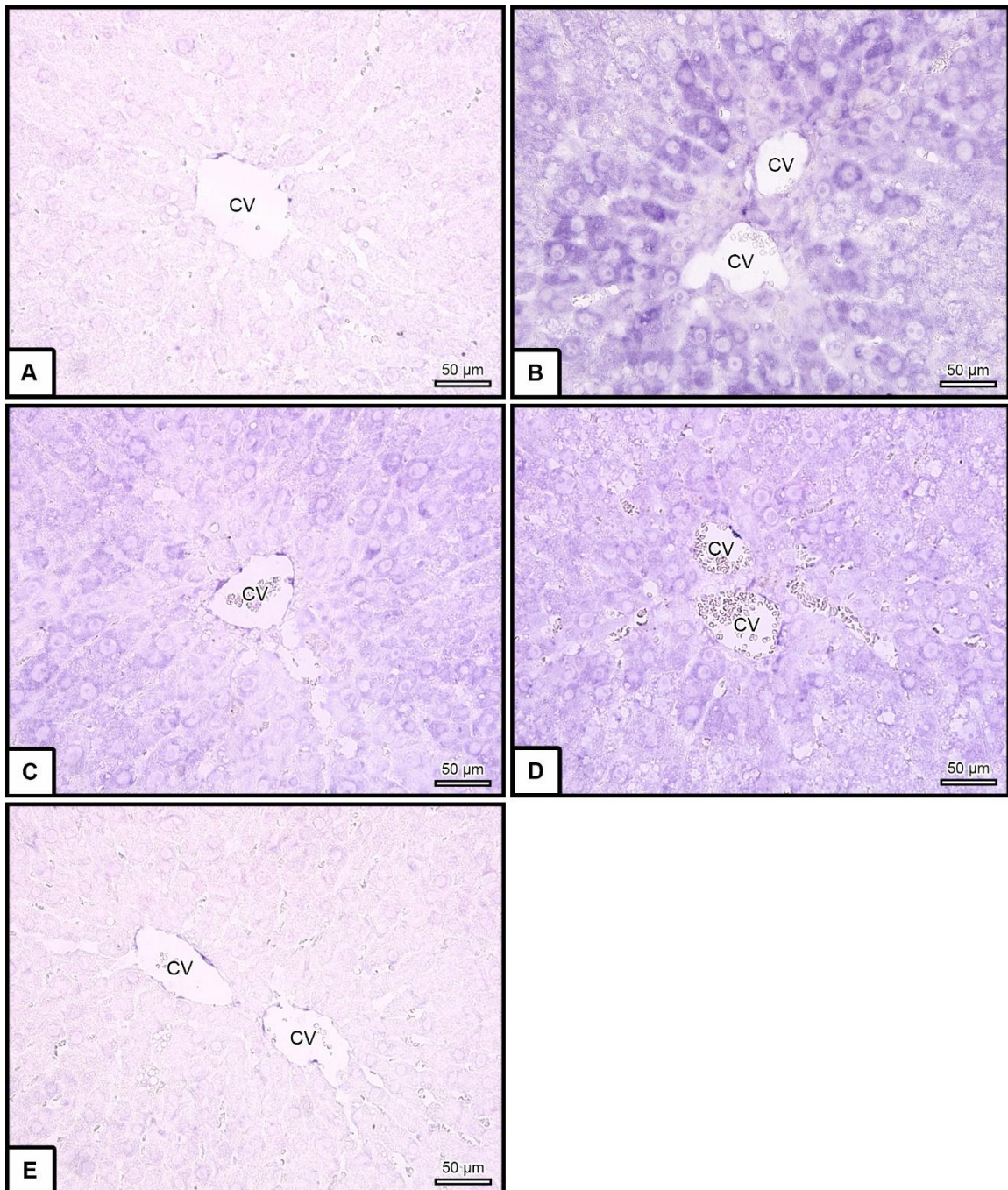


Figure 48 Photomicrographs at higher magnification showing immunoreactivity of α -SMA in rat liver sections of all animal groups

Positive immunostaining of α -SMA was strongest in the TAA-treated group (B), moderate in the TAA+Probiotics (C) and TAA+Silymarin (D) groups while very weak in the control (A) and probiotics only (E) groups. CV= central vein.

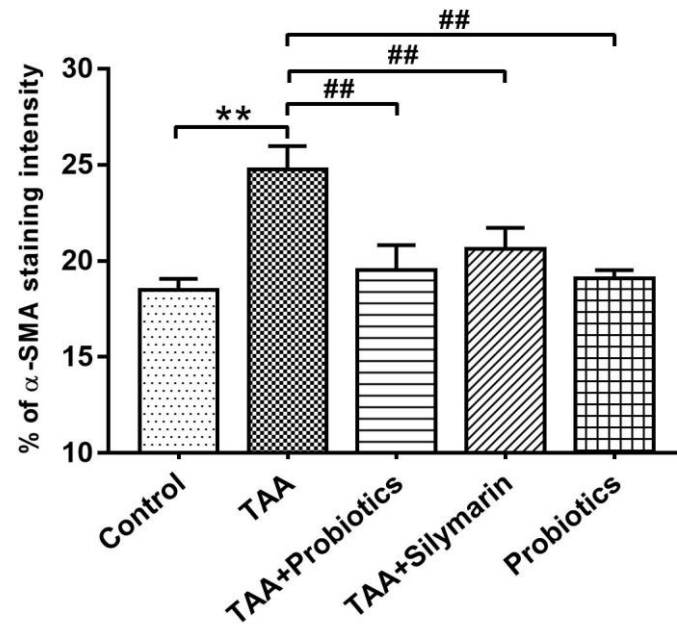


Figure 49 Quantitative analysis of α -SMA expression was shown as a percentage of positive staining intensity

The data are presented as the mean \pm S.E.M. ** P < 0.01 compared with the control group; and ## P < 0.01 compared with the TAA-treated group.

Western blot analysis

The hepatic contents of TNF- α , TGF- β 1, and α -SMA proteins were used as inflammation and fibrogenesis markers, and were determined by Western blot analysis. In the TAA group expressions of TNF- α , TGF- β 1, and α -SMA proteins were increased to 203 \pm 12, 219 \pm 35, and 547 \pm 67 % of the control group, respectively. In the TAA+silymarin group, the TNF- α protein content had decreased to a similar extent as that in of the TAA+probitoics group. In contrast, TGF- β 1 protein content in the TAA+probitoics and TAA+silymarin groups were decreased, but not significantly different from the TAA group. In the probiotics-only group, TNF- α , TGF- β 1, and α -SMA protein contents were not significantly different from the control group. The expression and the quantitative analysis of TNF- α , TGF- β 1, and α -SMA are illustrated in Figures 50-52 and Table 11.

Table 11 Comparison of the relative quantitative analysis of TNF- α , TGF- β 1, and α -SMA expression (% of control) in liver tissues

Parameters	Groups				
	Control	TAA	TAA+Probitoics	TAA+Silymarin	Probitoics
TNF- α	100 \pm 0.00	203 \pm 12**	123 \pm 16 [#]	133 \pm 22 [#]	97 \pm 13 ^{##}
TGF- β 1	100 \pm 0.00	219 \pm 35**	135 \pm 6 [#]	144 \pm 9	113 \pm 9 ^{##}
α -SMA	100 \pm 0.00	547 \pm 67**	285 \pm 50 [#]	380 \pm 70	85 \pm 17 ^{##}

The data are presented as the mean \pm S.E.M. ** P < 0.01 compared with the control group; [#] P < 0.05 and ^{##} P < 0.01 compared with the TAA-treated group.

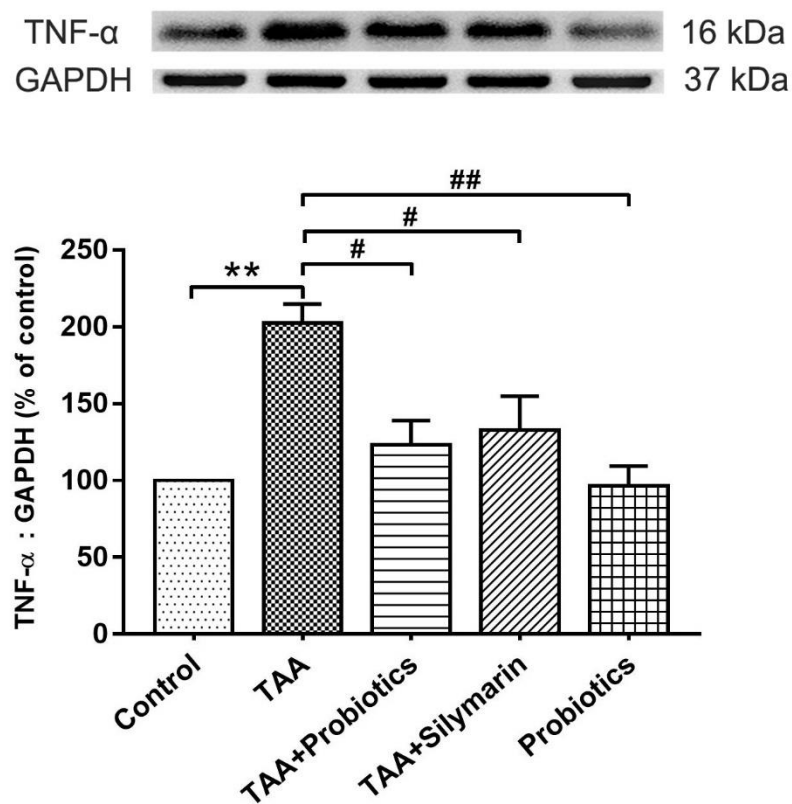


Figure 50 Hepatic TNF- α protein content was measured by Western blot analysis

Representative bands from each of the five groups were shown. The protein bands were quantified by densitometry and normalized relative to GAPDH content. All Western blot data were shown as a percentage of the control. The data are presented as the mean \pm S.E.M. $**P < 0.01$ compared with the control group; $\#P < 0.05$ and $##P < 0.01$ compared with the TAA-treated group.

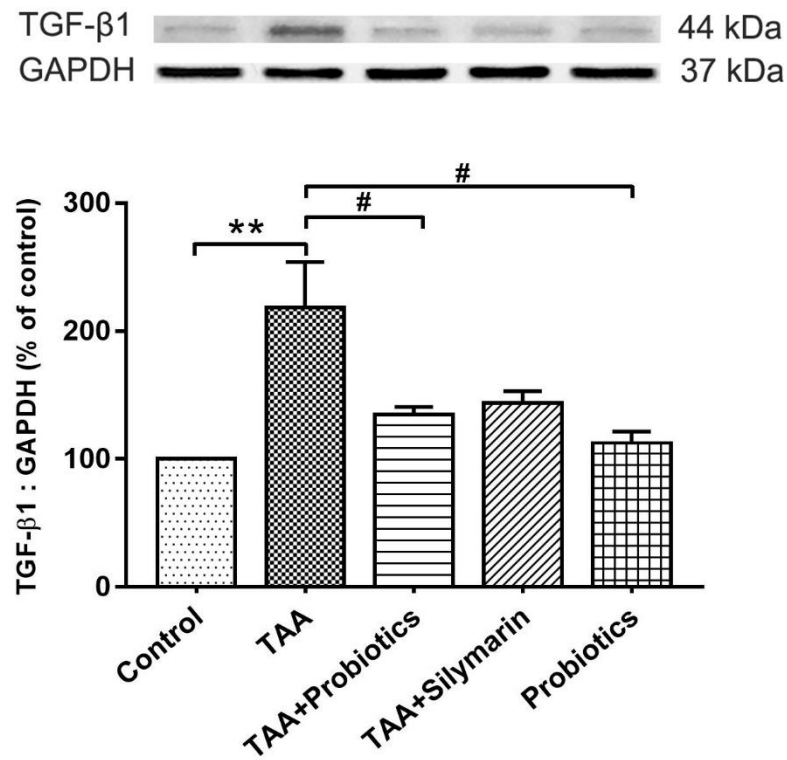


Figure 51 Hepatic TGF- β 1 protein content was measured by Western blot analysis

Representative bands from each of the five groups were shown. The protein bands were quantified by densitometry and normalized relative to GAPDH content. All Western blot data were shown as a percentage of the control. The data are presented as the mean \pm S.E.M. $**P < 0.01$ compared with the control group; $\#P < 0.05$ compared with the TAA-treated group.

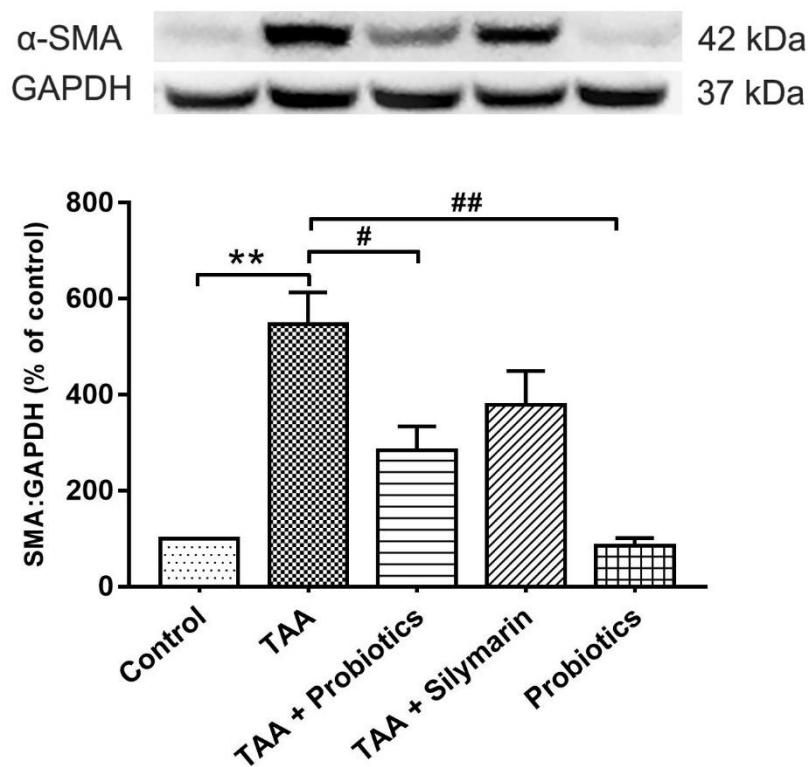


Figure 52 Hepatic α -SMA protein content was measured by Western blot analysis

Representative bands from each of the five groups were shown. The protein band were quantified by densitometry and normalized relative to GAPDH content. All Western blot data were shown as a percentage of the control. The data are presented as the mean \pm S.E.M. ** P < 0.01 compared with the control group; # P < 0.05 and ## P < 0.01 compared with the TAA-treated group.

7. Effects of probiotics on the mRNA expression of *Tnf*, *Tgfb1*, and *Acta2* genes in liver tissues.

The mRNA expression levels of *Tnf*, *Tgfb1*, and *Acta2* genes were determined by real-time PCR and normalized to *Actb* mRNA. The mRNA levels of each gene were expressed as values relative to the mRNA level of control. The results from real-time PCR were summarized in Table 12

Table 12 The real-time PCR analysis of the *Tnf*, *Tgfb1*, and *Acta2* mRNA expression levels in liver tissues of all five animal groups

Parameters	Groups				
	Control	TAA	TAA+Probiotics	TAA+Silymarin	Probiotics
<i>Tnf</i>	1±0.00	2.0±0.20**	1.2±0.11 ^{##}	1.3±0.07 ^{##}	1.1±0.05 ^{##}
<i>Tgfb1</i>	1±0.00	1.5±0.08**	1.2±0.06 [#]	1.3±0.09	1.1±0.01 ^{##}
<i>Acta2</i>	1±0.00	4.7±0.75**	2.2±0.36 [#]	3.3±0.90	1.2±0.27 ^{##}

The data are presented as the mean ± S.E.M. ** $P < 0.01$ compared with the control group; [#] $P < 0.05$ and ^{##} $P < 0.01$ compared with the TAA-treated group.

Tnf mRNA

The level of *Tnf* mRNA expression was significantly two-folds increased in the TAA group compared with control group ($P < 0.01$, Figure 53). In contrast, its expression in the TAA+probiotics and TAA+silymarin groups were significantly decreased compared with TAA group ($P < 0.01$, Figure 53). However, there was no difference in the mRNA expression levels of this inflammation marker between the control and probiotics groups.

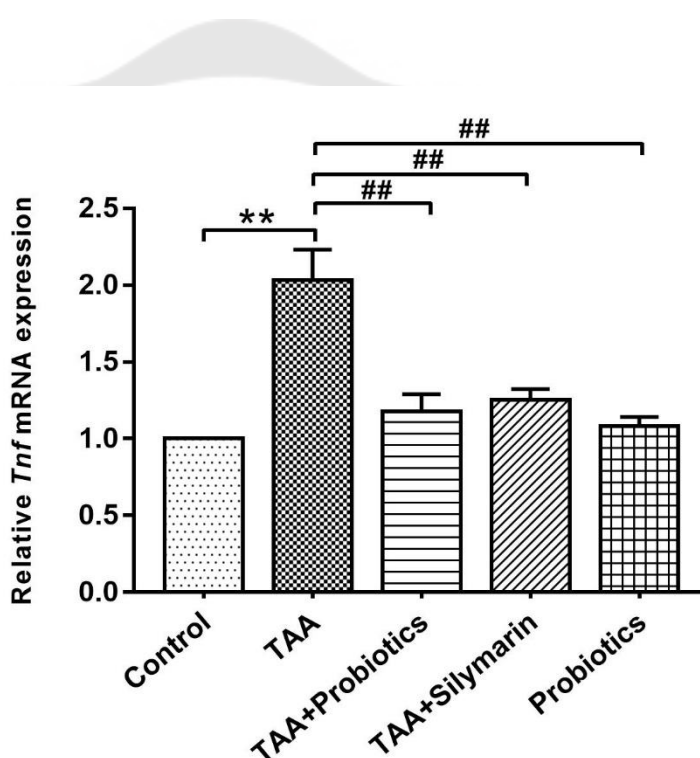


Figure 53 Quantitative real-time PCR analysis of the *Tnf* mRNA expression level in liver tissues

The mRNA level was normalized to *Actb* mRNA and expressed as relative values with respect to the mRNA of control. The data are presented as the mean \pm S.E.M. ** $P < 0.01$ compared with the control group; ## $P < 0.01$ compared with the TAA-treated group.

Tgfb1 mRNA

As expected, the level of *Tgfb1* mRNA expression was significantly increased in the TAA-treated group compared with the control group ($P < 0.01$, Figure 54). Its expression in the TAA+probiotics group was significantly lower than the TAA group ($P < 0.05$, Figure 54). Even though the mRNA expression level of this fibrogenic marker in the TAA+silymarin group was decreased but it was insignificantly different to the TAA-treated group. The expression of *Tgfb1* mRNA in the probiotics group was not different to that in the control group.

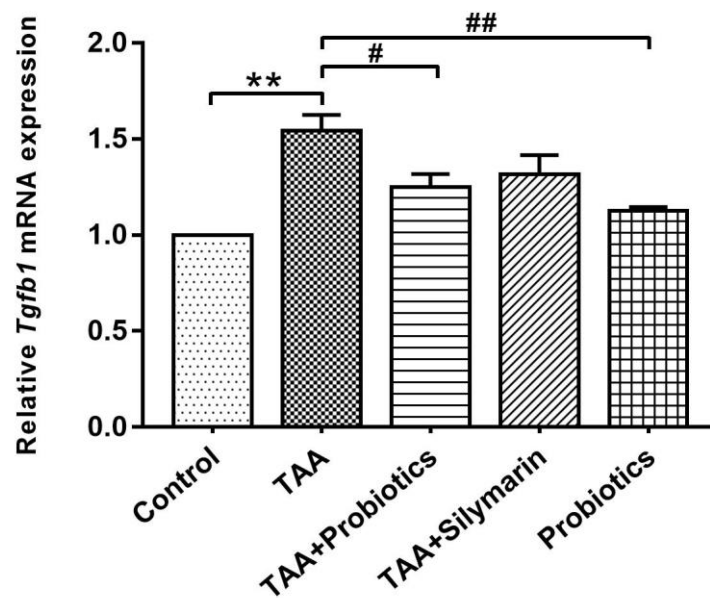


Figure 54 Quantitative real-time PCR analysis of the *Tgfb1* mRNA expression level in liver tissues

Its mRNA level was normalized by *Actb* mRNA and expressed as relative values with respect to the mRNA of control. The data are presented as the mean \pm S.E.M. ** $P < 0.01$ compared with the control group; ## $P < 0.05$ and # $P < 0.01$ compared with the TAA-treated group.

Acta2 mRNA

In the TAA-treated group, the level of *Acta2* mRNA expression was significantly increased compared with the control group ($P < 0.01$, Figure 55). Its expression level in the TAA+probiotics group was significantly decreased compared with the TAA group ($P < 0.05$, Figure 55). However, the mRNA expression level of *Acta2* in the TAA+silymarin group was higher than that in the TAA+probiotics group. There was no difference in expression of *Acta2* mRNA level between the control and probiotics group.

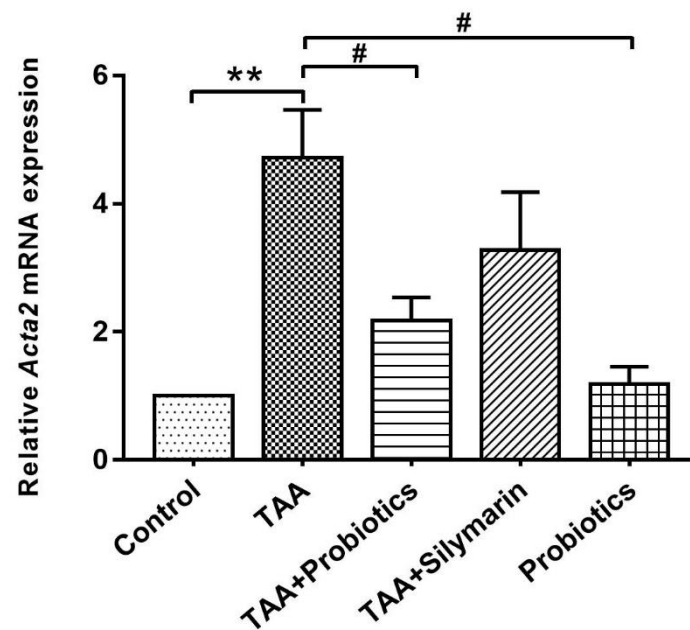


Figure 55 Quantitative real-time PCR analysis of the *Acta2* mRNA expression level in liver tissues

Its mRNA level was normalized by *Actb* mRNA and expressed as relative values with respect to the mRNA of control. The data are presented as the mean \pm S.E.M. ** $P < 0.01$ compared with the control group; # $P < 0.05$ compared with the TAA-treated group

CHAPTER 5

DISCUSSION

Recent studies have shown that probiotics protect against the sequels of common liver diseases such as fibrosis/cirrhosis, alcoholic liver disease, nonalcoholic fatty liver disease, and hepatic encephalopathy.^(60, 61, 126) In the present study, we selected 3 powerful probiotic strains with a strong inhibitory effect on TNF- α production in THP-1 human monocytic cell lines. These strains, *L. paracasei*, *L. casei*, and *W. confusa*, are lactic acid bacteria isolated from feces of a healthy Thai infant.⁽²⁵⁾ The effects of probiotics on gastrointestinal diseases are dependent on the bacterial strain, stage of the disease, dose of the probiotics administered, and the duration of treatment.⁽¹²⁷⁾

Dose of probiotic bacteria administered

The optimal concentration of probiotic bacteria that mediates a good clinical effect is generally stated to be 10^6 – 10^8 CFU/g, or 10^8 – 10^{10} CFU/day.⁽¹²¹⁾ Probiotics concentration at 10^6 CFU/ml and 10^8 CFU/g could lead to obtain a clinical benefit for the small bowel and in the large bowel.⁽¹²⁷⁾ In a preliminary study in fibrotic rats, we found that treatment with each of the used probiotic strains separately at a concentration of 10^9 CFU/day was most effective. At that concentration, the rats did not develop diarrhea, but produced normal-looking feces with a soft and smoothness texture. A concentration of 10^9 CFU/day for each of the probiotic bacteria used was also recommended by the Canadian Food Inspection Agency.⁽¹²⁸⁾ An earlier study with a combination of three live probiotic bacteria (*L. acidophilus*, *L. plantarum*, and *S. thermophiles*) at a concentration of 10^9 CFU/g p.o. for each of the bacteria has also been reported to confer hepatoprotective effects.⁽²⁴⁾ Similarly, addition viable *S. cerevisiae* and *L. acidophilus*, both at 10^9 CFU/g, has been reported to protect against liver fibrosis,⁽²²⁾ while treatment with 10^9 CFU/day of *L. johnsonii* La1 appears to exert antioxidant activity on intestinal flora, and reduction of endotoxemia and bacterial translocation in cirrhotic rats.⁽²³⁾

Beneficial effects of *Lactobacilli*

Lactobacilli are widely used in the probiotic research to prevent or treat various diseases. *L. casei*, *L. paracasei*, and *L. rhamnosus* are the most widely used probiotic *Lactobacillus* species in research and industry.⁽¹²⁹⁾ The probiotic *L. casei* bacterium may improve the antioxidant status and minimize the effects of oxidative stress in liver and red blood cells of rats,⁽¹³⁰⁾ and reduce lipopolysaccharide/d-galactosamine-induced production of proinflammatory cytokines and hepatic inflammation via modulation of the TLR-MAPK-PPAR- γ signaling pathways.⁽¹³¹⁾ *L. casei* CRL 431 reportedly exerts an antiinflammatory response in high-fat diet-induced obese mice by decreasing the expression of pro-inflammatory cytokines, such as IL-6, IL-17 and TNF- α .⁽¹³²⁾ Analogously, *L. casei* Shirota is reported to suppress liver inflammation and fibrosis induced by a methionine-choline-deficient (MCD) diet in a rat model by lowering the expression of α -SMA, TNF- α , and TIMP-1.⁽³³⁾ , while *L. paracasei* 9 Jlus66 appears to have a similar effect.⁽¹³³⁾ *L. acidophilus* and *L. casei* isolated from fresh cow milk decreases serum alanine aminotransferase (ALT) in enterotoxigenic *E. coli*-infected rats.⁽¹³⁴⁾ The combination of *L. paracasei* GMNL-32, *L. reuteri* GMNL-89, and *L. reuteri* GMNL-263 allegedly alleviates autoimmune diseases, in particular systemic lupus erythematosus (SLE) in NZB/W F1 mice, a lupus-prone animal model.⁽¹³⁵⁾ In addition, *L. paracasei* NFRI 7415 isolated from Japanese fermented fish (funa-sushi) appears to lower whole-body and fat-tissue weights, plasma lipid concentration and hepatic lipid contents in C57BL/6J mice.⁽¹³⁶⁾

Beneficial effects of *Weissella*

The genus *Weissella* contains gram-positive, catalase-negative, and nonendospore forming bacteria with a coccoid or rod-shaped morphology.⁽¹³⁷⁾ The *Weissella* genus encompasses lactic-acid bacteria, including *W. viridescens*, *W. cibaria*, and *W. confusa*. *W. confusa* is identical to *L. confusus* and is present in the normal microflora of the human intestine and in fermented foods.⁽¹³⁸⁾ Until now, only few studies have explored the probiotic effects of *Weissella* *in vivo* or *in vitro*. A combination of 3 lactic-acid bacteria including *Weissella* (*Pediococcus pentosaceus*, *L. plantarum*,

and *W. confusa*) had an anti-proliferative effect on a human colorectal adenocarcinoma cell line.⁽¹³⁹⁾ *W. confusa* PL9001, isolated from the urine of hospitalized female patients, was subsequently found potentially useful for both preventive and therapeutic treatment of genitourinary infections with *Candida albicans*, *Escherichia coli*, *Staphylococcus aureus*, or vancomycin-resistant *Enterococcus faecium*.⁽²⁰⁾ It should be noted that apart from being a probiotic, *W.confusa* may also be an opportunistic pathogenic microbial agent that can cause sepsis and other infections in humans and animals.⁽¹⁴⁰⁾ One should, therefore, exert caution when using *W.confusa* as a probiotic agent.^(138, 140)

Safety of our cocktail of probiotic bacteria

Our study clearly shows that the probiotic cocktail of *L. paracasei*, *L. casei*, and *W. confusa* itself, as used in the present study, did not induce any adverse effect on the rats. Furthermore, the study showed a hepatoprotective effect of the probiotic cocktail on TAA-induced liver fibrosis in rats. Accordingly, serum levels of liver-enriched enzymes, microscopic liver damage and inflammation, lipid peroxidation, collagen accumulation, liver content of the proinflammatory proteins TNF- α and TGF- β 1, and that of α -SMA, a marker for hepatic stellate cell activation, were all decreased substantially compared to the untreated group of TAA-fibrotic rats (Figure 56).

Hepatic effects of TAA treatment

Administration of TAA 300 mg/kg BW for consecutive 8 weeks is our standard protocol to induce liver fibrosis in all treated animals. This TAA treatment results in microscopically severe inflammation and accumulation of collagen fibers in the liver and an increase in serum concentrations of liver-enriched enzymes. TAA causes liver injury by conversion into two reactive metabolites: TAA-S-oxide (TASO) and TAA-S,S-dioxide (TASO₂).⁽¹⁰⁶⁾ Bioactivation of TAA is mediated by cytochrome P450 (CYP), in particular subtype CYP2E1, which is predominantly expressed in hepatocytes.⁽¹⁴¹⁾ Additionally, CYP2E1 is also expressed in the duodenum and jejunum.^(142, 143) but intestinal damage is not usually studied.

Disruption of the intestinal barrier, intestinal bacterial overgrowth, and bacterial translocation via the gut-liver axis are the factors to promote pathogenesis of hepatic

disorders, including fibrosis and cirrhosis.⁽¹⁴⁴⁾ Bacterial components, including lipopolysaccharide (LPS)⁽¹⁴⁵⁾, pathogen-associated molecular patterns (PAMPs), and damage-associated molecular patterns (DAMP) are translocated into the liver via the portal circulation following hepatic injury.^(145, 146) LPS and PAMP bind to TLR4 receptors on the hepatocyte membrane resulting in the production of pro-inflammatory cytokines (e.g., TNF- α , IL-6, and IFN- γ) and chemokines which enhanced liver inflammation (via up-regulation the p38 MAPK and NF- κ B activities, and liver fibrogenesis.⁽⁹⁸⁾ TLR4 activation can also lead to hepatic stellate cell (HSC) activation and transformation into myofibroblast-like cells which express α -SMA and produce collagen.⁽¹⁴⁷⁻¹⁵⁰⁾ (Figure 57).

After TAA treatment the intestinal barrier is weakened, which leads to translocation of pathogens from intestinal lumen into the portal circulation via the gut liver axis that, in turn, promotes more liver injury.^(151, 152) We, therefore, hypothesize that the mixture of three probiotics strains administered via oral gavage in the present study modulated gut microbiota and strengthened the intestinal barrier. Such an explanation is in accordance with previous studies using *Lactobacillus* to alleviate the fibrogenic status induced by TAA⁽¹⁵³⁾ or CCl₄.^(22, 154)

The present study confirms earlier reports that silymarin exerts hepatoprotective effects, as demonstrated by less liver damage index, oxidative stress, inflammation, and fibrosis. Silymarin appears to be a free-radical scavenger and increased the concentration of reduced glutathione (GSH).⁽¹⁵⁵⁾ It may also stabilize cell membrane integrity,⁽¹⁵⁶⁾ inhibit hepatic stellate cell activation.^(157, 158) and down-regulate the expression of fibrogenic markers, such as MMP-2, MMP-13, TIMP-1, TIMP-2, AP-1, KLF6, TGF- β 1, α -SMA, and COL- α 1⁽¹¹⁰⁾ and inflammatory cytokines.⁽¹⁵⁹⁾ Irrespective of these beneficial effects of silymarin, our combination of probiotic bacteria was more effective in reducing liver damage, MDA, and TGF- β 1, α -SMA, and TNF- α expression.

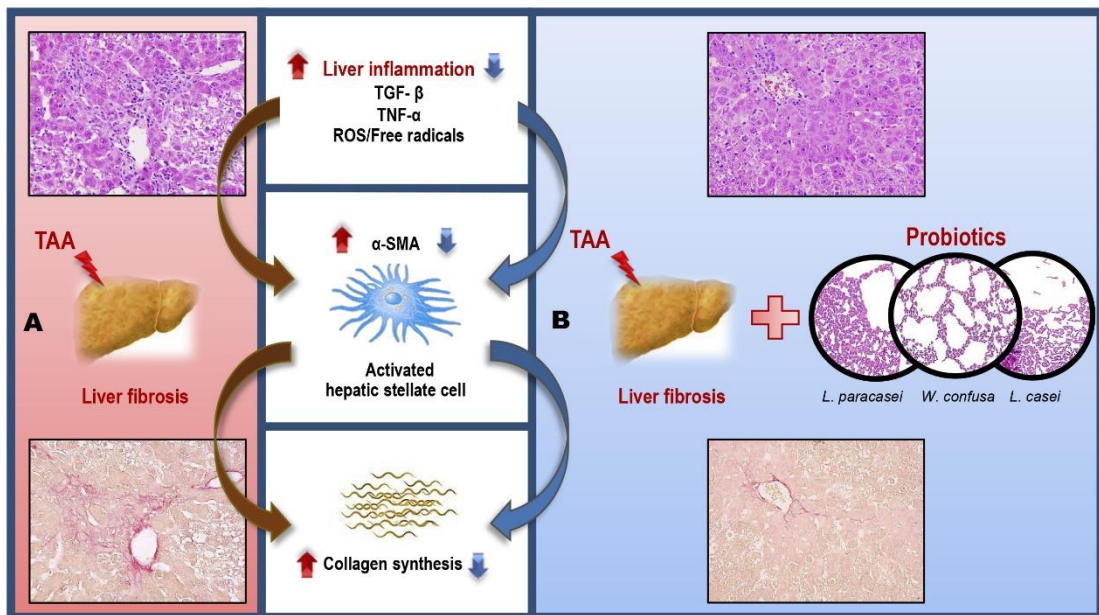


Figure 56 Schema showing of probiotic lactic acid bacteria protecting against liver fibrosis

(A) The pathway of collagen accumulation and fibrosis development involving inflammatory response and HSCs activation induced by TAA. (B) The probiotics reduces the inflammatory effect and attenuate liver fibrosis.

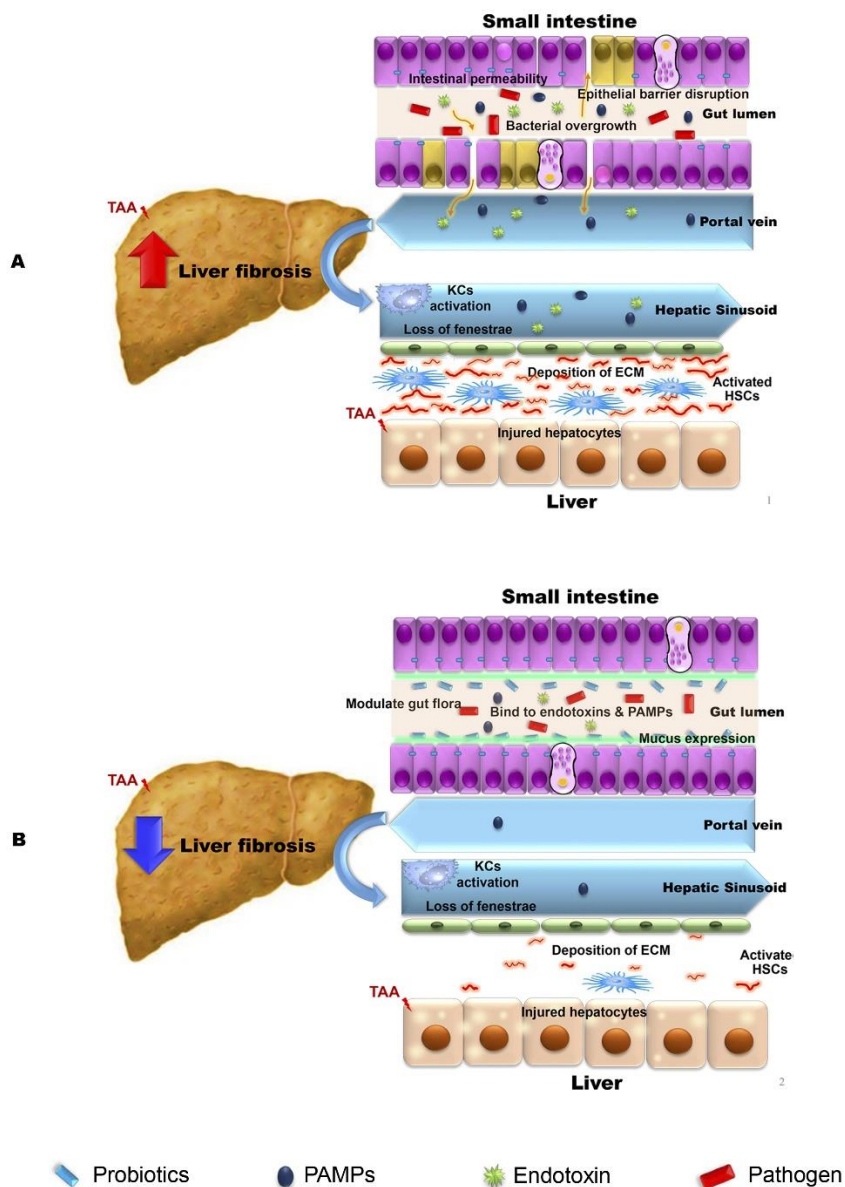


Figure 57 Schematic depicting the gut-liver axis following the liver fibrosis induced by thioacetamide (TAA)

Note the bacterial overgrowth, dysbiosis, and increased permeability in the intestine. Intestinal bacterial translocation via portal vein enhances the process of liver inflammation and liver fibrosis (A). Administration of probiotics lowers the intestinal bacterial overgrowth and intestinal permeability leading to reduce the inflammatory effect and attenuate liver fibrosis (B).

CHAPTER 6

CONCLUSION

The present study demonstrated that the combination of three probiotic lactic acid bacteria (*L. paracasei*, *L. casei*, and *W. confusa*) at the concentration of 10^9 CFU/ml/day each could alleviate the liver inflammation and liver fibrosis in the TAA-treated rat. TAA was suitable for being used to induce the liver fibrosis since its histopathogenesis is similar to that occur in human.⁽¹⁶⁰⁾ TAA caused overproduction of MDA reflecting high level of hepatic oxidative stress, up-regulation of TNF- α , TGF- β 1 reflecting high degree of liver inflammation, and up-regulation the α -SMA level reflecting high hepatic stellate cell activation,

From the present in vivo study, it demonstrated for the first time that administration of the cocktail of three combined strains of the viable lactic acid bacteria (*L. paracasei*, *L. casei*, and *W. confusa*) isolated from the Thai infant feces at the ratio of 1:1:1 (10^9 CFU/ml/day each) could attenuate the degree of liver oxidative stress, liver inflammation and liver fibrosis in TAA-treated rats. Treatment with such probiotics could lower the lipid peroxidation product, decrease the index of liver damage, percentage of leukocyte infiltration, collagen accumulation, and down-regulate the genes and proteins expression involved in inflammation and fibrogenesis. Therefore, consuming the probiotics lactic acid bacteria cocktail would be an alternative way to protect liver inflammation and liver fibrosis.

REFERENCES

1. Bataller R, Brenner DA. Liver fibrosis. *J Clin Invest*. 2005;115(2):209-18.
2. Mokdad AA LA, Shahrzad S, Lozano R, Mokdad AH, Stanaway J, et al. Liver cirrhosis mortality in 187 countries between 1980 and 2010: a systematic analysis. *BMC Med*. 2014;12(145):1-24.
3. Murray CJL, Lopez AD. Alternative projections of mortality and disability by cause 1990–2020: Global Burden of Disease Study. *The Lancet*. 1997;349(9064):1498-504.
4. Hernandez-Gea V, Friedman SL. Pathogenesis of liver fibrosis. *Annu Rev Pathol*. 2011;6:425-56.
5. Tsochatzidis EA, Bosch J, Burroughs AK. Liver cirrhosis. *Lancet*. 2014;383(9930):1749-61.
6. Lee UE, Friedman SL. Mechanisms of hepatic fibrogenesis. *Best Pract Res Clin Gastroenterol*. 2011;25(2):195-206.
7. Liu T, Wang X, Karsdal MA, Leeming DJ, Genovese F. Molecular serum markers of liver fibrosis. *Biomark Insights*. 2012;7:105-17.
8. Chakraborty JB, Oakley F, Walsh MJ. Mechanisms and biomarkers of apoptosis in liver disease and fibrosis. *Int J Hepatol*. 2012;2012:648915.
9. Ayala A, Munoz MF, Arguelles S. Lipid peroxidation: production, metabolism, and signaling mechanisms of malondialdehyde and 4-hydroxy-2-nonenal. *Oxid Med Cell Longev*. 2014;2014:360438.
10. Mitsuhashi M MK, Wanibuchi H, Kiyota A, Wada S, Nakatani T. Examination of the rat model of liver injury via thioacetamide (TAA) or carbon tetrachloride (CCl₄). *J Toxicol Pathol*. 2004;17:219-22.
11. Liedtke C, Luedde T, Sauerbruch T, Scholten D, Streetz K, Tacke F, et al. Experimental liver fibrosis research: update on animal models, legal issues and translational aspects. *Fibrogenesis Tissue Repair*. 2013;6(1):19.
12. Yanguas SC, Cogliati B, Willebrords J, Maes M, Colle I, van den Bossche B, et al. Experimental models of liver fibrosis. *Arch Toxicol*. 2016;90(5):1025-48.

13. Muñoz Torres E PBJ, López Bravo A, Abad Hernández MM, Carrascal Marino E. Experimental thioacetamide-induced cirrhosis of the liver. *Histol Histopathol.* 1991;6(1):95-100.
14. Stankova P, Kucera O, Lotkova H, Rousar T, Endlicher R, Cervinkova Z. The toxic effect of thioacetamide on rat liver *in vitro*. *Toxicol In Vitro.* 2010;24(8):2097-103.
15. Kang JS WH, Morimura K, Wongpoomchai R, Chusiri Y, Gonzalez FJ, et al. Role of CYP2 E1 in thioacetamide-induced mouse hepatotoxicity. *Toxicol Appl Pharmacol.* 2008;228(3):295-300.
16. FAO/WHO. Guidelines for the evaluation of probiotics in food. Report of a Joint FAO/WHO Working Group on Drafting Guidelines for the Evaluation of Probiotics in Food. 2002.
17. Sanders ME GG, Gill HS, Guarner F. Probiotics: their potential to impact human health. *Council for Agricultural Science and Technology.* 2007(36):1-20.
18. Holzapfel WH, Haberer P, Geisen R, Bjorkroth J, Schillinger U. Taxonomy and important features of probiotic microorganisms in food and nutrition. *Am J Clin Nutr.* 2001;73(2 Suppl):365S-73S.
19. Bermudez-Brito M, Plaza-Diaz J, Munoz-Quezada S, Gomez-Llorente C, Gil A. Probiotic mechanisms of action. *Ann Nutr Metab.* 2012;61(2):160-74.
20. Imani Fooladi AA MHH, Nourani MR, Khani S, Alavian SM. Probiotic as a novel treatment strategy against liver disease. *Hepat Mon.* 2013;13(2):e7521.
21. Lai JT, Hsieh WT, Fang HL, Lin WC. The protective effects of a fermented substance from *Saccharomyces cerevisiae* on carbon tetrachloride-induced liver damage in rats. *Clin Nutr.* 2009;28(3):338-45.
22. Liu Y, Liu Q, Ye G, Khan A, Liu J, Gan F, et al. Protective effects of Selenium-enriched probiotics on carbon tetrachloride-induced liver fibrosis in rats. *J Agric Food Chem.* 2015;63(1):242-9.
23. Chiva M, Soriano G, Rochat I, Peralta C, Rochat F, Llovet T, et al. Effect of *Lactobacillus johnsonii* La1 and antioxidants on intestinal flora and bacterial translocation in rats with experimental cirrhosis. *J Hepatol.* 2002;37(4):456-62.

24. Park JE, Lee DK, Kim KT, Seo JG, Chung MJ, Ha NJ, et al. Hepatoprotective effects of dual-coated and uncoated mixture of probiotics in rats. *Biotechnology & Biotechnological Equipment*. 2015;29(6):1164-8.
25. Ladda B, Theparee T, Chimchang J, Tanasupawat S, Taweechoitipatr M. In vitro modulation of tumor necrosis factor alpha production in THP-1 cells by lactic acid bacteria isolated from healthy human infants. *Anaerobe*. 2015;33:109-16.
26. Reid G, Jass J, Sebulsy MT, McCormick JK. Potential uses of probiotics in clinical practice. *Clin Microbiol Rev*. 2003;16(4):658-72.
27. R F. Probiotics in man and animals. *J Appl Bacteriol*. 1989;66(5):365-78.
28. Schrezenmeir J dVM. Probiotics, prebiotics, and synbiotics-approaching a definition. *Am J Clin Nutr*. 2001;73(2Suppl):361S-4S.
29. Kosin B RS. Microbial and processing criteria for production of probiotics: A review. *Food Technol Biotechnol*. 2006;44(3):371-9.
30. Tuomola E, Crittenden R, Playne M, Isolauri E, Salminen S. Quality assurance criteria for probiotic bacteria. *Am J Clin Nutr*. 2001;73(2 Suppl):393S-8S.
31. PL C. Selection criteria for probiotic microorganisms. *Asia Pac J Clin Nutr*. 1996;5(1):10-4.
32. Lee YK SS. The coming of age of probiotics. *Trends Food Sci Technol*. 1995;6(7):241-5.
33. Aureli P, Capurso L, Castellazzi AM, Clerici M, Giovannini M, Morelli L, et al. Probiotics and health: an evidence-based review. *Pharmacol Res*. 2011;63(5):366-76.
34. Sherman PM, Ossa JC, Johnson-Henry K. Unraveling mechanisms of action of probiotics. *Nutr Clin Pract*. 2009;24(1):10-4.
35. K Gogineni V, Morrow LE. Probiotics: Mechanisms of Action and Clinical Applications. *Journal of Probiotics & Health*. 2013;01(01):1000101.
36. Ohland CL, Macnaughton WK. Probiotic bacteria and intestinal epithelial barrier function. *Am J Physiol Gastrointest Liver Physiol*. 2010;298(6):G807-19.
37. Anderson RC, Cookson AL, McNabb WC, Park Z, McCann MJ, Kelly WJ, et al. *Lactobacillus plantarum* MB4 5 2 enhances the function of the intestinal barrier by

increasing the expression levels of genes involved in tight junction formation. *BMC Microbiol.* 2010;10(316):316.

38. Hummel S, Veltman K, Cichon C, Sonnenborn U, Schmidt MA. Differential targeting of the E-Cadherin/beta-Catenin complex by gram-positive probiotic lactobacilli improves epithelial barrier function. *Appl Environ Microbiol.* 2012;78(4):1140-7.

39. Mack DR, Michail S, Wei S, McDougall L, Hollingsworth MA. Probiotics inhibit enteropathogenic *E. coli* adherence in vitro by inducing intestinal mucin gene expression. *Am J Physiol.* 1999;276(4):G941-50.

40. Schiffrin EJ, Brassart D, Servin AL, Rochat F, Donnet-Hughes A. Immune modulation of blood leukocytes in humans by lactic acid bacteria: criteria for strain selection. *Am J Clin Nutr.* 1997;66(2):515S-20S.

41. COLLADO MC MGM, HERNANDEZ A, SANZ Y, SALMINEN S. Adhesion of Selected Bifidobacterium Strains to Human Intestinal Mucus and the Role of Adhesion in Enteropathogen Exclusion. *Journal of Food Protection.* 2005;68(12):2672-8.

42. Van Tassell ML, Miller MJ. *Lactobacillus* adhesion to mucus. *Nutrients.* 2011;3(5):613-36.

43. Caballero-Franco C, Keller K, De Simone C, Chadee K. The VSL#3 probiotic formula induces mucin gene expression and secretion in colonic epithelial cells. *Am J Physiol Gastrointest Liver Physiol.* 2007;292(1):G315-22.

44. Johnson-Henry KC, Hagen KE, Gordonpour M, Tompkins TA, Sherman PM. Surface-layer protein extracts from *Lactobacillus helveticus* inhibit enterohaemorrhagic *Escherichia coli* O157:H7 adhesion to epithelial cells. *Cell Microbiol.* 2007;9(2):356-67.

45. Wu X, Vallance BA, Boyer L, Bergstrom KS, Walker J, Madsen K, et al. *Saccharomyces boulardii* ameliorates *Citrobacter rodentium*-induced colitis through actions on bacterial virulence factors. *Am J Physiol Gastrointest Liver Physiol.* 2008;294(1):G295-306.

46. Penner R, Fedorak RN, Madsen KL. Probiotics and nutraceuticals: non-medicinal treatments of gastrointestinal diseases. *Curr Opin Pharmacol.* 2005;5(6):596-603.

47. Alakomi HL, Skytta E, Saarela M, Mattila-Sandholm T, Latva-Kala K, Helander IM.

Lactic acid permeabilizes gram-negative bacteria by disrupting the outer membrane. *Appl Environ Microbiol.* 2000;66(5):2001-5.

48. Kelsall BL. Innate and adaptive mechanisms to control pathological intestinal inflammation. *J Pathol.* 2008;214(2):242-59.

49. Duquesne S, Petit V, Peduzzi J, Rebuffat S. Structural and functional diversity of microcins, gene-encoded antibacterial peptides from enterobacteria. *J Mol Microbiol Biotechnol.* 2007;13(4):200-9.

50. Lievin-Le Moal V, Servin AL. The front line of enteric host defense against unwelcome intrusion of harmful microorganisms: mucins, antimicrobial peptides, and microbiota. *Clin Microbiol Rev.* 2006;19(2):315-37.

51. O'Shea EF, Cotter PD, Stanton C, Ross RP, Hill C. Production of bioactive substances by intestinal bacteria as a basis for explaining probiotic mechanisms: bacteriocins and conjugated linoleic acid. *Int J Food Microbiol.* 2012;152(3):189-205.

52. Corthésy B GH, Mercenier A. Some probiotic strains have the ability to promote the differentiation of B cells into plasma cells and increase the production of secretory immunoglobulin A. *J Nutr.* 2007;137(3 Suppl 2):781S-90S.

53. Gomez-Llorente C, Munoz S, Gil A. Role of Toll-like receptors in the development of immunotolerance mediated by probiotics. *Proc Nutr Soc.* 2010;69(3):381-9.

54. D A. Epithelial-cell recognition of commensal bacteria and maintenance of immune homeostasis in the gut. *Nat Rev Immunol.* 2008;8(6):411-20.

55. Di Giacinto C, Marinaro M, Sanchez M, Strober W, Boirivant M. Probiotics ameliorate recurrent Th1-mediated murine colitis by inducing IL-10 and IL-10-dependent TGF-beta-bearing regulatory cells. *J Immunol.* 2005;174(6):3237-46.

56. Tien MT, Girardin SE, Regnault B, Le Bourhis L, Dillies MA, Coppee JY, et al. Anti-inflammatory effect of *Lactobacillus casei* on *Shigella*-infected human intestinal epithelial cells. *J Immunol.* 2006;176(2):1228-37.

57. Bajaj JS, Hylemon PB, Younossi Z. The Intestinal Microbiota and Liver Disease. *The American Journal of Gastroenterology Supplements.* 2012;1(1):9-14.

58. Son G, Kremer M, Hines IN. Contribution of gut bacteria to liver pathobiology.

Gastroenterol Res Pract. 2010;2010(2010).

59. Compare D CP, Rocco A, Nardone OM, De Maria S, Carteni M, et al. Gut-liver axis: the impact of gut microbiota on non alcoholic fatty liver disease. *Nutr Metab Cardiovasc Dis.* 2012;22(6):471-6.
60. Sharma V, Garg S, Aggarwal S. Probiotics and liver disease. *Perm J.* 2013;17(4):62-7.
61. Gratz SW, Mykkanen H, El-Nezami HS. Probiotics and gut health: a special focus on liver diseases. *World J Gastroenterol.* 2010;16(4):403-10.
62. Cesaro C, Tiso A, Del Prete A, Cariello R, Tuccillo C, Cotticelli G, et al. Gut microbiota and probiotics in chronic liver diseases. *Dig Liver Dis.* 2011;43(6):431-8.
63. Goel A, Gupta M, Aggarwal R. Gut microbiota and liver disease. *J Gastroenterol Hepatol.* 2014;29(6):1139-48.
64. Gupta A, Dhiman RK, Kumari S, Rana S, Agarwal R, Duseja A, et al. Role of small intestinal bacterial overgrowth and delayed gastrointestinal transit time in cirrhotic patients with minimal hepatic encephalopathy. *J Hepatol.* 2010;53(5):849-55.
65. Lakshmi CP, Ghoshal UC, Kumar S, Goel A, Misra A, Mohindra S, et al. Frequency and factors associated with small intestinal bacterial overgrowth in patients with cirrhosis of the liver and extra hepatic portal venous obstruction. *Dig Dis Sci.* 2010;55(4):1142-8.
66. Gomez-Hurtado I, Santacruz A, Peiro G, Zapater P, Gutierrez A, Perez-Mateo M, et al. Gut microbiota dysbiosis is associated with inflammation and bacterial translocation in mice with CCl₄-induced fibrosis. *PLoS One.* 2011;6(7):e23037.
67. AL M. Junqueira's Basic histology: Text and Atlas.1 2 th ed. . New York, NY: McGraw Hill Medical;. 2010.
68. Ellis H. Anatomy of the liver. *Surgery (Oxford).* 2011;29(12):589-92.
69. Sibulesky L. Normal liver anatomy. *Clin Liver Dis (Hoboken).* 2013;2(Suppl 1):S1-S3.
70. Abdel-Misih SR, Bloomston M. Liver anatomy. *Surg Clin North Am.* 2010;90(4):643-53.
71. Vdoviakova K, Vdoviakova K, Petrovova E, Kresakova L, Maloveska M, Teleky J, et

- al. Importance Rat Liver Morphology and Vasculature in Surgical Research. *Med Sci Monit.* 2016;22:4716-28.
72. Martins PN, Neuhaus P. Surgical anatomy of the liver, hepatic vasculature and bile ducts in the rat. *Liver Int.* 2007;27(3):384-92.
73. V K. Chapter 13: gross anatomy. 2000
253-83.
74. Fiebig T BH, Figueiredo G, Kerl HU, Nittka S, Groden C, et al. Three-dimensional in vivo imaging of the murine liver: a micro-computed tomography-based anatomical study. *PLoS One.* 2012;7(2):e31179.
75. Madrahimov N, Dirsch O, Broelsch C, Dahmen U. Marginal hepatectomy in the rat: from anatomy to surgery. *Ann Surg.* 2006;244(1):89-98.
76. Kogure K, Ishizaki M, Nemoto M, Kuwano H, Makuuchi M. A comparative study of the anatomy of rat and human livers. *J Hepatobiliary Pancreat Surg.* 1999;6(2):171-5.
77. Fontana J ŠM, Mad'a P. Liver and biotransformation of xenobiotics [Internet] [cited 2018 Apr 4] Available from: http://fboltcz/en/skripta/ix-travici-soustava/5_jatra-a-biotransformace_xenobiotik/.
78. Ross MH PW. Digestive system III : Liver, Gallbladder, and Pancreas. In *Histology: A text and atlas* 2003;Philadelphia, Pa: Lippincott Williams & Wilkins Chicago:p.628-55.
79. Krishna M. Microscopic anatomy of the liver. *Clin Liver Dis (Hoboken).* 2013;2(Suppl 1):S4-S7.
80. DL CJB. Hepatobiliary System and Exocrine Pancreas [Internet]. . [cited 2018 Apr 4]. Available from: <https://veteriankey.com/hepatobiliary-system-and-exocrine-pancreas/>.
81. RK M. Hepatic stellate cells and liver fibrosis. *Arch Pathol Lab Med.* 2007;131:1728-34
82. Kuntz E KH. Biochemistry and functions of the liver. In: *Hepatology textbook and atlas.* 2008;Berlin, Heidelberg: Springer Berlin Heidelberg:35-76.
83. Tso P MJ. The physiology of the liver. In: Rhoades R, Tanner G, editors *Medical*

physiology 2nd ed Lippincott Williams & Wilkins; . 2003:p. 514–25.

84. Tsukada S, Parsons CJ, Rippe RA. Mechanisms of liver fibrosis. *Clin Chim Acta*. 2006;364(1-2):33-60.
85. Pellicoro A, Ramachandran P, Iredale JP, Fallowfield JA. Liver fibrosis and repair: immune regulation of wound healing in a solid organ. *Nat Rev Immunol*. 2014;14(3):181-94.
86. Shimizu I, Shimamoto N, Saiki K, Furujo M, Osawa K. Lipid Peroxidation in Hepatic Fibrosis. In *Lipid Peroxidation*; Catala, A, Ed; InTech Publisher: Rijeka, Croatia, . 2012:p. 483–92.
87. Zhou WC, Zhang QB, Qiao L. Pathogenesis of liver cirrhosis. *World J Gastroenterol*. 2014;20(23):7312-24.
88. Bautista M, Andres D, Cascales M, Morales-Gonzalez JA, Sanchez-Reus MI, Madrigal-Santillan E, et al. Role of Kupffer cells in thioacetamide-induced cell cycle dysfunction. *Molecules*. 2011;16(10):8319-31.
89. Czaja AJ. Hepatic inflammation and progressive liver fibrosis in chronic liver disease. *World J Gastroenterol*. 2014;20(10):2515-32.
90. Kisseleva T, Brenner DA. Hepatic stellate cells and the reversal of fibrosis. *J Gastroenterol Hepatol*. 2006;21 Suppl 3:S84-7.
91. Pinzani M. Pathophysiology of Liver Fibrosis. *Dig Dis*. 2015;33(4):492-7.
92. Friedman SL. Hepatic fibrosis -- overview. *Toxicology*. 2008;254(3):120-9.
93. Rockey DC FS. Hepatic fibrosis and cirrhosis. 2006.
94. M G. Noninvasive biochemical markers of liver fibrosis. *J Gastrointestin Liver Dis*. 2006;15(2):149-59.
95. SG S. Assessing liver function. *Curr Opin Crit Care*. 2007;13(2):207-14.
96. Goodman ZD. Grading and staging systems for inflammation and fibrosis in chronic liver diseases. *J Hepatol*. 2007;47(4):598-607.
97. Germani G, Hytiroglou P, Fotiadu A, Burroughs AK, Dhillon AP. Assessment of fibrosis and cirrhosis in liver biopsies: an update. *Semin Liver Dis*. 2011;31(1):82-90.
98. Huang Y dBW, Adams LA, MacQuillan G, Rossi E, Rigby P, et al. Image analysis of

liver collagen using sirius red is more accurate and correlates better with serum fibrosis markers than trichrome. *Liver Int.* 2013;33(8):1249-56.

99. Weng C-H, Ding F, Lin Y-T, Liu N. Effective decolorization of polyazo direct dye Sirius Red F3 B using persulfate activated with Fe₀ aggregate. *Sep Purif Technol.* 2015;147:147-55.

100. Standish RA, Cholongitas E, Dhillon A, Burroughs AK, Dhillon AP. An appraisal of the histopathological assessment of liver fibrosis. *Gut.* 2006;55(4):569-78.

101. Pellicoro A, Ramachandran P, Iredale JP. Reversibility of liver fibrosis. *Fibrogenesis Tissue Repair.* 2012;5(Suppl 1):S26.

102. Sun M, Kisseleva T. Reversibility of liver fibrosis. *Clin Res Hepatol Gastroenterol.* 2015;39 Suppl 1:S60-3.

103. Akhtar T, Sheikh N. An overview of thioacetamide-induced hepatotoxicity. *Toxin Reviews.* 2013;32(3):43-6.

104. Thioacetamide. [Internet] [cited 2018 Apr 10] Available from: <https://pubchem.ncbi.nlm.nih.gov/compound/thioacetamide>.

105. Axhausen J, Ritter C, Lux K, Kornath A. The Protonation of Acetamide and Thioacetamide in Superacidic Solutions: Crystal Structures of [H₃CC(OH)NH₂]⁺AsF₆⁻ and [H₃CC(SH)NH₂]⁺AsF₆⁻. *Zeitschrift für anorganische und allgemeine Chemie.* 2013;639(1):65-72.

106. Hajovsky H, Hu G, Koen Y, Sarma D, Cui W, Moore DS, et al. Metabolism and toxicity of thioacetamide and thioacetamide S-oxide in rat hepatocytes. *Chem Res Toxicol.* 2012;25(9):1955-63.

107. Skottová N KV. Silymarin as a potential hypocholesterolaemic drug. *Physiol Res.* 1998;47(1):1-7.

108. Abenavoli L, Capasso R, Milic N, Capasso F. Milk thistle in liver diseases: past, present, future. *Phytother Res.* 2010;24(10):1423-32.

109. Tsai JH, Liu JY, Wu TT, Ho PC, Huang CY, Shyu JC, et al. Effects of silymarin on the resolution of liver fibrosis induced by carbon tetrachloride in rats. *J Viral Hepat.* 2008;15(7):508-14.

110. Chen IS, Chen YC, Chou CH, Chuang RF, Sheen LY, Chiu CH. Hepatoprotection of silymarin against thioacetamide-induced chronic liver fibrosis. *J Sci Food Agric*. 2012;92(7):1441-7.
111. Vargas-Mendoza N, Madrigal-Santillan E, Morales-Gonzalez A, Esquivel-Soto J, Esquivel-Chirino C, Garcia-Luna YG-RM, et al. Hepatoprotective effect of silymarin. *World J Hepatol*. 2014;6(3):144-9.
112. Rasool M, Iqbal J, Malik A, Ramzan HS, Qureshi MS, Asif M, et al. Hepatoprotective Effects of *Silybum marianum* (Silymarin) and *Glycyrrhiza glabra* (Glycyrrhizin) in Combination: A Possible Synergy. *Evid Based Complement Alternat Med*. 2014;2014(2014):641597.
113. Féher J LG. Silymarin in the prevention and treatment of liver diseases and primary liver cancer. *Curr Pharm Biotechnol*. 2012;13(1):210-7.
114. Saller R MR, Brignoli R. The Use of Silymarin in the Treatment of Liver Diseases. *Drugs*. 2001;61(14):2035-63.
115. Fraschini F DG, Esposti D. Pharmacology of Silymarin. *Clinical Drug Investigation*. 2002;22(1):51-65.
116. Radko L CW. Application of silymarin in human and animal medicine. *J Pre-Clinical Clin Res*. 2007;1(1):22-6.
117. Jia JD BM, Cho JJ, Ruehl M, Milani S, Boigk G, et al. Antifibrotic effect of silymarin in rat secondary biliary fibrosis is mediated by downregulation of procollagen alpha1 (I) and TIMP-1. *J Hepatol*. 2001;35(3):392-8.
118. Lin YL, Hsu YC, Chiu YT, Huang YT. Antifibrotic effects of a herbal combination regimen on hepatic fibrotic rats. *Phytother Res*. 2008;22(1):69-76.
119. Abdel-Moneim AM, Al-Kahtani MA, El-Kersh MA, Al-Omair MA. Free Radical-Scavenging, Anti-Inflammatory/Anti-Fibrotic and Hepatoprotective Actions of Taurine and Silymarin against CCl₄ Induced Rat Liver Damage. *PLoS One*. 2015;10(12):e0144509.
120. Vinderola G, Binetti A, Burns P, Reinheimer J. Cell viability and functionality of probiotic bacteria in dairy products. *Front Microbiol*. 2011;2:70.
121. Champagne CP, Ross RP, Saarela M, Hansen KF, Charalampopoulos D.

Recommendations for the viability assessment of probiotics as concentrated cultures and in food matrices. *Int J Food Microbiol.* 2011;149(3):185-93.

122. Mahli A KA CB, Peterburs P, Lechner A, Haunschild J, et al. . Hepatoprotective effect of oral application of a silymarin extract in carbon tetrachloride-induced hepatotoxicity in rats. *Clinical Phytoscience.* 2015;1(5):1-5.

123. P Govind SY. A review on hepatoprotective activity of silymarin. *IJRAP.* 2011;2(1):75-9.

124. Camargo CA, Jr., Madden JF, Gao W, Selvan RS, Clavien PA. Interleukin-6 protects liver against warm ischemia/reperfusion injury and promotes hepatocyte proliferation in the rodent. *Hepatology.* 1997;26(6):1513-20.

125. Thurman RG MI, Seitz G, Thies J, Lemasters JJ, Zimmermann FA. . Hepatic reperfusion injury following

orthotopic liver transplantation in the rat. *Transplantation.* 1988;46(4):502-6.

126. Imani Fooladi AA, Mahmoodzadeh Hosseini H, Nourani MR, Khani S, Alavian SM. Probiotic as a novel treatment strategy against liver disease. *Hepat Mon.* 2013;13(2):e7521.

127. Minelli EB BA. Relationship between number of bacteria and their probiotic effects. *Microbial Ecology in Health and Disease.* 2008;20:180-3.

128. CFIA (Canadian Food Inspection Agency) PcVfhwigcfr-a-glih-cec. Probiotic claims. Variable form <http://www.inspection.gc.ca/food/requirements-and-guidance/labelling/industry/health-claims/eng/1392834838383/1392834887794?chap=10>

2009.

129. Hill D SI, Tobin C, Hill C, Stanton C, Ross RP. The *Lactobacillus casei* Group: History and Health Related Applications. *Front Microbiol.* 2008;9:2107.

130. Kapila S KR, Reddi R, Sinha PR. Oral administration of probiotic *Lactobacillus casei spp. casei* ameliorates oxidative stress in rats. *IntJCurrMicrobiolAppSci* 2014;3(9):670-84.

131. Wang Y, Li Y, Xie J, Zhang Y, Wang J, Sun X, et al. Protective effects of probiotic

- Lactobacillus casei* Zhang against endotoxin- and d-galactosamine-induced liver injury in rats via anti-oxidative and anti-inflammatory capacities. *Int Immunopharmacol.* 2013;15(1):30-7.
132. Novotny NI MG, de Moreno de LeBlanc A, Perdigón G. *Lactobacillus casei* CRL 4 3 1 administration decreases inflammatory cytokines in a diet-induced obese mouse model. *Nutrition.* 2015;31(7-8):1000-7.
133. Wei Wang QL, Wenhui Chai, Chunyan Sun, Tiehua Zhang, Changhui Zhao, Yuan Yuan, Xinyu Wang, Huiqin Liu, Haiqing Ye. *Lactobacillus paracasei* Jlus6 6 extenuate oxidative stress and inflammation via regulation of intestinal flora in rats with non alcoholic fatty liver disease. *Food Sci Nutr* 2019 7(8):2636–46.
134. Oyetayo VO AF, Akinyosoye FA. Safety and protective effect of *Lactobacillus acidophilus* and *Lactobacillus casei* used as probiotic agent *in vivo*. *Afr J Biotechnol.* 2003;2(11):448-52.
135. Hsu TC, Huang CY, Liu CH, Hsu KC, Chen YH, Tzang BS. *Lactobacillus paracasei* GMNL-32, *Lactobacillus reuteri* GMNL-89 and *L. reuteri* GMNL-263 ameliorate hepatic injuries in lupus-prone mice. *Br J Nutr.* 2017;117(8):1066-74.
136. Komatsuzaki N YY, Ueki Y, Shima J, Morikawa S. *Lactobacillus paracasei* NFRI 7415 reduces liver lipid contents in C57BL/6J mice fed a high-fat diet. *Int J Clin Nutr Diet.* 2016;2(1):108.
137. Björkroth J D, L. M. T., Endo A. The genus *Weissella*. *Lactic Acid Bacteria*. In W H Holzappel, & B J B Wood (Eds),. 2014; *Lactic Acid Bacteria: Biodiversity and Taxonomy* (Chichester, West Sussex, UK: John Wiley & Sons Ltd.):417-28.
138. Fusco V, Quero GM, Cho GS, Kabisch J, Meske D, Neve H, et al. The genus *Weissella*: taxonomy, ecology and biotechnological potential. *Front Microbiol.* 2015;6:155.
139. Er S, Kopal AT, Kivanc M. Cytotoxic effects of various lactic acid bacteria on Caco-2 cells. *Turkish Journal of Biology.* 2015;39(1):23-30.
140. Fairfax MR, Lephart PR, Salimnia H. *Weissella confusa*: problems with identification of an opportunistic pathogen that has been found in fermented foods and proposed as a probiotic. *Front Microbiol.* 2014;5:254.

141. Kang JS, Wanibuchi H, Morimura K, Wongpoomchai R, Chusiri Y, Gonzalez FJ, et al. Role of CYP2 E1 in thioacetamide-induced mouse hepatotoxicity. *Toxicol Appl Pharmacol.* 2008;228(3):295-300.
142. Matuskova Z, Siller M, Tunkova A, Anzenbacherova E, Zacharova A, Tlaskalova-Hogenova H, et al. Effects of *Lactobacillus casei* on the expression and the activity of cytochromes P450 and on the CYP mRNA level in the intestine and the liver of male rats. *Neuro Endocrinol Lett.* 2011;32 Suppl 1(Suppl 1):8-14.
143. Matuskova Z, Tunkova A, Anzenbacherova E, Vecera R, Siller M, Tlaskalova-Hogenova H, et al. Effects of probiotic *Escherichia coli* Nissle 1917 on expression of cytochromes P450 along the gastrointestinal tract of male rats. *Neuro Endocrinol Lett.* 2010;31 Suppl 2(Suppl 2):46-50.
144. Arab JP M-MR, Shah VH. Gut-liver axis, cirrhosis and portal hypertension: the chicken and the egg. *Hepatol Int* 2018;12(Suppl 1):24-33.
145. Konturek PC HI, Konturek K, Schink M, Konturek T, Neurath MF, Zopf Y. Gut-Liver Axis: How Do Gut Bacteria Influence the Liver? *Med Sci (Basel)* 2018;6(3):pii: E79.
146. Szabo G. Gut-liver axis in alcoholic liver disease. *Gastroenterology.* 2015;148(1):30-6.
147. Li Z, Yang S, Lin H, Huang J, Watkins PA, Moser AB, et al. Probiotics and antibodies to TNF inhibit inflammatory activity and improve nonalcoholic fatty liver disease. *Hepatology.* 2003;37(2):343-50.
148. Lirussi F, Mastropasqua E, Orando S, Orlando R. Probiotics for non-alcoholic fatty liver disease and/or steatohepatitis. *Cochrane Database Syst Rev.* 2007(1):CD005165.
149. Esposito E, Iacono A, Bianco G, Autore G, Cuzzocrea S, Vajro P, et al. Probiotics reduce the inflammatory response induced by a high-fat diet in the liver of young rats. *J Nutr.* 2009;139(5):905-11.
150. Arthur JS, Ley SC. Mitogen-activated protein kinases in innate immunity. *Nat Rev Immunol.* 2013;13(9):679-92.
151. Ortega MA TM, Fernández MI, Rios A, Sánchez-Pozo A, Gil A. Hepatotoxic agent thioacetamide induces biochemical and histological alterations in rat small intestine. *Dig*

Dis Sci. 1997;42(8):1715-23.

152. al-Bader AA MT, Abul H, al-Mosawi M, Panigrahi D, Dashti H. Bacterial translocation in thioacetamide induced liver cirrhosis in rat. *J R Coll Surg Edinb.* 1998;43(4):278-82.

153. Mahfouz MK AE-HO, Emam MA, Bakr MA. . Biochemical and histopathological effect of probiotics on experimentally induced liver fibrosis in rat. . *Banha Vet Med J* 2016;31(2):248-53.

154. Park JE LD, Kim KT, Seo JG, Chung MJ, Ha NJ, et al. Hepatoprotective effects of dual-coated and uncoated mixture of probiotics in rats. . *Biotechnology & Biotechnological Equipment.* 2015;29(6):1164-8.

155. Kang JS, Jeon YJ, Kim HM, Han SH, Yang KH. Inhibition of inducible nitric-oxide synthase expression by silymarin in lipopolysaccharide-stimulated macrophages. *J Pharmacol Exp Ther.* 2002;302(1):138-44.

156. Basiglio CL, Sanchez Pozzi EJ, Mottino AD, Roma MG. Differential effects of silymarin and its active component silibinin on plasma membrane stability and hepatocellular lysis. *Chem Biol Interact.* 2009;179(2-3):297-303.

157. Trappoliere M, Caligiuri A, Schmid M, Bertolani C, Failli P, Vizzutti F, et al. Silybin, a component of silymarin, exerts anti-inflammatory and anti-fibrogenic effects on human hepatic stellate cells. *J Hepatol.* 2009;50(6):1102-11.

158. Clichici S, Olteanu D, Nagy AL, Oros A, Filip A, Mircea PA. Silymarin inhibits the progression of fibrosis in the early stages of liver injury in CCl(4)-treated rats. *J Med Food.* 2015;18(3):290-8.

159. Kim M, Yang SG, Kim JM, Lee JW, Kim YS, Lee JI. Silymarin suppresses hepatic stellate cell activation in a dietary rat model of non-alcoholic steatohepatitis: analysis of isolated hepatic stellate cells. *Int J Mol Med.* 2012;30(3):473-9.

160. Wallace MC, Hamesch K, Lunova M, Kim Y, Weiskirchen R, Strnad P, et al. Standard operating procedures in experimental liver research: thioacetamide model in mice and rats. *Lab Anim.* 2015;49(1 Suppl):21-9.



VITA

NAME Mr.Chittapon Jantararussamee

DATE OF BIRTH 30 June 1987

PLACE OF BIRTH Songkhla, Thailand

INSTITUTIONS ATTENDED 2010 Bachelor of Science (Physical Therapy)
Faculty of Physical Therapy
Mahidol University, Bangkok, Thailand

2013 Master of Science (Anatomy)
Faculty of Medicine Siriraj Hospital
Mahidol University, Bangkok, Thailand

2019 Doctor of Philosophy (Biomedical Science)
Biomedical Sciences Program, Faculty of Medicine
Srinakharinwirot University, Bangkok, Thailand

HOME ADDRESS 260 Moo11, Kampanget, Rattaphum, Songkhla, 90180,
Thailand

